1970

Relative apparent molal heat contents of some aqueous rare earth salt solutions at 25° C

Michael Allen Mohs
Iowa State University

Recommended Citation

Mohs, Michael Allen, "Relative apparent molal heat contents of some aqueous rare earth salt solutions at 25° C " (1970). *Retrospective Theses and Dissertations*. 4253.
https://lib.dr.iastate.edu/rtd/4253

70-25,810

MOHS, Michael Allen, 1943-
RELATIVE APPARENT MOLAL HEAT CONTENTS OF
SOME AQUEOUS RARE EARTH SALT SOLUTIONS
AT 25° C.

Iowa State University, Ph.D., 1970
Chemistry, physical

University Microfilms, A XEROX Company, Ann Arbor, Michigan

RELATIVE APPARENT MOLAL HEAT CONTENTS OF SOME AQUEOUS RARE EARTH SALT SOLUTIONS AT 25° C

by

Michael Allen Mohs

A Dissertation Submitted to the
Graduate Faculty in Partial Fulfillment of
The Requirements for the Degree of
DOCTOR OF PHILOSOPHY

Major Subject: Physical Chemistry

Approved:

Signature was redacted for privacy.

In Charge of Major Work

Signature was redacted for privacy.

Head of Major Department

Signature was redacted for privacy.

Dean of Graduate College

Iowa State University
Ames, Iowa

1970

TABLE OF CONTENTS

I. INTRODUCTION

Although interest in electrolytic solution behavior has steadily increased since 1887, the development of a sound theory of electrolytic solutions for any but the most dilute solutions has not been realized.

The electrolytic solution theory of Debye and Hückel (1) was successful in predicting the behavior of the thermodynamic properties of solutions of strong electrolytes in the concentration range approaching infinite dilution. The complexity of the problem above this concentration range is magnified many times by such effects as ion-solvent interactions, modification of the solvent by the hydrated ions, and short range interactions of the ions. Due to this additional complexity attempts to modify or extend the theory of Debye and Hückel have in general been of little success.

A prerequisite for the successful development of a theory of electrolytic solutions applicable up to concentrated solutions appears to be the determination of the effects of the interactions mentioned above on the various thermodynamic properties of electrolytic solutions. It is thus desirable to collect data on strong electrolytes over the concentration range of infinite dilution to saturation. Ideally one would make measurements on a series of electrolytes which differed in only one variable such as the degree of complexation, ionic size, or degree of interaction with the solvent. Although this ideal series does not exist it is approximated by the rare earths.

The rare earth salts provide an excellent series for the study of electrolytic solution behavior due to their chemical similarity across the series. Since the electronic structures of the rare earth ions differ only in the extent of filling of the 4f subshell, which is shielded by the filled 5s and 5p subshells, the chemical properties of the rare earths are quite similar. The rare earths all form trivalent cations in aqueous solution which exhibit a fairly regular decrease of ionic radius with increase of atomic number. The rare earths do not hydrolyze as extensively as most other tripositive ions in aqueous solution. The salts formed by the rare earths are very soluble in water and thus afford an opportunity to study systems approaching the fused salt system. The study of the thermodynamic properties of the rare earth salts of a given anion will provide information on the effect of cation size. By varying the anion information on the effects of anion size and degree of complexation can be obtained.

Shortly after large scale ion exchange processes were developed at Ames Laboratory (2) capable of producing large quantities of high purity rare earths, this laboratory undertook an extensive study of the thermodynamic and transport properties of aqueous rare earth salt solutions from infinite dilution to saturation (3,4,5,6,7,8,9,10,11, 12).

One of the thermodynamic properties of interest in this program is the relative apparent molal heat constant ϕ_L. This quantity, which is directly related to the heat of dilution, provides a sensitive indicator of energy changes occurring during a dilution process due to complex dissociation, hydrolysis, ion-solvent interactions, and electrical work of separating charges. It was of interest in this investigation to study these effects as well as to provide additional data on 3-1 electrolytes for comparison with existing electrolytic solution theories.

The limiting law of Debye and Hückel has been shown to quantitatively describe the heat of dilution data of a number of very dilute univalent electrolyte solutions (13, 14). For a number of higher charge type electrolytes (14, 15,16,17) the limiting law has not been as successful due to the complicating effects of hydrolysis and complexation. The study of 3-1 electrolytes of the rare earths thus provides an opportunity to investigate the behavior of salts which differ in their tendencies to form complexes, but which have the important property that their degree of hydrolysis can be controlled.

Heat of dilution data are valuable for the practical reason that they are needed to correct heats of reaction involving electrolytes to the standard state which is usually infinite dilution.

This thesis is a report of the measurement of the heats of dilution of $La(NO_3)_3$, $Nd(NO_3)_3$, $Gd(NO_3)_3$, $Ho(NO_3)_3$, $Er(NO_3)_3$, $Lu(NO_3)_3$, $La(ClO_4)_3$, $Nd(ClO_4)_3$, $Gd(ClO_4)_3$, $Er(ClO_4)_3$, and $Lu(ClO_4)_3$ in aqueous solutions from infinite dilution to saturation. The heats of solution of $La(NO_3)_3 \cdot 6H_2O$, $Nd(NO_3)_3 \cdot 6H_2O$, $Gd(NO_3)_3 \cdot 6H_2O$, $Ho(NO_3)_3 \cdot 6H_2O$, $Er(NO_3)_3 \cdot 6H_2O$, $Lu(NO_3)_3 \cdot 5H_2O$, $La(ClO_4)_3 \cdot 8H_2O$, $Nd(ClO_4)_3 \cdot 8H_2O$, $Gd(ClO_4)_3 \cdot 8H_2O$, and $Er(ClO_4)_3 \cdot 8H_2O$ were also measured. The relative partial molal heat contents were calculated from the heat of dilution data. Wherever possible the derived relative partial molal heat contents were combined with activity data to calculate the partial molal excess entropies of dilution.

Studies of the partial molal volumes (9, 12) of some aqueous rare earth chlorides, nitrates, and perchlorates indicate that a hydration change occurs across the middle section of the rare earth series. The heat of dilution data of thirteen rare earth chlorides (3, 10) have been interpreted in terms of this hydration change. It was of interest to see if this trend could be detected from the heat of dilution data of the perchlorates and nitrates also.

II. THEORY

The ionization theory postulated by Arrhenius (18) in 1887 marked the beginning of the development of the modern theory of electrolytes. Although Arrhenius' theory of partial dissociation adequately described weak electrolytic solution behavior, it was readily apparent that it could not describe the behavior of strong electrolytes satisfactorily. The calculation of the electrical work of separating ions in solution was the object of several attempts to account for the various properties of strong electrolytes (19,20,21,22,23,24,25,26,27) and led to the general acceptance of the hypothesis of complete dissociation. In 1912 Milner (28, 29) analyzed the problem mathematically and was able to show the correct concentration dependence of the activity coefficient in dilute solutions. The complexity of Milner's treatment precluded its application to the derivation of expressions for related thermodynamic properties.

The first successful solution to this problem was obtained by Debye and Hückel in 1923 (1). These workers developed an interionic attraction theory from which they were able to derive an expression for the excess free energy of an electrolytic solution. In their treatment the excess free energy of an electrolytic solution was defined as that free energy resulting from the electrostatic interactions of the ions.

The primary problem confronting Debye and Hückel was that of deriving an expression for the average electrostatic potential about any given ion in an electrolytic solution. The basic assumptions which were made to simplify the problem are listed as follows:

1. Strong electrolytes are completely dissociated into spherical unpolarizable ions having a mean distance of closest approach.
2. All deviations from ideality are caused by the electrostatic interactions of the ions.
3. The ions move in a continuous medium of uniform dielectric constant. For dilute aqueous solutions the dielectric constant of pure water is used.
4. In the absence of external fields the distribution of ions about any given ion is spherically symmetric. In order to satisfy the condition of electrical neutrality each ion, on a time average basis, is surrounded by an excess of oppositely charged ions which constitute an ionic atmosphere of equal and opposite charge. This time average distribution is assumed to be described by the Boltzmann distribution function

$$n_i' = n_i \exp\left[\frac{-z_i \varepsilon \psi_j}{kT}\right] \qquad (2.1)$$

where n_i' is the number of ions of type i per unit volume at a point j in the solution, the quantity $z_i \epsilon \psi_j$ is the electrical potential energy of an i ion, having a charge $z_i \epsilon$, at point j at which the electrostatic potential is ψ_j, and n_i is the average number of i ions per unit volume of solution.

5. The average electrostatic potential of an i ion at any point j in the solution can be determined using the Poisson equation, which relates the electrostatic potential to the charge density $\rho_j(r)$.

$$\nabla^2 \psi_j(r) = -\frac{4\pi}{D} \rho_j(r) \qquad (2.2)$$

Since $\rho_j(r)$ is directly proportional to the Boltzmann distribution function given by Equation 2.1, Equation 2.2 is in violation of the principle of linear superposition of fields. In order to circumvent this problem Debye and Hückel considered only dilute solutions where it is valid to approximate Equation 2.1 by the truncated series expansion given in Equation 2.3.

$$n_i \exp\left[\frac{-z_i \epsilon \psi_j}{kT}\right] = n_i\left(1 - \left[\frac{z_i \epsilon \psi_j}{kT}\right]\right) \qquad (2.3)$$

Using these assumptions Debye and Hückel derived an expression for the average potential, actually the potential of average force, at any given point in the solution. The work required to charge an ion from zero to $z_i \epsilon$ in the field of the average electrostatic potential was then calculated and equated with the excess free energy of the solution per mole of solute. The expression obtained by Debye and Hückel is given in Equation 2.4.

$$\Delta\bar{F}^{ex} = \nu NkT \ln(f_\pm) = -\sum_i \frac{\nu_i z_i^2 \epsilon^2 N K \tau}{3D} \qquad (2.4)$$

Equations 2.5 and 2.6 define the functions τ and K.

$$K = \left(\sum_i \nu_i z_i^2\right)^{1/2} \left[\frac{4\pi N \epsilon^2}{1000\ DkT}\right]^{1/2} c^{1/2} \qquad (2.5)$$

$$\tau = \frac{3}{(Ka^o)^3} \left[\frac{1}{2}(Ka^o)^2 - Ka^o + \ln(1 + Ka^o)\right] \qquad (2.6)$$

The symbols contained in the previous equations pertain to the following quantities:

$\Delta\bar{F}^{ex}$	excess molar free energy of the solute
ν	total number of ions into which one molecule of solute dissociates
N	Avogadro's number
k	Boltzmann's constant
T	absolute temperature
$f_\pm$	mean rational ionic activity coefficient

ν_i	number of ions of charge $z_i\,\varepsilon$ obtained from the dissociation of one molecule of solute
ε	fundamental electronic charge
D	dielectric constant of the pure solvent
c	molar concentration of the solute
a^o	mean distance of closest approach of the ions

The excess molar enthalpy of dilution is obtained by substituting Equation 2.4 into the Gibbs-Helmholtz equation given below.

$$\frac{\partial}{\partial T}\left[\frac{\Delta\overline{F}}{T}\right] = -\frac{\Delta\overline{H}}{T^2} \tag{2.7}$$

Since $\Delta\overline{H}$ represents the relative molar enthalpy of dilution with respect to infinite dilution it can be equated with the relative apparent molal heat content ϕ_L. Thus we have the expressions

$$\phi_L = -T^2\frac{\partial}{\partial T}\left[\frac{\Delta\overline{F}^{ex}}{T}\right] \tag{2.8}$$

and

$$\phi_L = -T^2\frac{\partial}{\partial T}\left[\frac{-N\varepsilon^2}{3}\sum_i \nu_i z_i^2\,\frac{\tau K}{DT}\right] \tag{2.9}$$

to represent the excess molar enthalpy of dilution. The differentiation indicated in Equation 2.9 has been carried out by Owen and Brinkley (30) and was corrected later by Swanson (31). The expression obtained for ϕ_L is given in Equation 2.10,

$$\phi_L = -A\left[\frac{1}{1 + Ka^{o}}\left(\frac{1}{T} + \frac{\partial \ln D}{\partial T}\right) + \frac{\sigma\alpha}{3}\right] c^{1/2}$$

$$+ A\left[\sigma - \frac{1}{1 + Ka^{o}}\right]\left[\frac{\partial \ln(a^{o})}{\partial T}\right] c^{1/2} \tag{2.10}$$

in which α is the thermal expansibility of the solvent and the functions σ and A are as defined below.

$$A = \frac{NT\varepsilon^2}{2D}\left[\frac{4\pi N\varepsilon^2}{1000\ DkT}\right]^{1/2}\left[\sum_i \nu_i z_i^2\right]^{3/2} \tag{2.11}$$

$$\sigma = \frac{\partial(\tau Ka^{o})}{\partial Ka^{o}} = \frac{3}{(Ka^{o})^3}\left[1 + Ka^{o} - \frac{1}{1 + Ka^{o}} - 2\ln(1 + Ka^{o})\right] \tag{2.12}$$

In the limit of infinite dilution the functions τ, σ, and Ka^{o} approach values of 1, 1, and 0, respectively. Substitution of these values into Equation 2.10 yields the limiting form of the concentration dependence of the enthalpy of dilution.

$$\phi_L = -A\left[\frac{\partial \ln D}{\partial T} + \frac{1}{T} + \frac{\alpha}{3}\right] c^{1/2} \tag{2.13}$$

This equation can be expressed in terms of molality by employing the following conversion

$$m = \frac{c}{d_o}\left[1 - \left[\frac{c\ \phi_V}{1000}\right]\right]^{-1} \tag{2.14}$$

where d_o is the density of pure water and ϕ_V is the apparent molal volume of the solution. This equation simplifies to the following form as the concentration approaches zero.

$$m = \frac{c}{d_o} \tag{2.15}$$

Substitution of Equation 2.15 into Equation 2.13 yields the limiting law expression for the relative apparent molal heat content as a function of molality.

$$\phi_L = A_H m^{1/2} \tag{2.16}$$

The term A_H is defined as

$$A_H = -A(d_o)^{1/2} \left[\frac{\partial \ln D}{\partial T} + \frac{1}{T} + \frac{\alpha}{3}\right] \tag{2.17}$$

and has been calculated by Harned and Owen (32) to be 6925 for an aqueous 3-1 electrolyte at 25° C. using the dielectric constant data of Wyman and Ingalls (33) and the density of water data tabulated in the "International Critical Tables" (34). Since the first term contained in the brackets of Equation 2.17 is negative and only slightly larger in magnitude than the sum of the two remaining positive terms, the calculated value of A_H is quite sensitive to uncertainties in these terms.

The validity of the Debye-Hückel limiting law equations as infinite dilution is approached has been well established by critical examinations of the statistical mechanical basis of the theory carried out by Kramers (35), Fowler (36), Onsager (37), Kirkwood (38), Fowler and Guggenheim (39), and Kirkwood and Poirier (40).

In general, attempts to extend the theory to more concentrated solutions have been of two types. Those of the first type have been concerned with the electrostatic effects of higher terms in the Poisson-Boltzmann equation. Calculations of this type were undertaken by Gronwall *et al.* (41), LaMer *et al.* (42), and Guggenheim (43). The retention of higher terms of the Poisson-Boltzmann equation, however, leads to inconsistencies in the theory as pointed out by Fowler and Guggenheim (39).

The second general method of attack on this problem is exemplified by the attempts of several workers to extend the theory by inclusion of parameters which are intended to take into account effects such as hydration of the ions and incomplete dissociation of the solute at higher concentrations. Work in this area has been carried out by Hückel (44), Scatchard (45), Robinson and Stokes (46), Eigen and Wicke (47, 48), and Glueckauf (49). Although their treatments have led to expressions which, in many cases, are capable of representing activity and osmotic coefficient data to moderate concentrations, the calculation of related thermodynamic properties from these expressions would, at best, be qualitative in nature due to the lack of knowledge of the temperature and pressure dependences of the various parameters. A striking example of this appears in Equation 2.10 in which the temperature dependence of a^o is unknown and is, therefore, either assumed to be zero or used as an empirical parameter to fit experimental data.

Bjerrum (50) proposed an association theory which predicted the existence of ion pairs in solution under certain conditions using a simple coulombic potential function. This theory was extended to include the formation of triple ions and the interaction of two ion pairs to form quadruple ions by Fuoss and Kraus (51, 52). The effects of ion pair interactions were also considered by Mayer (53) who applied his cluster theory of imperfect gases (54) to ionic solutions. Poirier (55) obtained expressions for the thermodynamic properties of solutions using Mayer's results.

Recently Glueckauf (56) has derived equations which describe the behavior of activity coefficient and osmotic coefficient data up to moderate concentrations using the results of Kirkwood (38).

The treatises of Harned and Owen (32) and Robinson and Stokes (57) on electrolytic solution chemistry include comprehensive accounts of the Debye-Hückel theory and its various extensions.

Although the Debye-Hückel theory adequately describes electrolytic solution behavior as infinite dilution is approached, it is evident that development of a theory for concentrated solutions will be dependent upon the successful determination of the effects of such factors as solvent structure, ion-solvent interaction, and short range repulsive forces between ions.

III. THERMODYNAMICS

A thermodynamic property is defined as a thermodynamic function having an exact differential. The line integral of an exact differential depends only upon the limits of the integration irrespective of the path over which the integration is carried out. The value of a thermodynamic property is therefore determined solely by the state of the system. Energy, pressure, and volume are typical thermodynamic properties.

The first law of thermodynamics relates the change in the internal energy of a system, ΔE, to the amount of heat Q absorbed by, and the amount of work W done on, the system.

$$\Delta E = Q + W \tag{3.1}$$

The quantities Q and W, as defined above, are designated as positive quantities in accordance with usual convention. The energy change associated with a process which takes place in the absence of any external fields and involves only mechanical work can be expressed by Equation 3.2,

$$\Delta E = Q - \Delta(PV) \tag{3.2}$$

where P and V represent the pressure and volume of the system, respectively. Since E, P, and V are thermodynamic functions which depend only on the state of the system, the heat absorbed by the system under the conditions just described must also be dependent only upon the particular state of the system. This absorbed heat is thus a thermodynamic property and is called the enthalpy H.

$$H = E + PV \tag{3.3}$$

$$\Delta H = \Delta E + \Delta(PV) \tag{3.4}$$

The change in enthalpy for an isobaric process is given by Equation 3.5 which is of particular use to thermochemists since many experiments are carried out under constant pressure.

$$\Delta H = \Delta E + P\Delta V \tag{3.5}$$

Thermodynamic properties are classified as extensive or intensive functions. Extensive properties, such as volume and energy, are dependent upon the mass of the system while intensive properties, such as temperature and pressure, are independent of the mass of the system. An extensive thermodynamic function is more precisely defined as a homogeneous function of first degree with respect to the number of moles of material present in the system. Consider the extensive function G defined by Equation 3.6.

$$G = f\,(T, P, n_1, n_2, \ldots, n_j) \tag{3.6}$$

By the above definition, increasing the number of moles of each component of a system by some constant factor k would increase the value of the extensive function G by the same factor.

$$kG = f\ (T,\ P,\ kn_1,\ kn_2,\ \ldots,\ kn_j) \tag{3.7}$$

For many applications of thermodynamics to chemical and physical problems it is convenient to employ partial molal quantities. The partial molal properties are derived from the application of Euler's theorem to homogeneous thermodynamic functions. Equation 3.8 expresses Euler's theorem for the homogeneous extensive function G,

$$G = \sum_i n_i \left(\frac{\partial G}{\partial n_i}\right)_{T,\ P,\ n_j} \tag{3.8}$$

where the subscripts T, P, and n_j imply that these variables are held constant during the differentiation. The partial molal G of component i at constant temperature and pressure, $\bar{G}_i$, is defined by Equation 3.9.

$$\bar{G}_i = \left(\frac{\partial G}{\partial n_i}\right)_{T,\ P,\ n_j} \tag{3.9}$$

Physically, $\bar{G}_i$ can be pictured as the total change in G upon addition of one mole of component i to an infinite amount of the system.

This research involved the measurement of the heat absorbed or evolved upon dilution of a rare earth nitrate or perchlorate solution or upon solution of a hydrated crystal of one of these rare earth salts. All experiments involved two-component rare earth salt-water systems and were conducted at constant temperature and pressure. Under these conditions the measured heats were enthalpies.

The partial molal enthalpy, or partial molal heat content, $\overline{H}_i$, of component i in a system is defined in Equation 3.10.

$$\overline{H}_i = \left(\frac{\partial H}{\partial n_i}\right)_{T,\ P,\ n_j} \tag{3.10}$$

Throughout this work i = 1 refers to the solvent and i = 2 refers to the solute. At constant temperature and pressure the total enthalpy of the system can be expressed as,

$$H^i = n_1\overline{H}_1 + n_2\overline{H}_2 \tag{3.11}$$

where superscript i refers to the state of the system. The quantities $\overline{H}_1$ and $\overline{H}_2$ represent the partial molal heat contents of water and rare earth nitrate or perchlorate, respectively.

Unlike the volume of a solution, no absolute value can be determined for the enthalpy of a solution. It is thus necessary to choose some standard or reference state for the system under study and to calculate the difference between the enthalpies of the system in its present and standard states. Solution thermodynamic functions are usually expressed with respect to the solvent standard state of pure solvent and with respect to the hypothetical one-molal ideal solute standard state. The partial molal heat content of the solute in this hypothetical standard state is the same as the partial molal heat content of the solute in an infinitely dilute solution. For this reason it is convenient to use the infinitely dilute solution as a reference state for the partial molal heat content of the solute. The enthalpy of a two-component system in its standard state is expressed by Equation 3.12 as

$$H^o = n_1\overline{H}_1^o + n_2\overline{H}_2^o \qquad (3.12)$$

where $\overline{H}_1^o$ is the partial molal heat content of pure water and $\overline{H}_2^o$ is the partial molal heat content of rare earth nitrate or perchlorate in an infinitely dilute solution.

The total enthalpy of the solution in state i, with respect to its standard state enthalpy, is called the relative total enthalpy L^i.

$$L^i = H^i - H^o \qquad (3.13)$$

The relative total enthalpy is expressed in terms of the two components of the solution in Equation 3.14.

$$L^i = n_1(\overline{H}_1^i - \overline{H}_1^o) + n_2(\overline{H}_2^i - \overline{H}_2^o) \qquad (3.14)$$

Since L^i is an extensive property, inspection of Equations

3.8, 3.10, and 3.14 leads to the equation,

$$L^i = n_1\overline{L}_1^i + n_2\overline{L}_2^i \qquad (3.15)$$

where $\overline{L}_1^i$ and $\overline{L}_2^i$ are the relative partial molal heat contents of the solvent and solute in the solution in state i, respectively.

It is convenient for carrying out calculations from experimental data to define an apparent molal quantity ϕ_G.

$$\phi_G^i = \frac{G^i - n_1\overline{G}_1^o}{n_2} \qquad (3.16)$$

The relative apparent molal heat content ϕ_L, in state i, is defined as

$$\phi_L^i = \frac{L^i - n_1\overline{L}_1^o}{n_2} \qquad (3.17)$$

It is obvious that $\overline{L}_1^o$, the relative partial molal heat content of the pure solvent in the state of the pure solvent, is identically zero by inspection of its definition.

$$\overline{L}_1^o = \overline{H}_1^o - \overline{H}_1^o \qquad (3.18)$$

Combination of Equations 3.15 and 3.17 leads to the following expression for the relative apparent molal heat content of a system in state i.

$$n_2\phi_L^i = L^i = n_1\overline{L}_1^i + n_2\overline{L}_2^i \qquad (3.19)$$

Differentiation of Equation 3.19 with respect to n_2 yields $\overline{L}_2$ in the form

$$\overline{L}_2 = \left(\frac{\partial L}{\partial n_2}\right)_{T,\ P,\ n_1} = n_2 \left(\frac{\partial \phi_L}{\partial n_2}\right)_{T,\ P,\ n_1} + \phi_L \tag{3.20}$$

which, when substituted back into Equation 3.19, leads to an expression for $\overline{L}_1$.

$$\overline{L}_1 = \frac{-\,n_2^2}{n_1} \left(\frac{\partial \phi_L}{\partial n_2}\right)_{T,\ P,\ n_1} \tag{3.21}$$

Equations 3.20 and 3.21 are the fundamental equations upon which calorimetric determinations of $\overline{L}_1$ and $\overline{L}_2$ are based. In the preceding section the theoretical concentration dependence of ϕ_L was predicted to be a function of the square root of the molality. The concentration scale used throughout this work was molality. In order to transform Equations 3.20 and 3.21 into forms which are more amenable to the experimental data, the following conversion factors are employed,

$$n_2 = m \tag{3.22}$$

$$n_1 = \frac{1000}{M_1} \tag{3.23}$$

where m is the molality and M_1 is the molecular weight of water. Substitution of these quantities into Equations 3.20 and 3.21 leads to the following expressions for the relative partial molal heat contents in terms of the square root of the molality.

$$\bar{L}_2 = \frac{m^{1/2}}{2} \left(\frac{\partial \phi_L}{\partial m^{1/2}}\right)_{T,\ P,\ n_1} + \phi_L \tag{3.24}$$

$$\bar{L}_1 = \frac{-\ m^{3/2}}{2000} \left(\frac{\partial \phi_L}{\partial m^{1/2}}\right)_{T,\ P,\ n_1} \cdot \ M_1 \tag{3.25}$$

All calculations of $\bar{L}_1$ and $\bar{L}_2$ made during the course of this research were based on Equations 3.24 and 3.25.

Consider the dilution of a solution containing n_1 moles of water and n_2 moles of rare earth nitrate or perchlorate into n_1^* moles of pure water. The relative heat content of the solution before the dilution is

$$L^i = n_1\bar{L}_1^i + n_2\bar{L}_2^i + n_1^*\bar{L}_1^o \tag{3.26}$$

and the relative heat content of the solution after the dilution is

$$L^f = (n_1 + n_1^*)\ \bar{L}_1^f + n_2\bar{L}_2^f \tag{3.27}$$

The difference between the relative heat contents of the initial and final states of the solution is the enthalpy of dilution.

$$\Delta H_{Dil.} = L^f - L^i = (n_1 + n_1^*)\ \bar{L}_1^f + n_2\bar{L}_2^f - n_1\bar{L}_1^i - n_2\bar{L}_2^i \tag{3.28}$$

The relative apparent molal heat contents of the initial and final states of the solution may be related to the enthalpy of dilution using Equation 3.19.

$$\Delta H_{Dil.} = n_2\phi_L^f - n_2\phi_L^i \qquad (3.29)$$

From Equation 3.29 it is evident that knowledge of the heat of dilution and the relative apparent molal heat content of one of the two states will enable the relative apparent molal heat content of the other state to be calculated. Assuming that ϕ_L^f is known, the corresponding value for the initial solution may be calculated by Equation 3.30,

$$\phi_L^i = \phi_L^f - \Delta H_D \qquad (3.30)$$

in which ΔH_D is the enthalpy of dilution per mole of solute. The value of ϕ_L at infinite dilution is zero. If the heat of dilution is measured for very dilute solutions, an extrapolation function can be found which will enable values of the relative apparent molal heat contents to be determined. The particular procedure used in this research is discussed in a later section.

Consider the dissolution of n_2 moles of a crystalline rare earth nitrate or perchlorate hydrate into n_1 moles of pure water. The relative enthalpy of the system before the dissolution is given by

$$L^i = n_1\bar{L}_1^o + n_2\bar{L}^{\cdot} \qquad (3.31)$$

where $\overline{L}^{\bullet}$ is the relative molar enthalpy of the pure hydrate. The relative enthalpy of the system after the dissolution is given by

$$L^f = (n_1 + n_1')\overline{L}_1^f + n_2\overline{L}_2^f \tag{3.32}$$

where n_1' is the number of moles of water present in n_2 moles of hydrate crystals. The difference between the relative enthalpies of the initial and final states is the enthalpy of solution to the final state.

$$\Delta H_{sol.} = L^f - L^i = (n_1 + n_1')\overline{L}_1^f + n_2\overline{L}_2^f - n_2\overline{L}^{\bullet} \tag{3.33}$$

The enthalpy of solution can be related to the relative apparent molal heat content of the final solution by Equation 3.34.

$$\Delta H_{sol.} = n_2\phi_L^f - n_2\overline{L}^{\bullet} \tag{3.34}$$

The enthalpy of solution per mole of hydrate crystal is

$$\Delta H_S = \phi_L^f - \overline{L}^{\bullet} \tag{3.35}$$

All values of $\overline{L}^{\bullet}$ determined in this work were calculated by combining the relative apparent molal heat content data from the dilution studies with the measured enthalpies of solution using Equation 3.35.

The excess partial molal free energy of the solute is defined as

$$\bar{F}_2^{ex} = \nu RT\ln(\gamma_\pm) \qquad (3.36)$$

in which ν, R, T, and $\gamma_\pm$ represent the number of ions per molecule of solute, the universal gas constant, the absolute temperature, and the mean molal activity coefficient, respectively. Since the mean molal activity coefficient equals unity at infinite dilution and at the hypothetical standard state, the infinitely dilute solution can be used as a reference state for values of $\bar{F}_2^{ex}$. If $\gamma_\pm$ is known as a function of concentration, values of the excess partial molal free energy of the solute can be calculated using Equation 3.36 and combined with the experimentally determined relative partial molal heat contents to yield values of the relative partial molal excess entropy of the solute.

$$\bar{F}_2^{ex} - \bar{F}_2^{ex,o} = \bar{H}_2 - \bar{H}_2^o - T(\bar{S}_2 - \bar{S}_2^o) \qquad (3.37)$$

Since $\gamma_\pm$ is unity at infinite dilution, it is readily apparent that the value of $\bar{F}_2^{ex,o}$ is zero by inspection of Equation 3.36. Substitution of Equation 3.36 and the definition of $\bar{L}_2$ into Equation 3.37 and rearranging yields the following equation.

$$T(\bar{S}_2 - \bar{S}_2^o) = \bar{L}_2 - \nu RT\ln(\gamma_\pm) \qquad (3.38)$$

Equation 3.38 was used for all calculations of $T(\bar{S}_2 - \bar{S}_2^o)$ made during the course of this research.

The usefulness of excess functions is twofold. First, experimental data are used to calculate derived quantities relative to a physically meaningful state (infinite dilution). Second, the problem of handling free energy and entropy functions which approach minus and plus infinity, respectively, as the concentration approaches zero is avoided.

The partial molal free energy of the solvent is given by Equation 3.39,

$$\bar{F}_1 = RT \ln \left[\frac{a_1}{N_1}\right] \tag{3.39}$$

where a_1 is the activity of water and

$$N_1 = \frac{55.51}{55.51 + \nu m} \tag{3.40}$$

The N_1 term takes account of the ideal free energy of mixing. Values of the partial molal entropy of the solvent were calculated using Equation 3.41.

$$T(\bar{S}_1 - \bar{S}_1^o) = \bar{L}_1 - RT \ln \left[\frac{a_1}{N_1}\right] \tag{3.41}$$

IV. EXPERIMENTAL APPARATUS

The differential adiabatic solution calorimeter used throughout this work was built by Naumann (58) following the design of an apparatus described by Gucker, Pickard, and Planck (59). Several modifications have since been made by Eberts (60), Csejka (61), DeKock (3), and Pepple (10).

A schematic diagram of the calorimeter is given in Figure 1. Figures 2 and 3 are schematic diagrams of the electrical circuits. Reference to the figures will be designated (i-X) where i refers to the figure and X to the alphabetically labeled parts.

The calorimetric apparatus was located in a room thermostated between 23.5 and 25.0° C.

A double-walled 22-gallon water bath was insulated with three inches of exploded mica between its inner and outer walls. This bath served as an adiabatic medium for the calorimeter. The bath contained copper cooling coils (1-A) and an auxiliary 500-watt Calrod heater. The insulated water bath lid rested 54 inches above the floor on a sturdy angle-iron frame. The water bath was mounted on a movable angle-iron platform and could be raised to the level of the water bath lid by means of a hydraulic bumper jack.

A 100 gallon per minute centrifugal stirrer circulated the water in the water bath. A copper baffle was soldered to the inside of the bath directly across from the stirrer in order to reduce thermal gradients.

The adiabatic temperature control system employed a 500-watt Calrod heater which was mounted on the bath lid. The heater leads passed through the lid, and the heater encircled the adiabatic heat shield (1-B).

The adiabatic heat shield, which served as a submarine jacket, surrounded the calorimeter containers and shielded them from the relatively large temperature oscillations of the water bath. The submarine walls were constructed of 1/8-inch monel sheet and the bottom was constructed of 1/4-inch monel plate. A horizontal cross section of the submarine would have parallel sides and semicircular ends. The submarine was attached to its lid by means of 20 machine screws countersunk in a 1/4-inch by 1/4-inch inconel strip which was welded to the upper inside edge of the submarine wall. A water-tight seal between the submarine and its lid was provided by an 1/8-inch rubber O-ring which rested on this strip inside the screws.

The 1/4-inch monel plate submarine lid was suspended eight inches below the water bath lid with eight brass tubes which housed the stirrer shafts, sample holder rods, and electrical leads from the calorimeter containers.

The calorimeter container lids were constructed from 30-mil tantalum sheet and were suspended from the submarine lid by two thin-walled stainless steel tubes (1-H). Each lid contained a heater well (1-D), and three holes for the control thermel (1-G), stirrer shaft (1-E), and sample holder rod (1-F).

The cylindrical calorimeter containers (1-C) were constructed from 15-mil tantalum. The containers were four inches in diameter and six inches deep. A rectangular well was welded into the side of each calorimeter container to hold the main thermopile (1-J). A 1/4-inch rim extended outward horizontally from the top of each calorimeter container. Eight machine screws were threaded, from beneath, through a brass ring located immediately below the container rim. A similar brass ring rested on top of the container lid. A container was attached to its lid by passing the screws through matching holes in the container rim, container lid, and second brass ring and bolting the system together. A thin coat of Apiezon L grease was put on the container rims before assembly to insure a vapor tight seal.

The heater well in each container lid held two heaters, a 99 ohm heater to supply heat for calorimeter measurements and a 1.5 ohm trickle heater to compensate for temperature drifts in the containers. The calorimeter heaters were made from noninductively wound 38 B and S gauge manganin wire, and the trickle heaters were made from 30 B and S gauge manganin wire. The wire was wound around a thin mica strip, annealed, and inserted into the heater wells. The free volume in the heater wells was filled with melted paraffin wax to increase heat conduction from the heaters.

All heater leads were made from 30 B and S gauge copper wire. Potential leads of 36 B and S gauge copper wire were soldered to the midpoints of the calorimeter heater leads.

The leads from each heater well were connected to a six conductor shielded cable at a teflon junction block (1-K) attached to the underside of the submarine lid. The calorimeter heater circuit is shown in Figure 2 and the trickle heater circuit in Figure 3. Two Leeds and Northrup 12-position silver contact rotary switches (2-C, 2-D) regulate the calorimeter heater circuit. Switch 2-C was wired so that the potential drop across either heater, across both heaters in series, across the standard resistor (2-E), or across a dummy heater (2-F) could be measured. Switch 2-D was wired so that current could be passed through either heater, through both heaters in series, or through a dummy heater. When switch 2-D was set to allow current to pass through either heater, or through both heaters in series, an electronic timer was engaged.

Low discharge lead storage batteries provided the current sources for the calorimeter heaters. The following arrangements were used: two two-volt batteries in parallel (2-V_1, 2-V_2); two six-volt batteries in parallel (2-V_3, 2-V_4); and five six-volt batteries (2-V_3, 2-V_4, 2-V_5, 2-V_6, 2-V_7)

connected to give a twelve-volt working potential. An A.C. source was used to bring the calorimeter containers to operating temperature and was disconnected at all other times.

The resistance of each calorimeter heater was determined by measuring the potential drop across the heater and across the standard resistor while the same current was flowing through each. The resistance of the heaters remained constant within 0.006 percent throughout the course of this work.

The potentiometer (2-I) was a Leeds and Northrup Type K-2. The standard resistor and standard cell had been calibrated by the National Bureau of Standards and were constant to within a few parts per one hundred thousand.

The electronic timer (2-G) used a 5-megacycle quartz crystal frequency standard whose output was divided down to 1000 cycles per second by a series of flip-flop frequency dividers. The time interval between turning a heater on and off was displayed on the timer to 0.001 second.

The liquid in the calorimeters was mixed by stirrers (1-E) which consisted of the following three parts: a lower section of tantalum rod, an upper section of stainless steel rod, and a one inch length of nylon spacer connecting the other two sections. Each stirrer was mounted so that the nylon spacer was immediately below the lower stirrer shaft bearing. Two New Departure number 77R4A sealed bearings were used for each stirrer shaft, one mounted immediately above the submarine lid and the other mounted just above the water bath lid.

A 325 rpm synchronous motor (1-M), mounted above the water bath lid, drove the stirrers by means of a pulley assembly using an O-ring as a drive belt.

The samples were contained in thin-walled annealed pyrex bulbs. The approximately spherical bulbs ranged in volume from 4 milliliters to 20 milliliters. The sample bulbs were held by their necks in a stainless steel support which could hold one or two sample bulbs depending upon bulb size.

The sample holder rods (1-F) extended above the bath lid so that the samples could be positioned over the sample breakers (1-N) when the calorimeter was assembled. Each sample holder rod consisted of three parts: a tantalum rod to which the sample holder was attached, a stainless steel rod extending above the bath lid, and a one inch length of stainless steel tube connecting the two rods.

The sample breakers were constructed from a 2-1/4 inch length of 1/4-inch tantalum tube which was flattened at the upper end and cut to form a point. A sample bulb was broken by manually lowering the sample holder rod toward the breaker which was cemented to the bottom of the container with melted Apiezon W wax.

Adiabatic control of the bath was maintained by monitoring the difference in temperature between the water bath and calorimeter containers with two 5-junction copper-constantan thermels (2-J, 2-J'). One end of each control thermopile was held by a copper tube (1-L) which extended into the water bath from the submarine lid. The other end of each control thermopile was held by a 1/4-inch tantalum tube welded into each calorimeter container lid (1-G). Melted paraffin wax was used to fill any remaining space in the two thermopile tubes.

The control thermels were made from 36 B and S gauge copper wire and 30 B and S gauge constantan wire. The 36 B and S gauge copper leads extending from the control thermels were connected to a teflon junction block mounted to the underside of the submarine lid. A shielded four-conductor cable carried the control thermel signals from the junction block to a Leeds and Northrup 12-position silver contact rotary switch (2-K). This switch was wired so that either thermel signal, both thermel signals in series, or the two signals in opposition could be sent to the bath controller (2-L). Since the maximum possible signal was desired the thermels were switched in series. From this switch the signal was passed through an Ayrton shunt (2-M) to the automatic bath controller. The bath controller amplified the signal from the thermels approximately 10^6 times and fed the output to a Thyratron relay switch which operated the bath control heater. The 500-watt Calrod bath heater was connected in series with a Variac (2-P) to control the heating rate.

By proper adjustment of the heating and cooling rates alternate heating and cooling periods of 15 to 30 seconds each were attained with a temperature oscillation in the water bath of $\pm$ 0.0005° C.

The temperature of the water bath was read to a hundredth of a degree from a mercury thermometer which was calibrated over the operating temperature range with an NBS platinum resistance thermometer in conjunction with a Leeds and Northrup Model G-2 Mueller Temperature Bridge.

The temperature difference between the calorimeter containers was detected with the main thermopile (1-J). The main thermopile consisted of two 30-junction thermopiles (3-U, 3-U') made from 36 B and S gauge copper wire and 30 B and S gauge constantan wire with 36 B and S gauge copper leads. Each half of the main thermopile was constructed over a thin 7 centimeter by 12 centimeter mica sheet. The two 30-junction thermopiles were separated with a thin mica sheet and placed in a copper casing which fit snugly into the thermopile wells in the calorimeter containers. The empty space was filled with melted paraffin wax.

The thermopile leads were connected to the teflon junction block described earlier. The thermopile signals were carried through four-conductor shielded cable to a Leeds and Northrup 12-position rotary silver contact switch (3-V) wired so that the signals could be passed individually, in series, or in opposition. From this switch the signal was fed to a Liston Becker Model 14 breaker type D.C. amplifier (3-W). The amplifier output was passed through a Liston Becker filter circuit (3-X) to reduce the noise level and displayed on a 60 millivolt Brown recording potentiometer (3-Y). A Stabiline type IE-5101 voltage regulator (3-Z) provided the constant power supply for the amplifier and recorder.

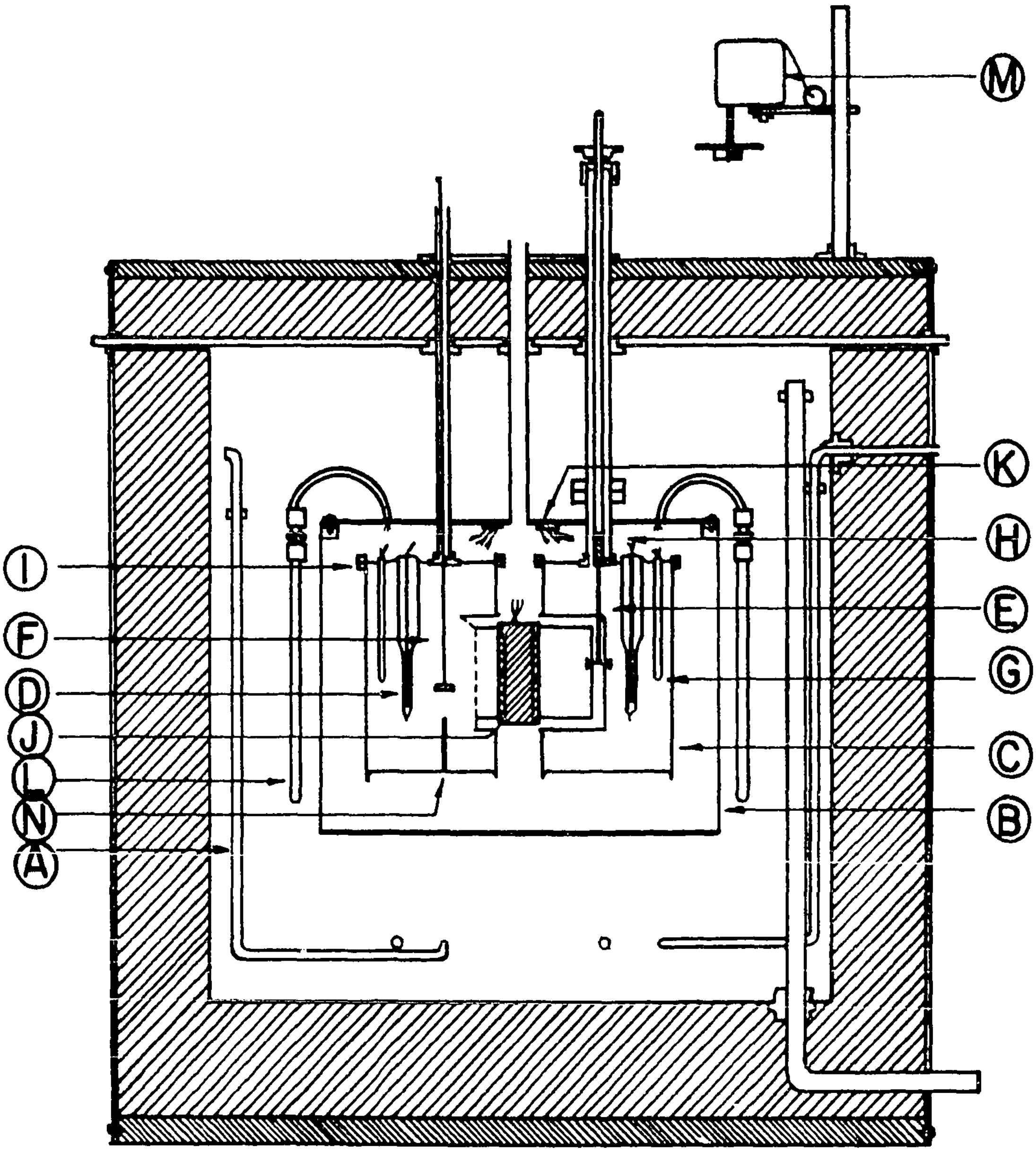

Figure 1. Adiabatic differential calorimeter

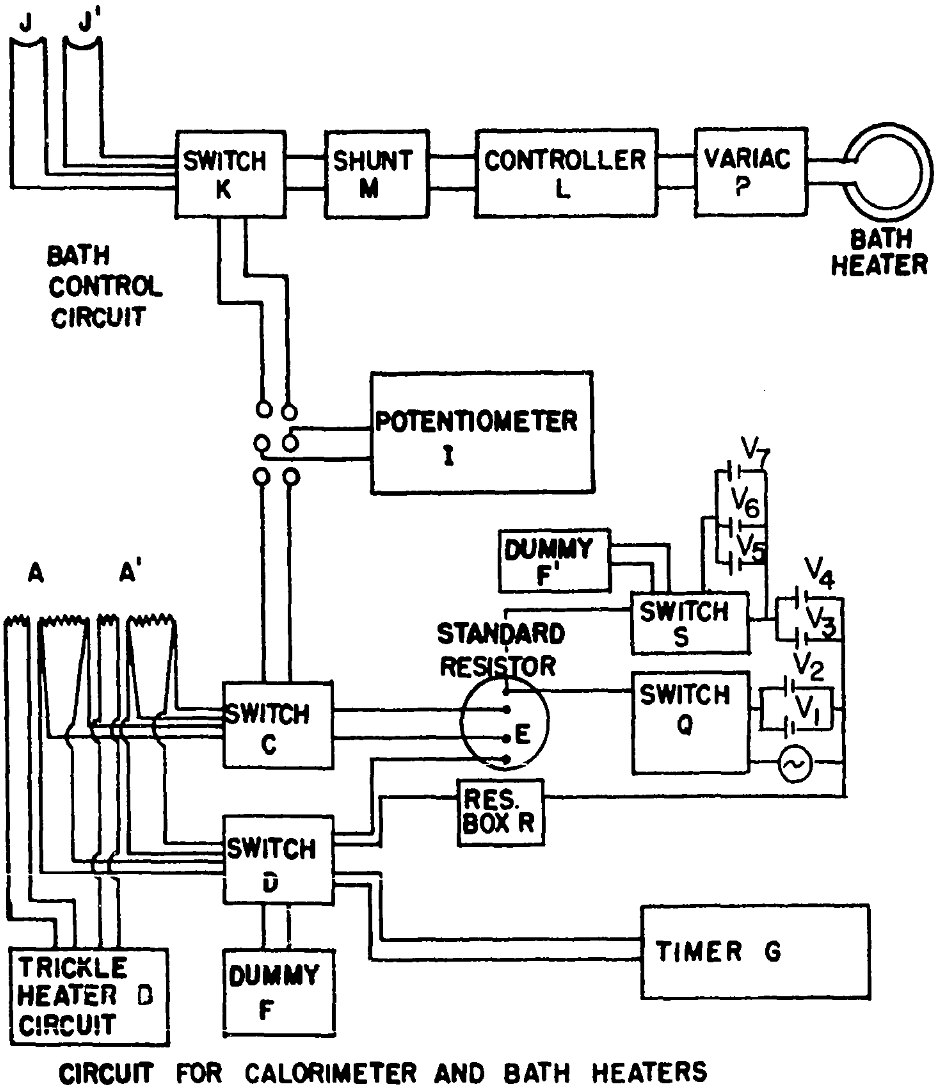

Figure 2. Schematic diagram of calorimeter heater circuit

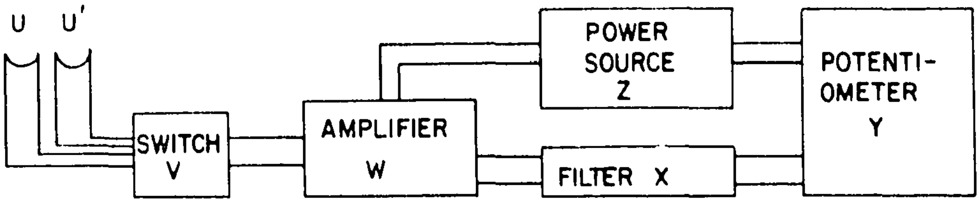

CIRCUIT FOR MAIN THERMEL

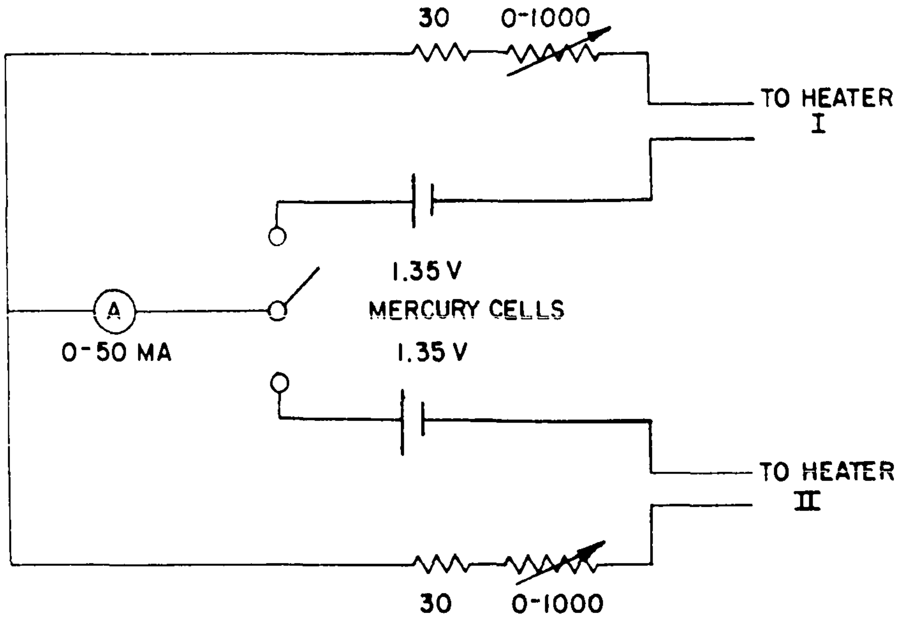

CURRENT SOURCE FOR TRICKLE HEATERS

Figure 3. Schematic diagrams of the thermopile and trickle heater circuits

V. SOLUTION PREPARATION

A stock solution of rare earth nitrate or perchlorate was prepared by dissolving an excess of the spectrographically pure rare earth oxide in the appropriate C.P. grade acid. The undissolved oxide was removed by filtering the hot solution through a sintered glass funnel. In order to remove the colloidal hydrolisis products present in the solution, a determination of the equivalence pH for the hydrolisis equilibrium represented by Equation 5.1 was made.

$$R^{3+} + H_2O \; = \; ROH^{2+} + H^+ \qquad (5.1)$$

Samples of the stock solution were titrated with a dilute solution of the appropriate acid on a Sargent Model D recording titrator. The equivalence pH of the solution was determined from the recorded pH versus titrant volume curves. The stock solution was adjusted to the equivalence pH and was heated to facilitate the reaction of the acid with the colloidal species. The solution was then repeatedly adjusted to the equivalence pH and heated until further heating did not change the room temperature pH of the solution. The stock solution was placed in a well stoppered Pyrex flask.

Dilutions were made by addition of weighed amounts of stock solution and freshly prepared conductivity water. The conductivity water, which had a specific conductance of less than 1 x 10^{-6} mho per centimeter, was prepared by distilling tap distilled water from an alkaline potassium permanganate solution. The dilutions were made at intervals of 0.1 in square root of molality over the concentration range from one-hundredth molal to saturation.

Saturated solutions of the nitrates and perchlorates were prepared by desiccating a portion of the stock solution over magnesium perchlorate until crystals began to form. The solution and crystals were transferred to a well stoppered Pyrex flask and placed in a water bath controlled at $25.00 \pm 0.01^\circ$ C. The solution was allowed to equilibrate for at least two weeks before samples of the saturated solution were drawn off with a pipette.

The rare earth concentrations of the stock and saturated solutions were determined by one or more of the following three methods:

1. Oxide analysis. Samples of rare earth salt solution were weighed into ceramic crucibles, the rare earth was precipitated with a 20 percent excess of twice recrystallized oxalic acid, and the precipitate was dried under infrared lamps and ignited to the oxide at 900° C in a muffle furnace. The samples were weighed as anhydrous rare earth oxides. The samples were then repeatedly heated and weighed until constant weight was obtained.

2. Sulfate analysis. Samples of rare earth salt solution were weighed into ceramic crucibles, the rare earth was

precipitated with an excess of one molar sulfuric acid, and the excess acid was removed as sulfur trioxide by heating with a Meeker burner. The samples were ignited in a muffle furnace at 550° C and were weighed as anhydrous rare earth sulfates. The samples were then repeatedly heated and weighed until constant weight was achieved.

3. EDTA analysis. Samples of rare earth salt solution were weighed into flasks, buffered to pH 5, and the rare earth was titrated with EDTA using xylenol orange as indicator and pyridine as an endpoint sharpener. The EDTA solution was standardized versus a zinc chloride solution prepared by weight from electrolytically prepared zinc metal. A second standard for the EDTA titration method was a gadolinium nitrate solution prepared by dissolving a weighed amount of pure gadolinium metal in the stoichiometric amount of nitric acid.

All analyses were performed in triplicate with a precision of ± 0.05 percent. Analyses made by different methods typically agreed within ± 0.1 percent. All weights determined in the course of this research were corrected to vacuum.

The concentrations of saturated $La(NO_3)_3$, $Gd(NO_3)_3$, $La(ClO_4)_3$, $Nd(ClO_4)_3$, and $Gd(ClO_4)_3$ were taken from the data of Walters (11).

Hydrated crystals of $La(NO_3)_3$, $Nd(NO_3)_3$, $Gd(NO_3)_3$, $Ho(NO_3)_3$, $Er(NO_3)_3$, $Lu(NO_3)_3$, $La(ClO_4)_3$, $Nd(ClO_4)_3$, and $Gd(ClO_4)_3$ were grown from their respective saturated solutions, dried over magnesium perchlorate, ground, and analyzed by EDTA titration to determine when the excess water was removed. The crystals of the rare earth hydrates were removed from the desiccant when an EDTA analysis indicated the rare earth composition to be within 0.1 percent of its theoretical composition. The crystals were never dehydrated below their theoretical water composition. The rare earth nitrate hydrates of lanthanum, neodymium, gadolinium, holmium, and erbium were hexahydrates. Lutetium nitrate formed a pentahydrate. The perchlorate crystals obtained for lanthanum, neodymium, and gadolinium contained eight waters of hydration per rare earth ion. The crystals grown for erbium perchlorate analyzed as having slightly less than eight waters of hydration which leads one to suspect the presence of more than one type of hydrate.

An attempt to grow a single type of hydrate was made by growing crystals from solutions containing an excess of perchloric acid. The mixture of rare earth perchlorate, perchloric acid, and water chosen to grow the hydrate was estimated from the solubility study of the $Ce(ClO_4)_3$-$HClO_4$-H_2O system carried out by Zinov'ev and Shchirova (62). The ratio of $Er(ClO_4)_3$-$HClO_4$-H_2O, in percent by weight, in the mixture was 35.2:24.7:35.2. The crystals grown from this mixture were washed with chloroform and dried under vacuum. The crystals were analyzed as previously described. Erbium perchlorate formed the octahydrate.

VI. EXPERIMENTAL PROCEDURE

All heat of dilution and heat of solution experiments were carried out at 25.00 ± 0.01° C by the following procedure.

All samples were introduced into the sample bulbs with either a stainless steel tipped syringe or a glass pipette. Teflon plugs were placed over the sample bulb necks while weighings were made. After the samples were weighed the sample bulbs were sealed with melted Apiezon W wax. Considerable care was exercised while handling the sample bulbs in order to prevent solution from sloshing up into the bulb neck. Solution lodged in a bulb neck and separated from the rest of the sample solution would not undergo dilution when the bulb was broken.

Samples of the hydrated crystals were transferred to the sample bulbs with only a brief exposure to the atmosphere. A small glass tube with one end drawn out was quickly filled with the crystals, inserted into a sample bulb neck, and the salt was tapped into the bulb. The sample bulbs were weighed and sealed in the same manner as described previously.

On the day of a run conductivity water was weighed into the calorimeter containers, subject to the condition that the total weight of conductivity water and samples equal approximately 900 grams, and the apparatus was assembled. Room temperature was always below 25° C and consequently the following steps always involved heating the water bath and calorimeter containers to the operating temperature. Immediately after assembly either the containers or the water bath, whichever was the cooler, was heated to within 0.001° C of the other and the adiabatic temperature control was switched on. The bath and calorimeter containers were then heated simultaneously to 24.9° C. An A.C. current source, in series, was used to heat the calorimeter containers during this step. The temperature differential between the calorimeter containers was then reduced to less than 0.0001° C. The temperature of the entire system was raised to 24.95° C using the regular calorimeter heater current sources and the auxiliary bath heater. Final adjustments were made in the heating and cooling rates and the system was allowed to equilibrate for two to three hours. At the end of this time near-equilibrium was established as evidenced by a constant-slope trace of the main thermopile e.m.f. signal.

The first heat to be carried out was the determination of the heat capacity ratio of the calorimeter containers. Before each heat made during the course of this research, the current was stabilized by passing it through a dummy resistance box set at the resistance of the heater to be used. The calorimeter heaters were switched in series and 30 calories were added to each container using the 12-volt current source. A difference in heat capacity between the two containers would cause an unequal temperature rise and was detected as a displacement of the recorder trace. The heat capacity ratio, which was used as a multiplicative correction to chemical heats, was calculated from this displacement.

The operation of differential calorimeters depends on the balancing of chemical heat in one container with electrical heat in the other container. It is therefore necessary to know the relative rise in temperature of one container with respect to the other upon addition of equal amounts of heat to each container. The heat capacity ratio determined during each run rarely differed from unity by more than 0.05 percent.

Two chart calibrations were made after the heat capacity determination. Unless an adjustment was made in the system between two heats the afterslope of the previous heat was also the foreslope of the following heat. The chart calibrations determined the sensitivity of the main thermopile in terms of calories per millimeter recorder chart displacement. Most of the experiments were carried out at a setting on the Liston Becker amplifier of gain 19, which corresponded to a sensitivity of approximately 4.0×10^{-4} calories per millimeter of displacement. On gain 19 a full chart displacement corresponded to a temperature change of about 0.0001° C or to about 0.1 calories of heat. The 2-volt current source with resistance from a variable resistance box switched in series with the heater generated approximately 0.04 calories for each calibration heat. The amplifier gain was set at 20 for measurements made on dilute solutions involving very small heat changes. The thermopile sensitivity at this setting was about 2.5 x 10^{-4} calories per millimeter chart displacement.

The samples were run last. A dilution or solution experiment was carried out by switching the appropriate current source into the calorimeter heater in one container, reading the potential drop across the standard resistor and, halfway through the heating period, breaking the sample bulb in the other container. Electrical heat was supplied to the same container in which the sample was dissolved in the case of endothermic heats of solution. In cases where large heats of dilution or solution were involved, adiabatic conditions were maintained during the heating period by manually regulating the auxiliary water bath heater. The electrical heat required to balance a heat of dilution experiment could usually be estimated to within a few percent. Within 10 to 15 minutes of a break a smaller heat, with the 2-volt current source, could be estimated closely enough to bring the two containers to within 0.0001° C of each other.

Since the heating rate of electrical heaters is linearly dependent on time while chemical heat is an exponential function of time, the sample bulbs were broken halfway through the heating period to minimize the heat leak between the calorimeter containers. Heating periods for dilution and solution experiments rarely exceeded 90 seconds.

The electrical heat generated in a calorimeter container was calculated according to Equation 6.1, where R_H is the resistance of the heater, R_S the resistance of the standard resistor, E_S the potential drop across the standard resistor, t the time in seconds, and 4.184 the joulecalorie conversion constant.

$$q_{el.} = \frac{R_H(E_S)^2 t}{4.184\ (R_S)^2} \tag{6.1}$$

The heat evolved or absorbed during a sample break was calculated by making the following four corrections to the electrical heat.

The equilibrium vapor pressure of water above a rare earth salt solution decreases as the concentration of the solution increases. Consequently, water evaporates into the free volume of the sample bulb when a break is made. The importance of this effect increases with the concentration of the sample solution. The evaporation correction, although negligible for the lowest experimental concentrations, amounted to as much as 0.09 calories for a few concentrated solutions. The correction was estimated according to Equations 6.2 and 6.3,

$$q_{evap.} = \frac{273}{298}\ \frac{\Delta P}{760}\ \frac{V}{22400}\ 10514 \text{ calories} \tag{6.2}$$

$$q_{evap.} = 0.000566V\Delta P \text{ calories} \tag{6.3}$$

where V is the free volume in milliliters of the sample bulb, ΔP is the difference in millimeters mercury between the vapor pressure over the sample solution and over pure water, and 10514 is the latent heat of vaporization of water according to Rossini (63). The evaporation is endothermic.

The breaking of a sample bulb is accompanied by the evolution of a small amount of heat. A correction for this effect, though usually small enough to be within the limits of accuracy of the measurements, was applied to all experimental determinations. The extremely thin-walled sample bulbs would deform elastically when pressed against a small postal scale platform. The bulbs were separated into groups according to the observed scale reading at which deformation began. The heats of breaking of bulbs from each group were measured and the results are given by Equation 6.4 where S is the magnitude of the scale reading in ounces.

$$q_{open} = 0.00080 \text{ S calories} \tag{6.4}$$

Due to the extremely small heats of opening involved a 50 percent uncertainty is estimated for the heats of opening calculated using Equation 6.4. All but a very few of the sample bulbs used throughout this work began to deform at readings of two ounces or less.

The chemical heat associated with a sample break was rarely exactly balanced with electrical heat. The correction for the amount by which the electrical heat exceeded or fell short of the chemical heat was based on the distance of separation, measured at the point of the break, between the foreslope and afterslope. The chart correction was calculated by multiplying this distance of separation by the sensitivity determined from the calibration experiments.

The last correction to be considered is the heat capacity correction. This correction is applied in the following manner. Consider an experiment in which chemical heat is evolved in container I and is balanced by electrical heat in container II. The corrected heat evolved in container I is given by Equation 6.5, where C_I/C_{II} is the ratio of the heat capacity of container I plus contents to that of container II plus contents.

$$q_I = \frac{C_I}{C_{II}} q_{II} \tag{6.5}$$

This correction was applied only to the sum of the electrical heat plus the chart correction. If electrical heat was added to the container in which the sample break occurred no heat capacity correction was necessary.

The chemical heat evolved due to the dilution or solution of a sample is given by Equation 6.6,

$$q_{dil.} = C'(q_{el.} \pm q_{chart}) + q_{evap.} - q_{open} \tag{6.6}$$

where the various quantities are identified by their subscripts, and C' refers to the heat capacity ratio. The chemical heat absorbed due to the endothermic dissolution of a sample is given by Equation 6.7.

$$q_{sol.} = q_{el.} \pm q_{chart} - q_{evap.} + q_{open} \qquad (6.7)$$

The operation of the calorimeter was tested by measuring the enthalpy of neutralization of hydrochloric acid with sodium hydroxide. The neutralization of HCl was chosen as a test reaction because it was well-characterized and could be carried out in almost exactly the same manner as a dilution experiment.

The hydrochloric acid was made up to a concentration of 0.15857 molal by a co-worker by weight dilution from constant boiling hydrochloric acid according to the procedure of Foulk and Hollingsworth (64). Standardization versus potassium hydrogen phthalate indicated an acid concentration of 0.15846 molal. The acid was reanalyzed during this research. The mean value obtained from triplicate analyses was 0.15849 molal with a precision of 0.03 percent. Samples of the acid were introduced into the sample bulbs, weighed, and sealed as described previously.

Carbonate free concentrated sodium hydroxide was prepared by a standard method (65).

Conductivity water was weighed into the calorimeter containers and, immediately prior to attaching the containers to their lids, enough concentrated sodium hydroxide solution was pipetted into each container to give a carbonate free solution of 0.003 molal sodium hydroxide. This gave approximately a fourfold excess of base over acid in each calorimeter container which minimized the effects of any absorbed carbon dioxide in the solution on the heat of neutralization measurements.

Since the hydrochloric acid was the limiting reactant it was only necessary to know the concentration of the sodium hydroxide to within ten percent.

The neutralization reaction is given by Equations 6.8 and 6.9 where ΔH_N is the enthalpy of neutralization of the acid at an ionic strength (μ) of 0.003 and ΔH_N^o is the enthalpy of neutralization at zero ionic strength (infinite dilution).

$$\text{NaOH (0.003m)} + \text{HCl (0.003m)} = \text{NaCl (0.003m)} + H_2O \; ; \; \Delta H_N \qquad (6.8)$$

$$OH^-_{aq.} + H^+_{aq.} = H_2O \; ; \; \Delta H_N^o \qquad (6.9)$$

Equation 6.8 was obtained by combining Equations 6.10, 6.11, 6.12, and 6.13.

$$\text{4NaOH (0.003m)} + \text{HCl (0.1585m)} = \text{NaCl (0.00075m)} + H_2O + \text{3NaOH (0.00225m)}; \; \Delta H_{exp.} \qquad (6.10)$$

$$\text{3NaOH (0.003m)} = \text{3NaOH (0.00225m)}; \; \Delta H_I \qquad (6.11)$$

$$\text{NaCl } (0.003\text{m}) = \text{NaCl } (0.00075\text{m}) \; ; \Delta H_{II} \tag{6.12}$$

$$\text{HCl } (0.1585\text{m}) = \text{HCl } (0.003\text{m}) \; ; \Delta H_{III} \tag{6.13}$$

The heat of neutralization was calculated using Equation 6.14,

$$\Delta H_N = \Delta H_{exp.} - \Delta H_I - \Delta H_{II} - \Delta H_{III} \tag{6.14}$$

where the values of ΔH_I, ΔH_{II}, and ΔH_{III} were calculated using the relative apparent molal heat contents of NaOH, NaCl, and HCl taken from the literature (63, 66).

The heat of neutralization was corrected to infinite dilution using Equation 6.15.

$$\Delta H_N^o = \Delta H_N - \phi_L \text{ (NaCl, 0.003m)} + \phi_L \text{ (NaOH, 0.003m)} + \phi_L \text{ (HCl, 0.003m)} \tag{6.15}$$

A total of 15 samples were run. The average enthalpy of neutralization at 25° C was $\Delta H_N = -13364$ calories per mole with a mean deviation of 27 calories per mole. The average enthalpy of neutralization at infinite dilution was $\Delta H_N^o = -13339 \pm 27$ calories per mole. This result is in good agreement with the value obtained by Vanderzee and Swanson (66), and by Hale, Izatt, and Christensen (67) who both reported -13336 ± 18 calories per mole.

The experimental precision of these measurements was 0.2 percent. An additional uncertainty of 0.05 percent in the hydrochloric acid concentration would lead to a total uncertainty in ΔH_N^0 of 0.25 percent.

VII. TREATMENT OF DATA AND RESULTS

The heat of dilution experiments carried out during the course of this work were of two types: (1) dilution of a sample solution containing n_2 moles of solute into pure water with the evolution of q_1 calories of heat, and (2) dilution of a sample solution containing n_2' moles of solute into the solution resulting from the first type of dilution with the evolution of q_2 calories of heat. The integral heats of dilution of these two processes are given by Equations 7.1 and 7.2, where ΔH_{i-f} corresponds to the dilution of a sample from molality m_i to molality m_f.

$$\Delta H_{1-2} = q_1/n_2 \tag{7.1}$$

$$\Delta H_{1-3} = (q_1 + q_2)/(n_2 + n_2') \tag{7.2}$$

These integral heats of dilution are referred to as long chords since they correspond to dilutions which range from several hundredfold to nearly two thousandfold.

The heat evolved upon dilution of one mole of solute from molality m_3 to molality m_2 can be calculated by combining Equations 7.1 and 7.2 to get Equations 7.3. This process corresponds to a dilution of about

$$\Delta H_{3-2} = \Delta H_{1-2} - \Delta H_{1-3} \tag{7.3}$$

twofold and is referred to as a short chord. The short chords provide heat of dilution data in the concentration range from 0.0009 molal to approximately 0.007 molal.

As it was shown earlier, the relative apparent molal heat content is a function of the square root of molality as infinite dilution is approached. An appropriate extrapolation function for extrapolating the heat of dilution data to infinite dilution would therefore be the derivative of the relative apparent molal heat content with respect to the square root of molality. Since the limiting value of this derivative at infinite dilution has been theoretically evaluated, a comparison of the data obtained in this work with the theoretical value may be made. The extrapolation function used throughout this work is given by Equation 7.4.

$$\begin{aligned} \bar{P}_i &= -\Delta H_{3-2}/(m_3^{1/2} - m_2^{1/2}) \\ &= (\phi_{L(m_3)} - \phi_{L(m_2)})/(m_3^{1/2} - m_2^{1/2}) \qquad (7.4) \end{aligned}$$

The short chord method of Young and co-workers (14, 68, 69) was used for the extrapolations. In this method the slope, S, of the ϕ_L versus $m^{1/2}$ curve in very dilute solutions is represented by a power series in $m^{1/2}$. This is shown in Equation 7.5 where A is the limiting slope obtained at infinite dilution. The average value of the slope at

$$S = \frac{\partial \phi_L}{\partial m^{1/2}} = A + Bm^{1/2} + Cm \qquad (7.5)$$

the midpoint of a short chord, may be written as

$$\bar{P}_i = \frac{\int_{m_2^{1/2}}^{m_3^{1/2}} S dm^{1/2}}{m_3^{1/2} - m_2^{1/2}} \qquad (7.6)$$

where the midpoint of the chord is given by Equation 7.7.

$$\overline{m_f^{1/2}} = \frac{1}{2}(m_3^{1/2} + m_2^{1/2}) \qquad (7.7)$$

The $\bar{P}_i$ data for the nitrates and perchlorates studied in this work were represented by Equations 7.8 and 7.9, respectively. The

$$\bar{P}_i = A + Bm^{1/2} \qquad (7.8)$$

$$\bar{P}_i = A + Bm^{1/2} + Cm \qquad (7.9)$$

parameters in these equations were generated from a standard double-precision orthogenal polynomial least squares program run on an IBM 360 computer. The parameters occurring in polynomial expressions for ϕ_L, $\bar{L}_2$, and $\bar{L}_1$ were generated in the same manner.

The extrapolated values obtained for the A parameter for the nitrates were within experimental error of the theoretical value of 6925. Since the data indicated that the nitrates were approaching the Debye-Hückel limiting law slope, the $\overline{P}_1$ data were forced to this value and B was re-evaluated using the same least squares program described previously. A typical plot of the $\overline{P}_1$ data for the nitrates is shown in Figure 4 using the data obtained for $La(NO_3)_3$.

The limiting slopes obtained for the perchlorates using an equation of the form of Equation 7.8 did not approach the theoretical value in the case of the perchlorates. The $\overline{P}_1$ data were then fit to equations of the form of Equation 7.9. The limiting slopes obtained for $La(ClO_4)_3$ and $Nd(ClO_4)_3$ were still much lower than the Debye-Hückel value. In order to determine whether or not it would be justifiable to force the data to the Debye-Hückel limit inspite of this apparent deviation from theory, a second extrapolation of the data was made using an extrapolation function which recognized the dependence of ϕ_L on ion size. This second extrapolation function, designated $\overline{P}_1'$, included the average distance of closest approach of the ions, a^o, which should affect the perchlorates more than the nitrates due to the larger size of the former. Equation 7.10 defines $\overline{P}_1'$, where K and a^o are as defined previously. The value of K for a 3-1 electrolyte in water at 25^o C is 0.806 $m^{1/2}$ and a^o is expressed in angstroms. Using the a^o

$$\overline{P}_1' = (1 + K\,a^o)^2\,\overline{P}_1 = A' + 2B'\left[\frac{m^{1/2}}{1 + K\,a^o}\right] \qquad (7.10)$$

values obtained from activity coefficient and conductance data (70), limiting slopes were obtained which agreed within experimental error with the predicted value. Figure 5 shows the $\overline{P}_1'$ data of $La(ClC_4)_3$ using an a^0 parameter of 7.0. The agreement between A' and 6925 indicated that the $\overline{P}_1$ data of the rare earth perchlorates studied in this work could be forced to the limiting law value. The standard deviation of the fit obtained when the $\overline{P}_1$ data were represented by Equation 7.9 with A set equal to 6925 was approximately 50 percent lower than that obtained using Equation 7.10. The $\overline{P}_1$ data for the rare earth perchlorates were therefore fit to Equation 7.9 with A = 6925. The $\overline{P}_1$ data of $La(ClO_4)_3$ is shown in Figure 6. The dashed and solid curves represent the $\overline{P}_1$ data fit to Equations 7.8 and 7.9, respectively. The standard deviation of the fit was nearly the same for both curves.

The parameters in Equations 7.8 and 7.9 are listed in Tables 12 and 13, respectively. The relative apparent molal heat contents of solutions in the concentration range from which the $\overline{P}_1$ data were taken were calculated by substituting Equations 7.8 and 7.9 into Equation 7.11 and performing the integration. The relative apparent molal heat contents of the nitrates and perchlorates, in this concentration range, are calculated by Equations 7.12 and 7.13, respectively.

$$\phi_L(m) = \int_0^{m^{1/2}} \overline{P}_1 \, dm^{1/2} \qquad (7.11)$$

$$\phi_L(m) = Am^{1/2} + \frac{B}{2} m \qquad (7.12)$$

$$\phi_L(m) = Am^{1/2} + \frac{B}{2} m + \frac{C}{3} m^{3/2} \qquad (7.13)$$

The relative apparent molal heat contents of solutions above this concentration range were calculated using Equation 3.30. The ϕ_L values obtained for dilute solutions of $La(NO_3)_3$ and $La(ClO_4)_3$ are compared with data of other investigators (60, 71, 72) in Figures 7 and 8, respectively.

The heat of dilution data for the nitrates and perchlorates studied are presented in Tables 1 through 11. The column headings from left to right represent the following quantities: molality of the sample solution, the number of moles of solute contained in the sample, the square root of molality of the solution resulting from the dilution, the amount of heat evolved upon dilution, in calories, calculated using Equation 6.6, the integral heat of dilution in calories per mole of solute, $\overline{P}_1$, the relative apparent molal enthalpy of the final solution, in calories per mole, calculated from Equations 7.12 and 7.13, the relative apparent molal enthalpy of the sample solution in calories per mole of solute, and the average value of the relative apparent molal enthalpy of the sample solution in calories per mole of solute.

The integral heat of dilution of a sample solution diluted into a solution resulting from a previous dilution, for which no heat of dilution was measured, was calculated using Equation 7.14, where

$$\Delta H_{1-3} = \frac{q_2 - n_2(\phi_L(m_2) - \phi_L(m_3))}{n_2'} \qquad (7.14)$$

$\phi_L(m_2)$ and $\phi_L(m_3)$ are calculated using Equation 7.12 or 7.13.

The relative apparent molal heat contents were expressed as empirical least squares polynomial equations over three concentration ranges: (1) very dilute, (2) moderate, and (3) concentrated.

1. The dilute range pertained to solutions below 0.008 molal. The equations used to calculate ϕ_L in this region have already been discussed.

2. The moderate concentration range extended from zero molal to approximately 1.1 molal.

3. The concentrated range pertained to all solutions above 1.1 molal.

The ϕ_L values for the rare earth nitrate solutions in the moderate concentration range were fit to Equation 7.15 with an average standard deviation of less than 9 calories per mole.

$$\phi_L = am^{1/3} + bm^{1/2} + cm^{2/3} + dm + em^{4/3} + fm^{3/2} \qquad (7.15)$$

The ϕ_L data of the rare earth perchlorate solutions in the moderate concentration range were fit to Equation 7.16 with an average standard deviation of less than 8 calories per mole. Lanthanum perchlorate was the only salt requiring the last term in Equation 7.16.

$$\phi_L = Am^{1/3} + Bm^{1/2} + Cm^{2/3} + Dm + Em^{4/3} + Fm^{3/2} + Gm^2 \qquad (7.16)$$

The ϕ_L data of the rare earth nitrate solutions above 1.1 molal, excluding $Nd(NO_3)_3$, were fit to Equation 7.17. Equation 7.18 was used to represent the ϕ_L data of $Nd(NO_3)_3$ above 1.1 molal. The average standard deviation of the fit obtained for these two equations was less than 5 calories per mole.

$$\phi_L = a'm^{1/2} + b'm + c'm^{3/2} + d'm^2 + e'm^3 + f'm^4 \qquad (7.17)$$

$$\phi_L = a'' + b''m^{1/3} + c''m^{1/2} + d''m + e''m^{4/3} + f''m^{3/2} + g''m^2 + h''m^{5/2} \qquad (7.18)$$

The ϕ_L data of the rare earth perchlorate solutions above 1.1 molal were represented by Equation 7.19 with an average standard deviation of less than 12 calories per mole.

$$\phi_L = A' + B'm^{1/2} + C'm + D'm^{3/2} + E'm^2 + F'm^{5/2} \qquad (7.19)$$

The parameters for Equations 7.15, 7.17, and 7.18 are listed in Tables 14 and 15. The parameters appearing in Equations 7.16 and 7.19 are presented in Tables 20 and 21, respectively.

The purpose of representing the ϕ_L data by these polynomial equations was to enable the derivative of ϕ_L with respect to $m^{1/2}$ to be calculated and combined with the ϕ_L data to obtain expressions for $\bar{L}_1$ and $\bar{L}_2$. It is to be emphasized that the equations representing the ϕ_L data are strictly empirical and should not be used to calculate values of ϕ_L outside of the stated regions of validity. For certain concentration ranges the ϕ_L data were best described by empirical equations composed of a linear combination of power series in $m^{1/2}$ and $m^{1/3}$.

The mean average deviation of $\bar{\phi}_L(m_1)$, determined for the 241 sample solutions listed in Tables 1 through 11, was less than 3 calories per mole. The uncertainties in $\phi_L(m_f)$, $\phi_L(m_1)$, and ΔH_{1-f} were estimated by the method of propagation of precision indexes as described by Worthing and Geffner (73). This method enables the reliability of indirectly determined quantities to be evaluated. Consider the derived quantity

$$U = f(X_1, X_2, \ldots, X_n) \tag{7.20}$$

where X_1, X_2, ..., X_n represent the independent, directly measurable quantities from which U is derived. The probable error associated with the derived quantity is obtained from Equation 7.21, where P_U and P_{X_i} refer to the probable error associated with U and X_i, respectively.

$$P_U^2 = \sum_{i=1}^{i=n} \left(\frac{\partial U}{\partial X_i}\right)^2 P_{X_i}^2 \tag{7.21}$$

The values for ϕ_L were calculated using the following equations:

$$\phi_L(m_1) = \phi_L(m_f) - \Delta H_{1-f} \qquad (3.30)$$

$$\phi_L(m_f) = Am^{1/2} + \frac{B}{2}m \text{ (Nitrates)} \qquad (7.12)$$

$$\phi_L(m_f) = Am^{1/2} + \frac{B}{2}m + \frac{C}{3}m^{3/2} \text{ (Perchlorates)} \qquad (7.13)$$

$$\Delta H_{1-2} = \frac{q_1}{n_2} \qquad (7.1)$$

$$\Delta H_{1-3} = \frac{q_1 + q_2}{n_2 + n_2'} \qquad (7.2)$$

The equations used to calculate the probable errors in $\phi_L(m_f)$, $\phi_L(m_1)$, and ΔH_{1-f}, in that order, are given below.

$$P^2_{\phi_L(m_f)} = \left(\frac{\partial\phi_L(m_f)}{\partial A}\right)^2 P^2_A + \left(\frac{\partial\phi_L(m_f)}{\partial B}\right)^2 P^2_B + \left(\frac{\partial\phi_L(m_f)}{\partial C}\right)^2 P^2_C \qquad (7.22)$$

$$P^2_{\phi_L(m_1)} = \left(\frac{\partial\phi_L(m_1)}{\partial \Delta H_{1-f}}\right)^2 P^2_{\Delta H_{1-f}} + \left(\frac{\partial\phi_L(m_1)}{\partial\phi_L(m_f)}\right)^2 P^2_{\phi_L(m_f)} \qquad (7.23)$$

$$P^2_{\Delta H_{1-f}} = \left(\frac{\partial \Delta H_{1-f}}{\partial q}\right)^2 P^2_q + \left(\frac{\partial \Delta H_{1-f}}{\partial n_2}\right)^2 P^2_{n_2} \qquad (7.24)$$

Since the value of A in Equations 7.8 and 7.9 was set at the theoretical value of 6925, the uncertainties in $\phi_L(m_f)$ are contained only in the B and C terms. The first term of Equation 7.22 is, therefore, zero. The third term of this equation is also dropped in the case of the nitrates. The probable errors, calculated using Equations 7.22, 7.23, and 7.24, are listed for a number of sample solutions of $La(NO_3)_3$ and $La(ClO_4)_3$ in Tables 26 and 27, respectively.

Values of $\bar{L}_1$ and $\bar{L}_2$ were calculated for each salt solution studied during the course of this work by Equations 3.25 and 3.24. The polynomial expressions for ϕ_L were substituted into these equations in order to evaluate the derivative of ϕ_L with respect to $m^{1/2}$.

The equations obtained for $\bar{L}_2$ are of the same form as those representing ϕ_L over the corresponding concentration ranges. The values of $\bar{L}_2$ for the rare earth nitrates and perchlorates below 1.1 molal can be calculated using Equations 7.25 and 7.26. The parameters in these equations are listed in Tables 16 and 22, respectively.

$$\bar{L}_2 = a_1m^{1/3} + b_1m^{1/2} + c_1m^{2/3} + d_1m + e_1m^{4/3} + f_1m^{3/2} \tag{7.25}$$

$$\bar{L}_2 = A_1m^{1/3} + B_1m^{1/2} + C_1m^{2/3} + D_1m + E_1m^{4/3} + F_1m^{3/2} + G_1m^2 \tag{7.26}$$

The values of $\bar{L}_2$ for these solutions above 1.1 molal are calculated using Equations 7.27, 7.28, and 7.29. The parameters for these equations are given in Tables 17 and 23.

$$\overline{L}_2 = a_1' m^{1/2} + b_1' m + c_1' m^{3/2} + d_1' m^2 + e_1' m^3 + f_1' m^4$$

$$\text{(Nitrates-La, Gd, Ho, Er, Lu)} \qquad (7.27)$$

$$\overline{L}_2 = a_1'' + b_1'' m^{1/3} + c_1'' m^{1/2} + d_1'' m + e_1'' m^{4/3} + f_1'' m^{3/2}$$

$$+ \; g_1'' m^2 + h_1'' m^{5/2} \quad (\mathrm{Nd(NO_3)_3}) \qquad (7.28)$$

$$\overline{L}_2 = A_1' + B_1' m^{1/2} + C_1' m + D_1' m^{3/2} + E_1' m^2 + F_1' m^{5/2} \qquad (7.29)$$

The relative partial molal heat content of the solvent below 1.1 molal is given by Equations 7.30 and 7.31 for the nitrates and perchlorates, respectively. The parameters for these two equations are listed in Tables 18 and 24, respectively.

$$\overline{L}_1 = a_2 m^{4/3} + b_2 m^{3/2} + c_2 m^{5/3} + d_2 m^2 + e_2 m^{7/3} + f_2 m^{5/2} \qquad (7.30)$$

$$\overline{L}_1 = A_2 m^{4/3} + B_2 m^{3/2} + C_2 m^{5/3} + D_2 m^2 + E_2 m^{7/3}$$

$$+ \; F_2 m^{5/2} + G_2 m^3 \qquad (7.31)$$

The empirical expressions for $\overline{L}_1$ above 1.1 molal are given in Equations 7.32, 7.33, and 7.34 for $\mathrm{Nd(NO_3)_3}$, the other nitrates studied in this work, and the perchlorates, respectively. The parameters corresponding to these three equations are listed in Tables 19 and 25.

$$\overline{L}_1 = a_2'' m^{4/3} + b_2'' m^{3/2} + c_2'' m^2 + d_2'' m^{7/3} + e_2'' m^{5/2}$$

$$+ \; f_2'' m^3 + g_2'' m^{7/2} \qquad (7.32)$$

$$\bar{L}_1 = a_2'm^{3/2} + b_2'm^2 + c_2'm^{5/2} + d_2'm^3 + e_2'm^4 + f_2'm^5 \qquad (7.33)$$

$$\bar{L}_1 = A_2'm^{3/2} + B_2'm^2 + C_2'm^{5/2} + D_2'm^3 + E_2'm^{7/2} \qquad (7.34)$$

Values of $\bar{L}_1$ and $\bar{L}_2$, at given concentrations, are listed in Tables 28 through 31 for the six nitrates and five perchlorates studied in this research. Since $\bar{L}_1$ and $\bar{L}_2$ are functions of the derivative of ϕ_L with respect to square root of molality, the values of these two quantities calculated at about 1.1 molal are somewhat sensitive to which polynomial equation, that pertaining to solutions below 1.1 molal or that pertaining to solutions above 1.1 molal, is used for their calculation. For this reason, the values of $\bar{L}_1$ and $\bar{L}_2$ between 1.0 and 1.2 molal, used in constructing Figures 15 through 18, were averages of the values calculated using the polynomial equations corresponding to both concentration ranges.

It is difficult to estimate the uncertainties in quantities which are determined from the derivatives of least squares polynomial equations. It is unlikely, however, that an uncertainty greater than 1 percent can be associated with the values of $\bar{L}_1$ and $\bar{L}_2$ calculated from the derivatives of the ϕ_L polynomial equations, except in the neighborhood of the terminal concentrations of each concentration range to which the equations apply.

The partial molal excess entropy of the solute and solvent were calculated for solutions of $Er(NO_3)_3$, $Nd(ClO_4)_3$, $Gd(ClO_4)_3$, and $Lu(ClO_4)_3$. The values of $T(\bar{S}_2 - \bar{S}_2^o)$ and $T(\bar{S}_1 - \bar{S}_1^o)$ were calculated from Equations 3.38 and 3.41. These quantities were not calculated for the other salts studied in this work due to lack of activity coefficient data.

The activity coefficient data used to calculate the partial molal excess entropies were obtained from the osmotic coefficient studies of Weber[1] on the rare earth perchlorates, and of Petheram on the rare earth nitrates (74). The osmotic coefficient data of the latter worker were extended from 1.8 molal to saturation by means of a linear extrapolation. The use of a linear extrapolation seemed justifiable as the data from 0.6 molal to 1.8 molal could be fit to a straight line. The activity coefficients above 1.8 molal were calculated from the extrapolated osmotic coefficient "data" in the usual manner by Herman Weber. The osmotic coefficient data of $ErCl_3$ (74) and of the rare earth perchlorates[1] are linear within approximately 2 percent above 1.0 molal. For this reason the error introduced into the osmotic coefficients calculated for $Er(NO_3)_3$ solutions by the above method is estimated to be well within 10 percent. This error would not seriously effect the trends in the

---

[1] Weber, H. O., Ames Laboratory of the A.E.C., Ames, Iowa. Activity data of some rare earth perchlorate solutions at 25° C. Private communication. 1969.

calculated values of the partial molal excess entropies for this salt.

The values obtained for $T(\overline{S}_2 - \overline{S}_2^o)$ and $T(\overline{S}_1 - \overline{S}_1^o)$ for the above-mentioned rare earth salt solutions are listed in Tables 32 and 33, respectively. The number in parentheses immediately below the final value of $T(\overline{S}_2 - \overline{S}_2^o)$ and $T(\overline{S}_1 - \overline{S}_1^o)$ for each salt, in these two tables, is the molality of the saturated solution of that salt.

The integral heats of solution of $La(NO_3)_3 \cdot 6H_2O$, $Nd(NO_3)_3 \cdot 6H_2O$, $Gd(NO_3)_3 \cdot 6H_2O$, $Ho(NO_3)_3 \cdot 6H_2O$, $Er(NO_3)_3 \cdot 6H_2O$, $Lu(NO_3)_3 \cdot 5H_2O$, $La(ClO_4)_3 \cdot 8H_2O$, $Nd(ClO_4)_3 \cdot 8H_2O$, $Gd(ClO_4)_3 \cdot 8H_2O$, and $Er(ClO_4)_3 \cdot 8H_2O$ were measured as part of this research. The heats of solution were measured in the same manner as described previously for the heat of dilution experiments. In general, two samples of hydrate crystals were placed in each calorimeter container, the first being dissolved in pure water and the second sample being dissolved in the solution resulting from the dissolution of the first sample. These two processes are represented by the following equations:

$$n_2\ (RX_3 \cdot yH_2O) + xH_2O \;=\; n_2\ RX_3(m_2) \quad ; \quad q_{sol.} \qquad (7.35)$$

$$n_2\ RX_3(m_2) + n_2'\ (RX_3 \cdot yH_2O) \;=\; (n_2 + n_2')\ RX_3(m_3) \; ; \quad q'_{sol.} \qquad (7.36)$$

The integral heat of solution for the process represented by

Equation 7.35 is given by Equation 7.37, where $q_{sol.}$ is the heat evolved upon dissolution of the sample containing n_2 moles of hydrate. The integral

$$\Delta H_3 = \frac{q_{sol.}}{n_2} \tag{7.37}$$

heat of solution of n_2' moles of the hydrate, corresponding to the process designated by Equation 7.36, is given by Equation 7.38, where $q'_{sol.}$ calories of heat are evolved and values of $\phi_L(m_2)$ and $\phi_L(m_3)$ are taken from the heat of dilution data.

$$\Delta H_s = \frac{q'_{sol.} + n_2(\phi_L(m_2) - \phi_L(m_3))}{n_2'} \tag{7.38}$$

The integral heats of dilution were used to calculate the relative molal heat contents of the hydrated crystals using Equation 3.35. The heat of solution data of the nitrates and perchlorates, respectively, are listed in Tables 34 and 35, where $\overline{L}$ is the relative molar heat content of the rare earth nitrate or perchlorate hydrate and the remaining quantities are as previously defined.

The uncertainties in the heat of solution data are estimated to be ± 0.4 percent for the rare earth nitrates, and ± 0.05 percent for the rare earth perchlorates. These estimates include uncertainties in the composition of the hydrated crystals set at 0.1 and 0.2 percent for the nitrates and perchlorates, respectively. The higher uncertainty in composition of the perchlorate octahydrates is attributable to their very hygroscopic nature.

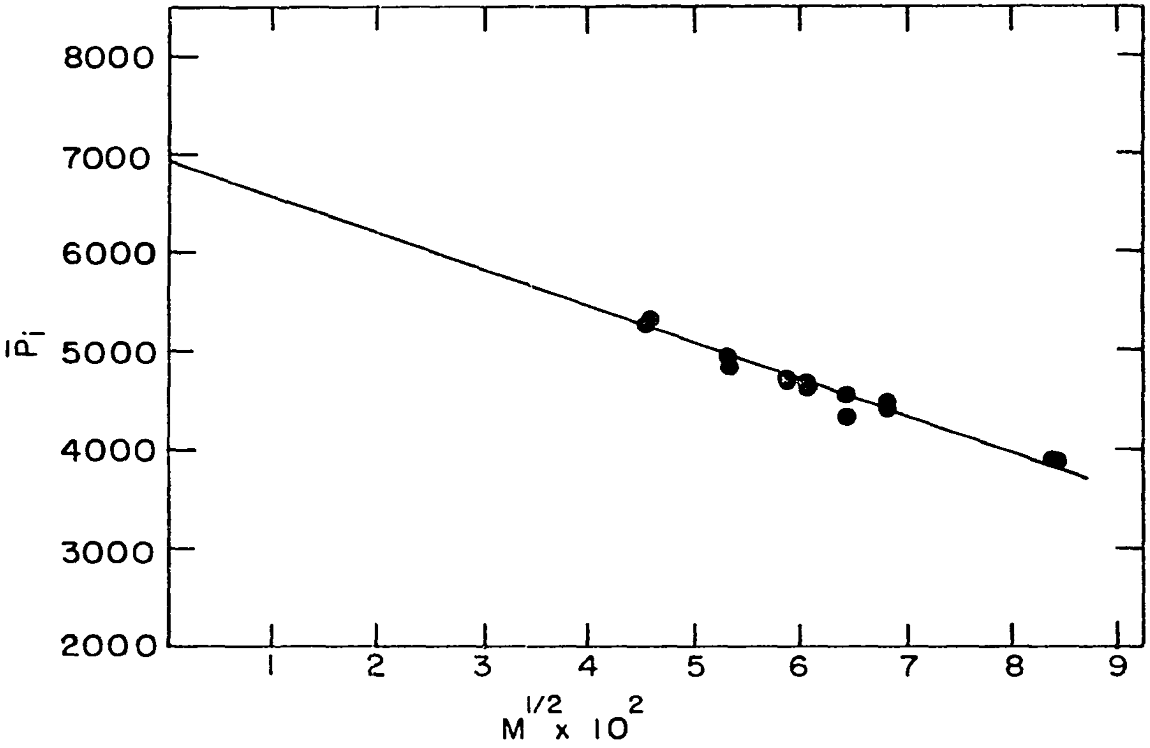

Figure 4. $\overline{P}_i$ versus $m^{1/2}$ for aqueous lanthanum nitrate solutions at 25° C

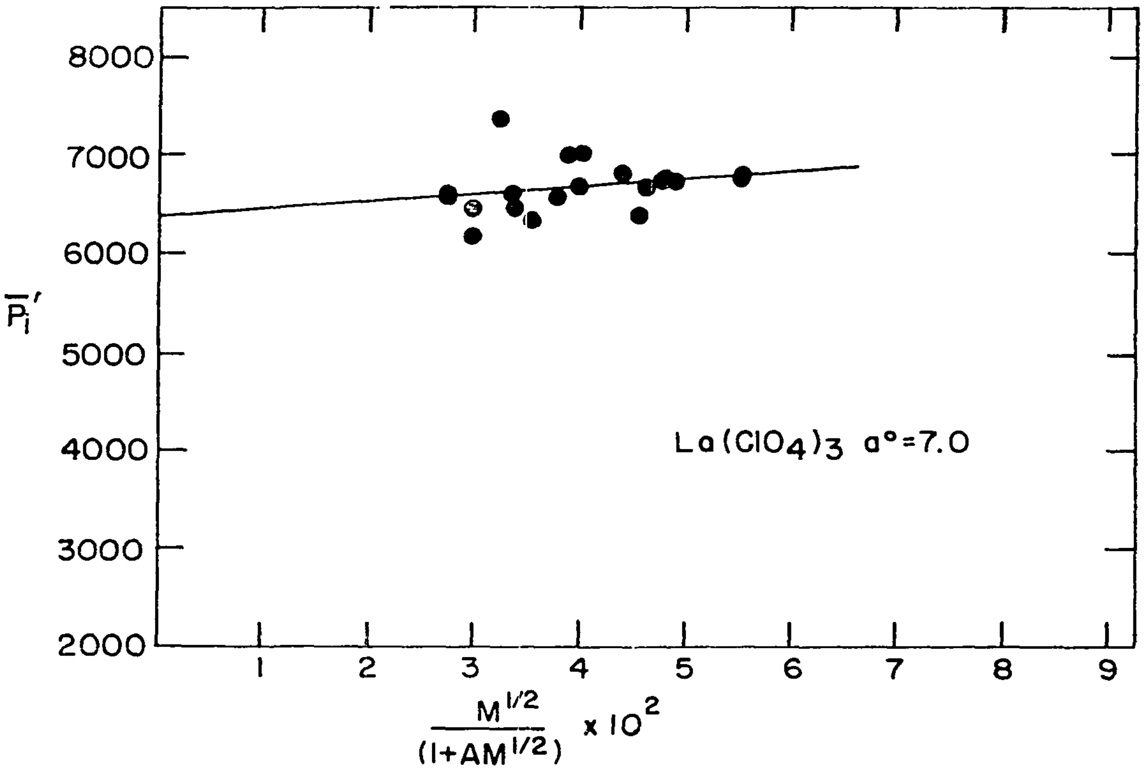

Figure 5. $\overline{P}_i'$ data of aqueous lanthanum perchlorate solutions at 25° C using $a^o = 7.0$

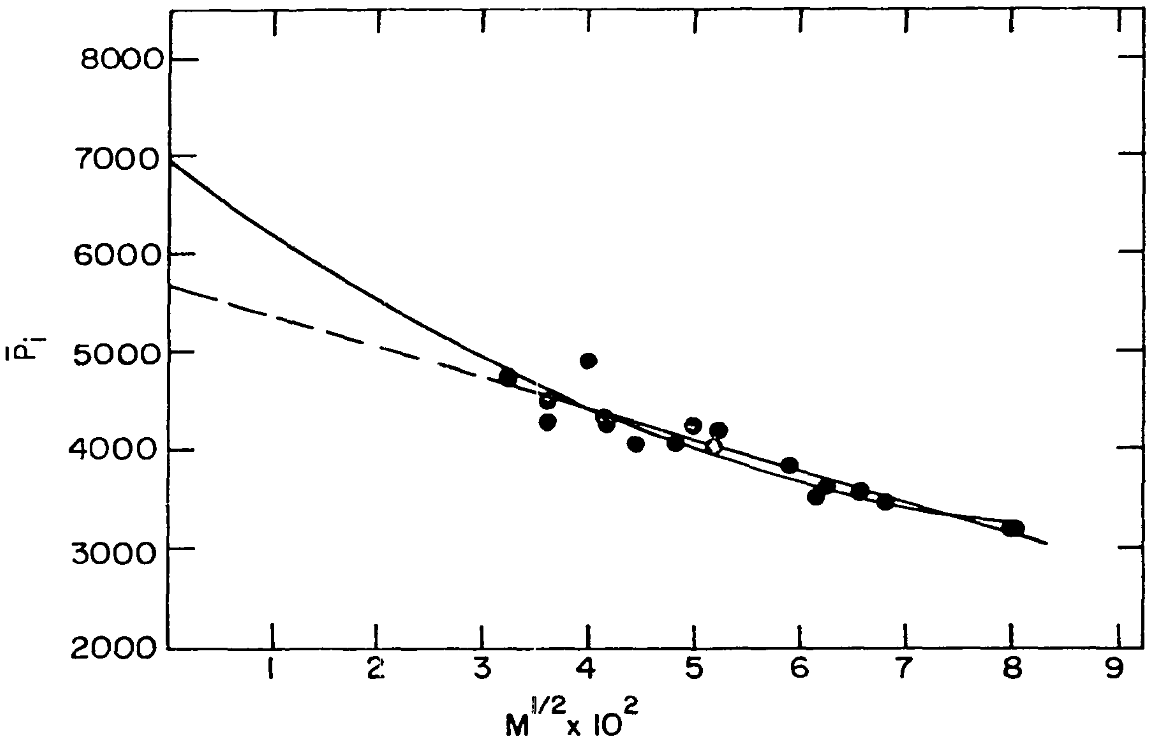

Figure 6. $\bar{P}_i$ versus $m^{1/2}$ for aqueous lanthanum perchlorate solutions at 25° C

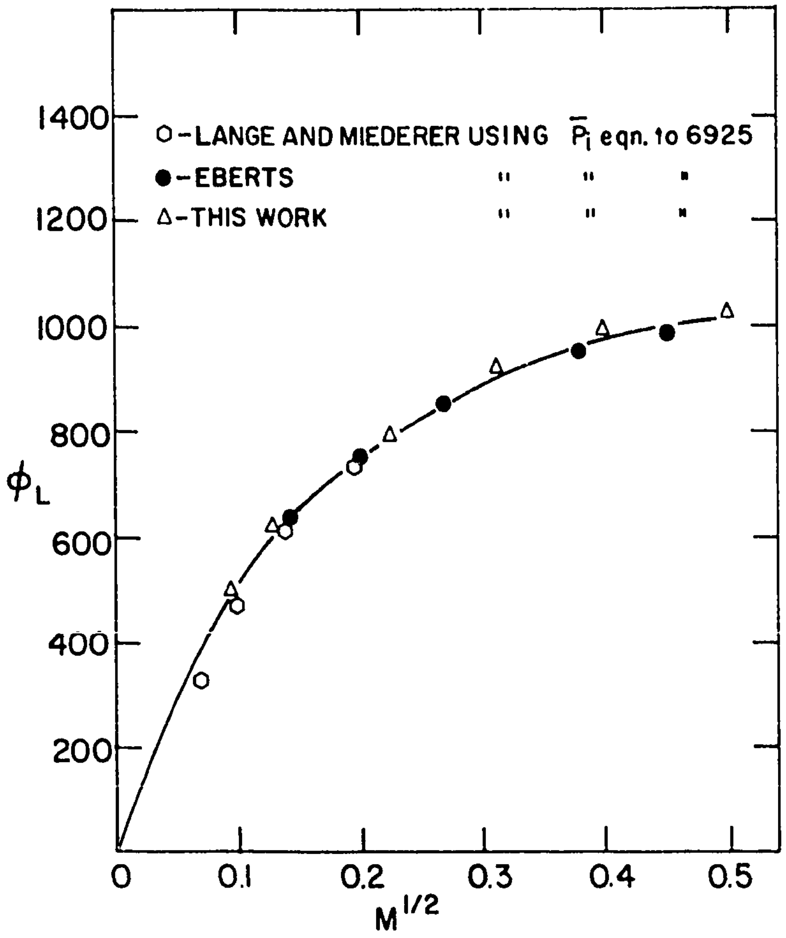

Figure 7. Comparison of the relative apparent molal heat contents of aqueous lanthanum nitrate solutions at 25° C using the Debye-Hückel limiting law

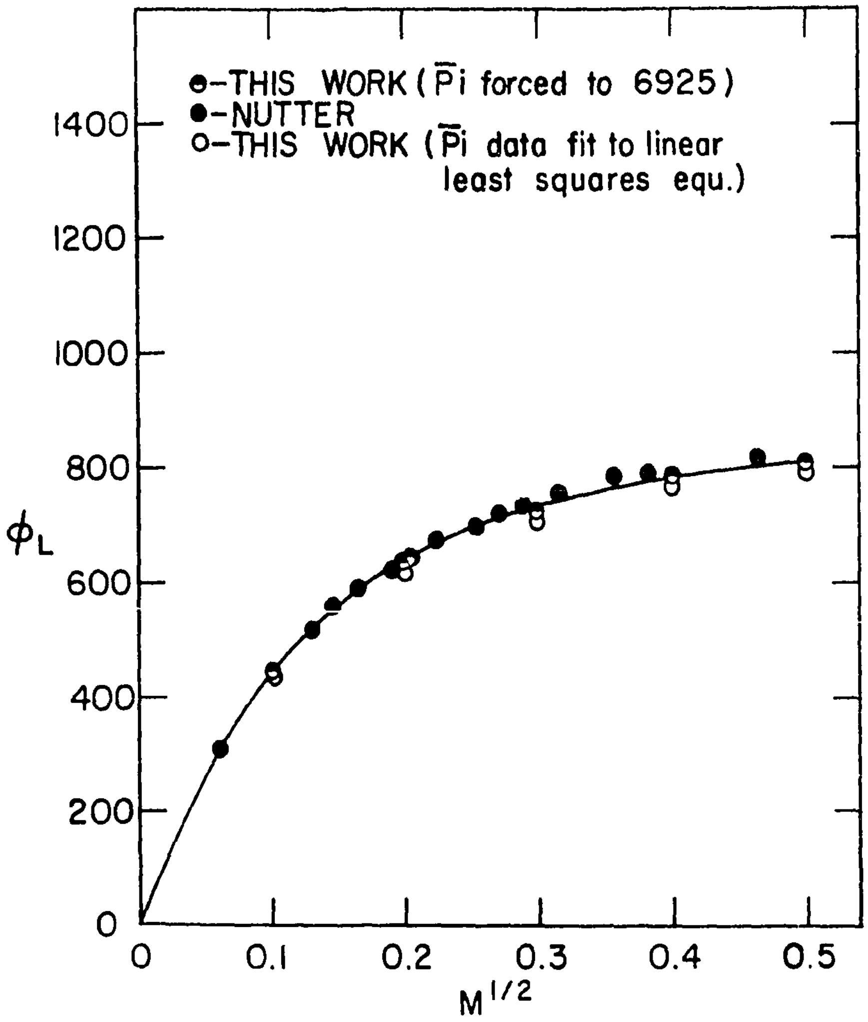

Figure 8. Comparison of the relative apparent molal heat contents of dilute aqueous lanthanum perchlorate solutions at 25° C as determined by Nutter (filled circles) and by this work (open and half-filled circles). The difference in ϕ_L between the open and half-filled circles is the uncertainty introduced into ϕ_L by the extrapolation of the data to infinite dilution

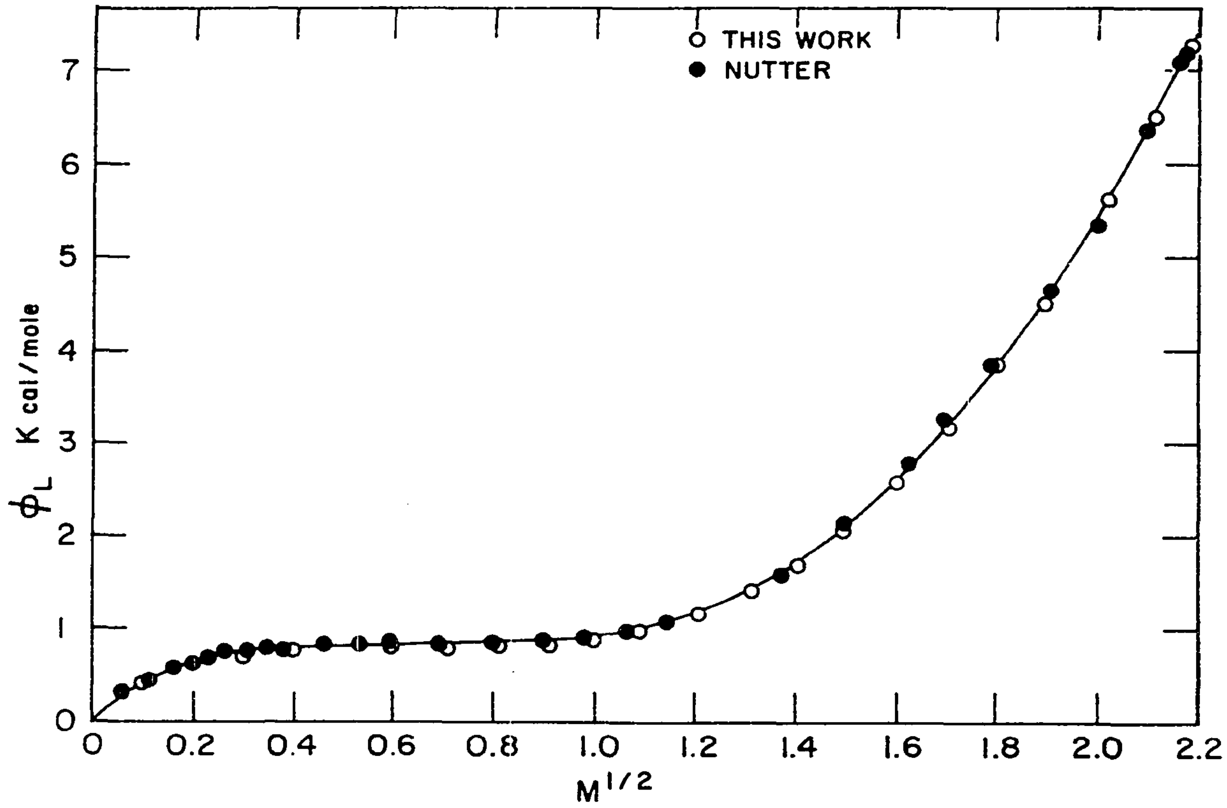

Figure 9. Comparison of the relative apparent molal heat contents of aqueous lanthanum perchlorate solutions at 25° C obtained by Nutter (closed circles) and by this work (open circles)

Table 1. Observed heats of dilution of aqueous lanthanum nitrate solutions at 25° C

m_1	$n_2 \times 10^4$	$m_f^{1/2} \times 10^2$	-q dil.(cal)	$\overline{P}_i$	$\phi_L(m_1)$	$\overline{\phi}_L(m_1)$
0.009027	0.8873	0.9930	0.037		484	497 ± 13
	0.8825	0.9903	0.039		509	
0.01702	1.075	1.093	0.058		613	622 ± 8
	1.155	1.133	0.064		630	
0.05013	3.732	2.037	0.243		784	789 ± 5
	3.227	1.894	0.216		793	
0.09897	9.908	3.319	0.708		924	919 ± 3
	10.212	3.369	0.723		920	
	13.722	3.906	0.923		915	
	10.112	3.353	0.713		916	
0.1599	23.464	5.137	1.585		983	983 ± 1
	23.773	5.170	1.606		984	
	15.693	4.177	1.137		982	
0.2498	24.271	5.196	1.710		1015	1017 ± 1
	24.621	5.232	1.740		1018	
0.3598	29.450	5.720	1.962		1001	1002 ± 1
	28.896	5.670	1.934		1002	
0.4891	19.880	4.710	1.386		982	980 ± 1
	47.393	7.263	2.727		980	
	47.102	7.241	2.707		979	

Table 1. (Continued)

m_1	$n_2 \times 10^4$	$m_f^{1/2} \times 10^2$	-q dil.(cal)	$\overline{P}_i$	$\phi_L(m_1)$	$\overline{\phi}_L(m_1)$
0.6397	50.533	7.500	2.657		941	941
	50.748	7.516	2.662		941	
0.8101	53.873	7.744	2.540		896	897 ± 1
	54.069	7.758	2.557		898	
1.000	46.578	7.200	2.115		856	857 ± 1
	46.511	7.195	2.119		858	
1.208	27.362	5.517	1.370		826	826 ± 1
	27.480	5.528	1.372		825	
1.341	23.579	5.121	1.208		818	817 ± 1
	18.315	4.513	0.991		816	
	18.334	4.515	0.993		817	
1.694	22.847	5.041	1.174		816	817 ± 1
	22.928	5.049	1.181		817	
1.960	25.302	5.305	1.347		847	847 ± 1
	24.777	5.249	1.322		846	
	31.536	5.923	1.587		848	
2.092	26.367	5.415	1.432		864	865 ± 1
	26.314	5.410	1.436		867	
	30.828	5.856	1.612		865	

Table 1. (Continued)

m_1	$n_2 \times 10^4$	$m_f^{1/2} \times 10^2$	-q dil.(cal)	$\bar{P}_i$	$\phi_L(m_1)$	$\bar{\phi}_L(m_1)$
2.557	21.564	4.901	1.477		980	981 ± 1
	20.997*	6.882	1.041	4710	981	
	21.504	4.894	1.478		981	
	21.150*	6.890	1.055	4684	983	
2.893	17.652	4.433	1.448		1090	1094 ± 2
	17.570*	6.260	1.129	4855	1093	
	17.698	4.439	1.460		1096	
	17.388*	6.248	1.121	4942	1096	
3.239	12.881	3.786	1.273		1224	1226 ± 3
	13.048*	5.370	1.073	5297	1222	
	12.886	3.786	1.279		1229	
	12.914*	5.357	1.069	5251	1228	
3.606	22.822	5.042	2.452		1376	1377 ± 1
	23.054*	7.146	2.026	4672	1376	
	22.745	5.034	2.446		1377	
	23.320*	7.160	2.058	4595	1379	
4.000	43.136	6.938	5.022		1555	1556 ± 2
	44.055*	9.858	4.137	3894	1553	
	43.550	6.971	5.082		1559	
	44.508*	9.907	4.193	3869	1557	

---

*Sample was diluted into the final molality of the immediately preceding sample.

Table 1. (Continued)

m_1	$n_2 \times 10^4$	$m_f^{1/2} \times 10^2$	-q dil.(cal)	$\bar{P}_1$	$\phi_L(m_1)$	$\bar{\phi}_L(m_1)$
4.456	25.420	5.321	3.713		1777	1775 ± 2
	26.203*	7.581	3.298	4540	1776	
	25.518	5.332	3.714		1771	
	25.930*	7.568	3.276	4325	1777	
4.608	27.373	5.523	4.173		1851	1852 ± 1
	32.239*	8.147	4.230	4378	1851	
	27.386	5.524	4.186		1855	
	32.047*	8.135	4.204	4473	1852	

Table 2. Observed heats of dilution of aqueous neodymium nitrate solutions at 25° C

m_1	n_2 x 10^4	$m_f^{1/2}$ x 10^2	-q dil.(cal)	$\bar{P}_i$	$\phi_L(m_1)$	$\bar{\phi}_L(m_1)$
0.01022	0.7523	0.9144	0.029		446	471 ± 25
	0.7360	0.9043	0.032		496	
0.04035	3.016	1.831	0.176		703	703
0.1024	7.723	2.930	0.485		812	810 ± 2
	6.505	2.689	0.415		808	
0.1639	14.680	4.040	0.891		851	851 ± 1
	14.432	4.005	0.878		850	
0.2533	20.534	4.778	1.200		864	863 ± 1
	19.966	4.712	1.169		862	
0.3697	28.272	5.608	1.520		857	856 ± 2
	24.285	5.197	1.345		854	
0.4908	41.638	6.807	1.957		839	840 ± 1
	44.702	7.053	2.063		840	
0.6595	42.695	6.893	1.836		802	803 ± 1
	40.298	6.696	1.768		803	
0.8342	60.110	8.182	2.114		770	770 ± 1
	55.857	7.886	2.016		769	
1.032	48.129	7.319	1.744		750	748 ± 2
	56.753	7.949	1.907		747	
	64.171	8.454	2.047		746	

Table 2. (Continued)

m_1	$n_2 \times 10^4$	$m_f^{1/2} \times 10^2$	-q dil.(cal)	$\overline{P}_i$	$\phi_L(m_1)$	$\overline{\phi}_L(m_1)$
1.250	43.290	6.941	1.590		741	741 ± 1
	44.194	7.013	1.605		740	
1.491	40.229	6.691	1.543		748	748 ± 1
	27.184	5.499	1.178		747	
1.755	23.240	5.090	1.134		783	785 ± 1
	23.663*	7.225	0.736	4183	784	
	23.148	5.080	1.139		787	
	25.323*	7.345	0.780	4247	785	
2.033	26.626	5.448	1.421		846	843 ± 2
	25.532*	7.620	0.900	4084	844	
	27.821	5.569	1.455		840	
	24.957*	7.665	0.874	3898	842	
2.368	14.930	4.077	1.048		948	951 ± 2
	17.200*	5.979	0.922	4669	949	
	16.235	4.251	1.135		953	
	16.516*	6.036	0.883	4644	953	
2.662	16.021	4.223	1.300		1064	1064 ± 1
	16.596*	6.024	1.072	4675	1064	
	18.396	4.525	1.465		1064	
	15.113*	6.106	0.955	4693	1062	

---

*Sample was diluted into the final molality of the immediately preceding sample.

Table 2. (Continued)

m_1	$n_2 \times 10^4$	$m_f^{1/2} \times 10^2$	-q dil.(cal)	$\overline{P}_1$	$\phi_L(m_1)$	$\overline{\phi}_L(m_1)$
3.036	30.467	5.827	2.737		1226	1223 ± 3
	26.222*	7.945	1.883	3933	1225	
	30.266	5.808	2.696		1219	
	27.005*	7.985	1.939	3744	1221	
3.394	25.374	5.317	2.799		1409	1408 ± 1
	26.021*	7.564	2.392	4143	1407	
	29.692	5.752	3.218		1409	
	25.597*	7.846	2.307	4035	1406	
3.618	27.601	5.546	3.339		1526	1527 ± 1
	26.089*	7.731	2.690	4014	1525	
	29.518	5.735	3.553		1528	
	26.907*	7.926	2.747	3980	1527	
4.144	21.149	4.852	3.264		1827	1828 ± 1
	19.552*	6.730	2.685	4350	1828	
	18.509	4.539	2.887		1829	
	19.387*	6.493	2.687	4550	1827	
4.582	13.909	3.935	2.565		2082	2086 ± 3
	20.093*	6.150	3.367	4492	2087	
	15.493	4.153	2.842		2083	
	18.868*	6.183	3.157	4360	2090	

Table 3. Observed heats of dilution of aqueous $Gd(NO_3)_3$ solutions at 25° C

m_1	$n_2 \times 10^4$	$m_f^{1/2} \times 10^2$	-q dil.(cal)	$\bar{P}_1$	$\phi_L(m_1)$	$\bar{\phi}_L(m_1)$
0.03951	2.968	1.816	0.171		695	693 ± 2
	2.744	1.746	0.158		690	
0.09998	11.112	3.515	0.699		846	846
	9.202	3.198	0.595		846	
0.1566	12.430	3.717	0.826		892	892
0.2500	24.406	5.210	1.529		928	927 ± 1
	19.165	4.616	1.249		925	
0.3597	33.267	6.084	1.984		937	938 ± 1
	31.366	5.907	1.898		938	
0.4980	39.528	6.632	2.218		925	925
	47.671	7.284	2.557		925	
0.6417	45.290	7.100	2.417		916	916 ± 1
	54.422	7.784	2.761		914	
	49.617	7.432	2.591		917	
0.8114	60.272	8.193	2.879		899	900 ± 1
	56.946	7.963	2.771		901	
1.004	76.113	9.210	3.301		887	889 ± 1
	69.701	8.812	3.130		890	
1.211	69.953	8.828	3.165		894	895 ± 1
	57.859	8.026	2.778		896	

Table 3. (Continued)

m_1	$n_2 \times 10^4$	$m_f^{1/2} \times 10^2$	-q dil.(cal)	$\bar{P}_1$	$\phi_L(m_1)$	$\bar{\phi}_L(m_1)$
1.440	54.464	7.787	2.765		915	915
	53.389	7.710	2.721		915	
1.692	41.704	6.825	2.490		968	962 ± 4
	46.462*	9.909	1.795	3602	959	
	44.570	7.056	2.605		965	
	45.851*	10.035	1.743	3478	957	
1.967	27.432	5.531	2.007		1049	1050 ± 1
	25.928*	7.708	1.427	4042	1049	
	25.141	5.294	1.877		1053	
	26.527*	7.584	1.477	4258	1049	
2.254	19.014	4.602	1.682		1158	1162 ± 3
	19.826*	6.574	1.420	4356	1160	
	17.936	4.470	1.613		1165	
	22.563*	6.713	1.614	4570	1164	
2.566	17.371	4.399				
	22.667*	6.675	1.981		1317	1317 ± 1
	16.637	4.305	1.761		1316	
	22.677*	6.614	1.999	4422	1319	
2.896	10.407	3.403	1.346		1503	1511 ± 5
	14.176*	5.229	1.621	4737	1510	
	12.361	3.709	1.593		1516	
	12.112*	5.217	1.377	4980	1516	

---

*Sample was diluted into the final molality of the immediately preceding sample.

Table 3. (Continued)

m_1	$n_2 \times 10^4$	$m_f^{1/2} \times 10^2$	-q dil.(cal)	$\overline{P}_1$	$\phi_L(m_1)$	$\overline{\phi}_L(m_1)$
3.238	15.942	4.212	2.362		1735	1736 ± 1
	15.817*	5.944	2.090	4607	1737	
	15.743	4.146	2.291		1734	
	16.323*	5.945	2.164	4508	1737	
3.622	21.614	4.906	3.722		2009	2012 ± 3
	22.413*	7.000	3.460	4331	2009	
	20.920	4.827	3.622		2015	
	22.814*	6.977	3.536	4405	2014	
3.952	14.185	3.973	2.865		2261	2266 ± 3
	15.560*	5.752	2.900	4587	2264	
	14.707	4.046	2.975		2268	
	15.345*	5.782	2.857	4735	2269	
4.400	15.786	4.191	3.731		2616	2617 ± 1
	16.030*	5.949	3.531	4608	2617	
	14.786	4.056	3.508		2618	
	16.338*	5.884	3.606	4748	2618	

Table 4. Observed heats of dilution of aqueous holmium nitrate solutions at 25° C

m_1	$n_2 \times 10^4$	$m_f^{1/2} \times 10^2$	-q dil.(cal)	$\overline{P}_1$	$\phi_L(m_1)$	$\overline{\phi}_L(m_1)$
0.01578	1.171	1.141	0.054		537	550 ± 13
	1.170	1.140	0.057		563	
0.04989	3.494	1.970	0.242		822	820 ± 2
	2.859	1.782	0.200		817	
0.09920	5.887	2.558	0.476		974	976 ± 1
	5.844	2.549	0.475		977	
0.1682	10.344	3.391	0.905		1088	1086 ± 2
	10.330	3.389	0.900		1084	
0.2508	17.806	4.450	1.600		1169	1171 ± 2
	17.638	4.431	1.594		1173	
0.3598	18.622	4.562	1.769	4567	1226	1229 ± 1
	14.050*	6.029	1.116		1230	
	18.755	4.578	1.786	4778	1229	
	14.043*	6.041	1.108		1230	
0.4915	20.997	4.843	2.092	4462	1286	1289 ± 1
	21.698*	6.889	1.772		1290	
	23.394	5.114	2.305	4631	1289	
	19.599*	6.917	1.572		1289	
0.5403	24.497	5.231	2.436	4584	1303	1303 ± 1
	22.963*	7.264	1.841		1302	

---

*Sample was diluted into the final molality of the immediately preceding sample.

Table 4. (Continued)

m_1	$n_2 \times 10^4$	$m_f^{1/2} \times 10^2$	-q dil.(cal)	$\bar{P}_i$	$\phi_L(m_1)$	$\bar{\phi}_L(m_1)$
	23.623	5.141	2.360	4625	1304	
	24.095*	7.288	1.933		1302	
0.8020	37.683	5.494	3.812	4076	1380	1378 ± 1
	32.167*	8.822	2.591		1378	
	41.048	6.773	4.098	4104	1378	
	30.116*	8.900	2.335		1374	
0.9929	28.260	5.618	3.147	4479	1442	1439 ± 2
	27.433*	7.875	2.492		1439	
	27.598	5.550	3.076	4409	1440	
	30.970*	8.072	2.801		1436	
1.210	27.911	5.582	3.321	4425	1516	1515 ± 1
	27.665*	7.867	2.730		1514	
	28.718	5.659	3.403	4377	1515	
	27.044*	7.875	2.664		1514	
1.427	32.417	6.017	4.090	4264	1609	1607 ± 2
	34.475*	8.632	3.604		1604	
	33.265	6.091	4.189	4247	1609	
	31.805*	8.509	3.337		1606	
1.685	18.004	4.481				1740 ± 1
	26.671*	7.052	3.380		1740	
	17.377	4.400	2.558	4620	1739	
	28.115*	7.112	3.569		1742	

Table 4. (Continued)

m_1	$n_2 \times 10^4$	$m_f^{1/2} \times 10^2$	-q dil.(cal)	$\overline{P}_i$	$\phi_L(m_1)$	$\overline{\phi}_L(m_1)$
1.958	17.574	4.424				1898 ± 1
	17.873*	6.280	2.593		1898	
	18.887	4.584	3.061	4718	1898	
	16.238*	6.248	2.356		1899	
2.236	19.071	4.608	3.444	4805	2084	2085 ± 1
	14.084*	6.073	2.310		2084	
	17.421	4.402	3.167	4806	2085	
	15.556*	6.054	2.566		2086	
2.550	22.253	4.979	4.489	4583	2314	2318 ± 3
	21.249*	6.958	3.892		2315	
	22.123	4.962	4.482	4662	2322	
	23.503*	7.122	4.302		2320	
2.830	16.221	4.250	3.693	4887	2536	2537 ± 1
	17.877*	6.159	3.752		2536	
	17.851	4.456	4.046	4771	2537	
	17.773*	6.292	3.716		2538	
3.338	24.140	5.184	6.414	4509	2964	2967 ± 4
	26.527*	7.506	6.518		2963	
	25.526	5.333	6.787	4615	2973	
	26.107*	7.582	6.406		2969	
3.724	14.472	4.013	4.430	4790	3308	3311 ± 2
	13.574*	5.585	3.944		3313	
	15.156	4.105	4.634	4866	3310	
	14.993*	5.788	4.337		3312	

Table 4. (Continued)

m_1	$n_2 \times 10^4$	$m_f^{1/2} \times 10^2$	-q dil.(cal)	$\bar{P}_i$	$\phi_L(m_1)$	$\bar{\phi}_L(m_1)$
4.131	14.719	4.047	5.063	5117	3689	3684 ± 4
	15.581*	5.806	5.087		3687	
	15.588	4.163	5.337	4811	3679	
	14.181*	5.751	4.628		3681	
4.564	11.671	3.604	4.507	4886	4086	4090 ± 2
	14.120*	5.356	5.232		4091	
	11.961	3.646	4.619	5014	4089	
	11.289*	5.082	4.192		4092	
5.027	12.449	3.721	5.335		4516	4516 ± 4
	12.469	3.722				
	13.311*	5.352	5.498		4524	
	12.730	3.762	5.451		4515	
	14.958	4.076	6.372		4510	

Table 5. Observed heats of dilution of aqueous erbium nitrate solutions at 25° C

m_1	$n_2 \times 10^4$	$m_f^{1/2} \times 10^2$	-q dil.(cal)	$\overline{P}_i$	$\phi_L(m_1)$	$\overline{\phi}_L(m_1)$
0.009496	0.6753	0.866	0.026		443	443 ± 1
	0.8495	0.972	0.032		442	
0.03830	2.662	1.720	0.169		748	748
	2.545	1.682	0.162		748	
0.1011	10.484	3.414	0.787		964	968 ± 3
	10.466	3.411	0.793		971	
0.1770	15.761	4.186	1.306		1084	1085 ± 1
	15.470	4.147	1.288		1086	
0.2546	8.779	3.131	0.841		1155	1158 ± 2
	9.588*	4.519	0.790	5036	1160	
0.3516	13.354	3.861	1.299		1211	1215 ± 4
	11.283*	5.235	0.927	5036	1212	
	11.050	3.513	1.106		1220	
	12.317*	5.098	1.037	5287	1218	
0.4909	26.369	5.430	2.509		1268	1267 ± 1
	19.209*	7.123	1.475	4572	1266	
	25.107	5.299	2.403		1268	
	20.099*	7.094	1.557	4518	1267	
0.6428	20.734	4.812	2.129		1314	1315 ± 1
	19.380*	6.681	1.647	4575	1315	

---

*Sample was diluted into the final molality of the immediately preceding sample.

Table 5. (Continued)

m_1	$n_2 \times 10^4$	$m_f^{1/2} \times 10^2$	-q dil.(cal)	$\overline{P}_i$	$\phi_L(m_1)$	$\overline{\phi}_L(m_1)$
	20.747	4.813	2.130		1314	
	19.201*	6.567	1.637	4515	1316	
0.8138	26.833	5.475	2.811		1367	1366 ± 1
	23.732*	7.503	2.030	4448	1364	
1.005	38.106	6.527	4.046		1429	1428 ± 2
	29.985*	8.710	2.584	4035	1426	
	37.607	6.484	4.011		1432	
	30.680*	8.722	2.642	4124	1426	
1.209	25.189	5.301	3.029		1514	1513 ± 1
	22.313*	7.272	2.266	4455	1513	
	25.136	5.295	3.025		1514	
	22.357*	7.271	2.267	4514	1512	
1.422	28.998	5.690	3.737		1618	1620 ± 1
	31.102*	8.181	3.405	4026	1621	
	28.661	5.657	3.702		1620	
	31.166*	8.163	3.418	4054	1622	
1.712	28.016	5.590	4.097		1787	1786 ± 1
	27.150*	7.838	3.429	4368	1784	
	28.391	5.628	4.145		1787	
	27.548*	7.892	3.479	4289	1785	
1.969	22.253	4.980	3.707		1961	1962 ± 1
	24.199*	7.191	3.564	4545	1960	

Table 5. (Continued)

m_1	n_2 x 10^4	$m_f^{1/2}$ x 10^2	-q dil.(cal)	$\bar{P}_i$	$\phi_L(m_1)$	$\bar{\phi}_L(m_1)$
	22.160	4.970	3.697		1963	
	24.307*	7.192	3.590	4505	1963	
2.258	20.624	4.793	3.914		2184	2182 ± 1
	18.596*	6.606	3.192	4744	2182	
	20.715	4.804	3.926		2182	
	18.318*	6.591	3.147	4650	2182	
2.570	18.010	4.478	3.927		2450	2453 ± 3
	18.425*	6.367	3.690	4754	2451	
	18.438	4.531				
	17.990*	6.367	3.612		2457	
2.949	17.032	4.355				2790 ± 2
	17.091*	6.162	4.017		2788	
	16.964	4.346	4.281		2787	
	16.693	4.311				
	16.956*	6.119	3.991		2789	
	16.710	4.313	4.225		2790	
	16.866*	6.112	3.983	4658	2794	
3.288	16.044	5.954	4.444		3112	3111 ± 1
	16.108	4.234	4.590		3107	
	15.717*	5.950	4.225	4645	3111	
	16.030	4.224	4.575		3111	
	15.825*	5.953	4.250	4835	3112	
3.703	15.200	4.113	4.962		3515	3513 ± 2
	15.123*	5.808	4.684	4920	3516	

Table 5. (Continued)

m_1	$n_2 \times 10^4$	$m_f^{1/2} \times 10^2$	-q dil.(cal)	$\bar{P}_i$	$\phi_L(m_1)$	$\bar{\phi}_L(m_1)$
	15.056	4.093	4.909		3510	
	15.386*	5.819	4.764	4809	3513	
4.014	14.326	3.993	5.120		3819	3819 ± 1
	13.982*	5.611	4.766	5043	3818	
4.452	13.365	3.856	5.364		4250	4249 ± 1
	13.144*	5.430	5.062	5114	4250	
	13.343	3.853	5.351		4247	
	13.659*	5.480	5.256	5046	4248	
4.848	11.714	3.610	5.169		4637	4637 ± 1
	11.979*	5.133	5.096	5266	4636	
	11.816	3.626	5.211		4635	
	11.800*	5.125	5.026	5023	4638	
5.179	10.336	3.391	4.911		4963	4967 ± 2
	10.750*	4.842	4.950	5155	4966	
	10.848	3.474	5.157		4971	
	10.382*	4.859	4.774	5495	4967	
5.456	9.240	3.206	4.625		5207	5209 ± 1
	9.526*	4.568	4.636	5169	5210	

Table 6. Observed heats of dilution of aqueous lutetium nitrate solutions at 25° C

m_1	$n_2 \times 10^4$	$m_f^{1/2} \times 10^2$	$-q$ dil.(cal)	$\bar{P}_i$	$\phi_L(m_1)$	$\bar{\phi}_L(m_1)$
0.008001	0.7105	0.8885	0.026		426	408 ± 18
	0.6975	0.8799	0.023		389	
0.04795	3.347	1.929	0.220		783	780 ± 3
	3.051	1.840	0.200		776	
0.1016	5.777	2.534	0.439		922	927 ± 5
	6.257	2.636	0.478		932	
0.1604	7.727	2.931	0.644		1018	1019 ± 2
	7.962	2.973	0.663		1021	
	9.916	3.320	0.803		1017	
0.2466	16.554	4.290	1.388		1097	1096 ± 2
	15.513	4.151	1.306		1094	
	16.574	4.293	1.391		1098	
0.3599	15.316	4.134	1.369		1145	1143 ± 2
	13.496*	5.658	0.983	5085	1141	
	11.882	3.643	1.089		1142	
0.4881	19.752	4.695	1.780		1180	1181 ± 1
	17.779*	6.459	1.300	4563	1182	
	21.292	4.877	1.899		1180	
	16.689*	6.501	1.212	4483	1181	

---

*Sample was diluted into the final molality of the immediately preceding sample.

Table 6. (Continued)

m_1	n_2 x 10^4	$m_f^{1/2}$ x 10^2	-q dil.(cal)	$\overline{P}_i$	$\phi_L(m_1)$	$\overline{\phi}_L(m_1)$
0.6403	22.491	5.015	2.065		1213	1212 ± 1
	26.243*	7.366	1.895	4487	1210	
	24.879	5.272	2.252		1212	
	25.591*	7.492	1.829	4351	1211	
0.8135	26.447	5.434	2.456		1244	1241 ± 1
	27.067*	7.715	1.989	4296	1241	
	27.859	5.580	2.561		1241	
	26.868*	7.807	1.955	4221	1239	
0.9917	29.583	5.749	2.827		1285	1283 ± 2
	29.373*	8.103	2.222	4214	1281	
	30.153	5.801	2.876		1286	
	28.862*	8.103	2.184	4188	1282	
1.181	23.070	5.073	2.414		1344	1343 ± 1
	21.972*	7.081	1.905	4358	1345	
	22.337	4.989	2.344		1343	
	22.088*	7.028	1.911	4492	1342	
1.432	18.376	4.526	2.161		1447	1446 ± 1
	19.934*	6.529	1.997	4523	1448	
	18.233	4.506	2.144		1446	
	21.021*	6.606	2.089	4643	1445	
1.709	30.521	5.836	3.874		1602	1602 ± 1
	29.897*	8.203	3.209	4098	1600	

Table 6. (Continued)

m_1	$n_2 \times 10^4$	$m_f^{1/2} \times 10^2$	-q dil.(cal)	$\overline{P}_i$	$\phi_L(m_1)$	$\overline{\phi}_L(m_1)$
	30.017	5.785	3.822		1604	
	31.106*	8.247	3.334	4163	1601	
2.051	18.892	4.587	2.995		1859	1856 ± 3
	16.489*	6.274	2.335	4677	1859	
	18.461	4.532	2.917		1851	
	17.655*	6.336	2.499	4462	1855	
2.260	17.676	4.436	3.144		2045	2043 ± 2
	14.490*	5.982	2.341	4754	2045	
	17.637	4.429	3.130		2041	
	14.958*	6.019	2.411	4698	2041	
2.596	42.589	6.885	8.505		2375	2375
	22.566	5.011	4.694		2375	
	20.151*	6.891	3.837	4415	2375	
2.928	12.800	3.772	3.220		2748	2754 ± 5
	13.716*	5.428	3.238	4837	2751	
	14.341	3.995	3.610		2760	
	12.767*	5.491	3.008	5080	2759	
3.260	12.134	3.675				3166
	14.039*	5.395	3.900		3166	
	12.543	3.736	3.683		3166	
	11.978	3.649				
	14.173*	5.390	3.938		3166	

Table 6. (Continued)

m_1	$n_2 \times 10^4$	$m_f^{1/2} \times 10^2$	-q dil.(cal)	$\bar{P}_i$	$\phi_L(m_1)$	$\bar{\phi}_L(m_1)$
3.644	14.714	4.044				3634 ± 1
	14.717*	5.719	4.745		3634	
	15.098	4.099	5.108		3632	
	13.164*	5.607	4.253	4708	3635	
4.060	15.335	4.131	6.000		4164	4162 ± 4
	15.368*	5.844	5.769	4635	4167	
	16.321	4.259	6.362		4155	
	12.386*	5.648	4.655	4341	4163	
4.553	11.947	3.646	5.450		4787	4788 ± 2
	13.273*	5.296	5.858	4733	4792	
	12.541	3.733	5.714		4786	
	13.118*	5.339	5.770	5025	4786	
4.872	15.423	4.141	7.604		5181	5182 ± 1
	16.262*	5.934	7.746	4785	5183	
5.056	7.536	2.893	3.955		5431	5429 ± 2
	7.643*	4.106	3.904	5820	5427	
5.482	6.732	2.736	3.867		5918	5923 ± 4
	6.649	2.718	3.824		5924	
	7.799*	4.006	4.388	5233	5928	
5.804	8.215	3.021	5.005		6283	6289 ± 4
	6.235*	4.006	3.737	4335	6294	

Table 6. (Continued)

m_1	$n_2 \times 10^4$	$m_f^{1/2} \times 10^2$	-q dil.(cal)	$\bar{P}_i$	$\phi_L(m_1)$	$\Phi_L(m_1)$
	7.531	2.894	4.597		6287	
	7.379*	4.071	4.405	5650	6285	
5.792	5.218	2.407	3.731		7305	7325 ± 14
	4.848	2.322	3.486		7341	
	9.098*	3.938	6.402	6213	7330	

Table 7. Observed heats of dilution of aqueous lanthanum perchlorate solutions at 25° C

m_1	$n_2 \times 10^4$	$m_f^{1/2} \times 10^2$	-q dil.(cal)	$\bar{P}_i$	$\phi_L(m_1)$	$\bar{\phi}_L(m_1)$
0.01027	0.8766	0.9869	0.035		464	451 ± 3
	0.7400	0.9063	0.028		438	
0.03991	3.028	1.834	0.158		637	638 ± 1
	2.853	1.780	0.150		638	
0.08912	7.191	2.827	0.404		729	728 ± 1
	7.184	2.824	0.402		727	
0.1611	10.478	3.411	0.622		790	789 ± 2
	10.133	3.356	0.607		792	
	11.120	3.514	0.651		786	
0.2500	14.702	4.043	0.864		812	811 ± 1
	14.612	4.029	0.856		810	
0.3504	23.589	5.122	1.288		816	816 ± 1
	21.217	4.855	1.180		815	
0.4939	26.458	5.426	1.399		811	809 ± 2
	23.554	5.116	1.268		807	
0.6448	29.844	5.763	1.556		815	815
	28.937	5.671	1.516		815	

Table 7. (Continued)

m_1	$n_2 \times 10^4$	$m_f^{1/2} \times 10^2$	-q dil.(cal)	$\overline{P}_i$	$\phi_L(m_1)$	$\overline{\phi}_L(m_1)$
0.8167	29.788	5.757	1.622		839	839 ± 1
	29.680	5.744	1.614		838	
1.005	36.986	6.416	2.113		889	889
	36.261	6.350	2.076		889	
1.176	30.810	5.855	2.063		968	967 ± 2
	30.815	5.853	2.056		965	
1.465	39.053	6.611	3.270		1162	1164 ± 2
	42.182*	9.519	2.776	3200	1165	
	35.632	6.313	3.018		1162	
	48.668*	9.693	3.211	3200	1166	
1.733	28.393	5.630	3.190		1413	1413 ± 1
	29.129*	8.006	2.799	3460	1414	
	28.268	5.614				
	29.189*	7.997	2.802		1412	
1.982	24.324	5.205	3.484		1705	1707 ± 3
	23.857*	7.321	3.046	3640	1705	
	24.402	5.217	3.508		1711	
2.238	16.655	4.305				2062 ± 1
	17.839*	6.192	2.994		2057	
	16.773	4.322	3.063		2063	
	27.002	5.485	4.804		2063	
	25.947*	7.676	4.201	3580	2063	

---

*Sample was diluted into the final molality of the immediately preceding sample.

Table 7. (Continued)

m_1	n_2 x 10^4	$m_f^{1/2}$ x 10^2	-q dil.(cal)	$\bar{P}_i$	$\phi_L(m_1)$	$\bar{\phi}_L(m_1)$
	26.348	5.422	4.696		2063	
	28.178*	7.794	4.556	3610	2063	
2.565	16.615	4.299	3.916		2593	2591 ± 2
	17.544*	6.162	3.869	4180	2588	
	16.700	4.313	3.935		2592	
	16.351*	6.065	3.621	4000	2592	
2.902	15.992	4.217	4.733		3192	3192 ± 2
	14.089*	5.782	3.970	4240	3188	
	14.207	3.977	4.223		3194	
	14.893*	5.690	4.225	4050	3195	
3.255	10.891	3.481	4.004		3875	3875 ± 2
	10.688*	4.899	3.800	4220	3877	
	10.204	3.368	3.754		3873	
	11.914*	4.957	4.231	4320	3873	
3.581	21.945	4.942	9.350		4523	4521 ± 1
	20.468*	6.868	8.408	3830	4521	
	24.643	5.240	10.458		4518	
	20.364*	7.079	8.351	3520	4521	
4.093	9.054	3.174	4.934		5634	5626 ± 4
	11.968*	4.835	6.351	4900	5626	
	12.873	3.783	6.961		5620	
	10.750*	5.123	5.685	4050	5623	

Table 7. (Continued)

m_1	$n_2 \times 10^4$	$m_f^{1/2} \times 10^2$	-q dil.(cal)	$\overline{P}_1$	$\phi_L(m_1)$	$\overline{\phi}_L(m_1)$
4.465	6.522	2.692	4.140		6508	6511 ± 3
	6.615*	3.820	4.129	4730	6509	
	6.662	2.722	4.231		6513	
	6.231*	3.786	3.893	4680	6514	
4.791	8.064	2.995	5.717		7266	7269 ± 2
	8.142*	4.245	5.686	4260	7269	
	8.047	2.990	5.708		7268	
	8.110*	4.236	5.663	4450	7271	

Table 8. Observed heats of dilution of aqueous neodymium perchlorate solutions at 25° C

m_1	$n_2 \times 10^4$	$m_f^{1/2} \times 10^2$	$-q$ dil.(cal)	$\overline{P}_i$	$\phi_L(m_1)$	$\overline{\phi}_L(m_1)$
0.01050	0.6252	0.8335	0.026		471	467 ± 4
	0.6406	0.8432	0.026		462	
0.04221	3.268	1.906	0.169		635	621 ± 14
	2.799	1.763	0.139		607	
0.1004	5.771	2.533	0.325		714	716 ± 2
	6.108	2.604	0.343		717	
0.1599	10.031	3.339	0.571		760	758 ± 2
	9.808	3.300	0.557		757	
0.2496	13.597	3.888	0.747		764	764 ± 1
	14.575	4.023	0.790		763	
0.3606	21.023	4.836	1.053		756	754 ± 2
	21.638	4.902	1.072		752	
0.4763	24.924	5.266	1.178		744	743 ± 2
	23.907	5.154	1.132		741	
0.6390	29.525	5.732	1.274		720	722 ± 2
	31.423	5.910	1.345		723	
0.7945	41.946	6.835	1.644		719	719
	45.788	7.137	1.748		719	

Table 8. (Continued)

m_1	n_2 x 10^4	$m_f^{1/2}$ x 10^2	-q dil.(cal)	$\bar{P}_i$	$\phi_L(m_1)$	$\bar{\phi}_L(m_1)$
1.005	35.007	6.242	1.558		752	751 ± 1
	37.070	6.420	1.620		750	
1.227	44.291	7.023	2.172		823	826 ± 3
	42.928	6.910	2.142		828	
1.444	47.073	7.261	2.871		951	953 ± 3
	45.148*	10.146	1.964	2970	955	
	47.093	7.261	2.861		949	
	49.715*	10.390	2.147	2880	955	
1.670	29.878	5.774	2.515		1132	1130 ± 1
	34.773*	8.484	2.336	3380	1130	
	31.434	5.926	2.624		1131	
	33.728*	8.523	2.253	3330	1129	
1.964	24.763	5.256	2.858		1425	1424 ± 1
	27.930*	7.662	2.776	3530	1423	
	26.422	5.427	3.031		1424	
	27.255*	7.729	2.692	3520	1422	
2.254	18.659	4.559	2.893		1794	1794 ± 2
	17.442*	6.339	2.450	3960	1790	
	18.213	4.502	2.834		1797	
	17.438*	6.296	2.463	3910	1795	

---

*Sample was diluted into the final molality of the immediately preceding sample.

Table 8. (Continued)

m_1	$n_2 \times 10^4$	$m_f^{1/2} \times 10^2$	-q dil.(cal)	$\bar{P}_i$	$\phi_L(m_1)$	$\bar{\phi}_L(m_1)$
2.603	17.070	4.358	3.541		2309	2310 ± 1
	19.983*	6.419	3.857	3780	2310	
	17.685	4.439	3.666		2312	
	18.648*	6.359	3.596	3870	2310	
2.879	12.707	3.759	3.258		2774	2775 ± 1
	13.009*	5.346	3.170	4050	2774	
	11.899	3.639	3.062		2777	
	13.174*	5.281	3.216	4230	2776	
3.223	14.299	3.987	4.539		3394	3396 ± 4
	13.092*	5.517	3.982	4140	3392	
	12.629	3.750	4.032		3402	
3.625	15.337	4.132	6.022		4152	4152 ± 1
	15.658*	5.873	5.939	3880	4153	
	15.777	4.189	6.187		4150	
	14.894*	5.839	5.648	3810	4151	
4.075	13.452	3.869	6.550		5083	5082 ± 2
	13.350*	5.461	6.324	4130	5082	
	13.472	3.870	6.554		5079	
	12.670*	5.390	6.019	3650	5085	
4.509	7.857	2.954	4.665		6109	6110 ± 2
	7.917*	4.186	4.617	4300	6112	
	8.071	2.996	4.788		6106	
	7.637*	4.179	4.454	4130	6112	

Table 8. (Continued)

m_1	$n_2 \times 10^4$	$m_f^{1/2} \times 10^2$	-q dil.(cal)	$\bar{P}_i$	$\phi_L(m_1)$	$\bar{\phi}_L(m_1)$
4.685	7.733	2.933	4.936		6554	6547 ± 7
	8.615*	4.264	5.397	4680	6552	
	10.609	3.433	6.730		6539	
	7.600*	4.498	4.742	4090	6541	

Table 9. Observed heats of dilution of aqueous gadolinium perchlorate solutions at 25° C

m_1	$n_2 \times 10^4$	$m_f^{1/2} \times 10^2$	-q dil.(cal)	$\bar{P}_i$	$\phi_L(m_1)$	$\bar{\Phi}_L(m_1)$
0.02339	4.440	2.221	0.114		392	397 ± 4
	4.573	2.253	0.121		401	
0.05915	7.493	2.886	0.394		694	698 ± 4
	7.538	2.895	0.403		704	
	7.797	2.944	0.409		696	
0.1132	13.299	3.845	0.774		795	791 ± 3
	13.726	3.907	0.783		786	
	14.003	3.946	0.805		792	
0.1982	25.371	5.313	1.466		851	856 ± 3
	27.235	5.505	1.579		860	
	25.735	5.351	1.497		856	
0.3275	34.273	6.176	2.019		894	894 ± 1
	34.291	6.177	2.019		894	
	24.769	5.249	1.539		891	
	24.656	5.237	1.541		895	
0.4256	42.807	6.904	2.482		910	912 ± 1
	42.919	6.913	2.498		913	
	29.256	5.706	1.828		913	
	29.318	5.712	1.832		913	
0.5525	34.553	6.202	2.174		935	937 ± 2
	34.576	6.204	2.184		938	

Table 9. (Continued)

m_1	$n_2 \times 10^4$	$m_f^{1/2} \times 10^2$	-q dil.(cal)	$\bar{P}_1$	$\phi_L(m_1)$	$\bar{\phi}_L(m_1)$
	21.862	4.931	1.487		938	
	21.924	4.938	1.484		935	
0.7330	27.407	5.522	1.908		977	983 ± 5
	27.354	5.517	1.922		984	
	22.708	5.026	1.629		979	
	22.302	4.980	1.633		992	
0.9182	50.285	7.484	3.492		1044	1048 ± 2
	50.597	7.507	3.521		1047	
	27.552	5.538	2.112		1048	
	27.828	5.566	2.138		1051	
1.081	18.619	4.550	1.666		1133	1136 ± 3
	10.291*	5.669	0.793	3950	1137	
	18.839	4.579	1.682		1137	
	9.911*	5.653	0.770	3715	1139	
	39.300	6.630	3.180		1130	
	39.303	6.630	3.190		1133	
1.320	37.612	6.489	3.693		1298	1299 ± 2
	42.442*	9.450	3.385	3300	1299	
	37.492	6.479	3.666		1294	
	42.497*	9.447	3.409	3144	1299	
	19.671	4.678	2.070		1300	
	9.490*	5.694	0.891	3632	1302	

---

*Sample was diluted into the final molality of the immediately preceding sample.

Table 9. (Continued)

m_1	$n_2 \times 10^4$	$m_f^{1/2} \times 10^2$	-q dil.(cal)	$\bar{P}_i$	$\phi_L(m_1)$	$\bar{\phi}_L(m_1)$
1.556	13.176	3.828				1508 ± 4
	8.677*	4.928	1.024		1508	
	13.351	3.853	1.735		1515	
	8.491*	4.927	1.013	3855	1516	
	13.405	3.861	1.734		1507	
	8.576*	4.943	1.018	3835	1511	
	34.806	6.237	4.170		1505	
	32.160*	8.641	3.298	3448	1504	
	34.971	6.251	4.178		1502	
	32.138*	8.650	3.297	3368	1503	
1.823	26.637	5.452	4.058		1801	1800 ± 1
	25.494*	7.619	3.478	3590	1801	
	26.615	5.449	4.052		1800	
	25.329*	7.607	3.449	3628	1798	
2.074	22.079	4.962	4.083		2108	2110 ± 2
	22.251*	7.026	3.786	3595	2110	
	22.016	4.955	4.080		2112	
	22.298*	7.025	3.782	3816	2108	
2.389	18.786	4.575				2564 ± 3
	18.506*	6.443	4.024		2560	
	18.863	4.584	4.384		2568	
	18.338*	6.435	3.984	4036	2563	
2.891	13.227	3.837	4.233		3413	3411 ± 1

Table 9. (Continued)

m_1	$n_2 \times 10^4$	$m_1^{1/2} \times 10^2$	-q dil.(cal)	$\bar{P}_1$	$\phi_L(m_1)$	$\bar{\phi}_L(m_1)$
	13.127	3.822	4.197		3409	
	11.786*	5.265	3.625	3985	3411	
3.104	15.884	4.205	5.654		3788	3787 ± 1
	14.233*	5.789	4.877	3977	3788	
	15.718	4.183	5.592		3786	
	14.335*	5.783	4.913	3894	3786	
3.499	10.944	3.490	4.763		4549	4547 ± 2
	10.947	3.490	4.764		4549	
	10.328*	4.865	4.361	4567	4544	
3.827	7.153	2.821	3.602		5201	5204 ± 2
	7.399*	4.022	3.646	4563	5202	
	7.265	2.843	3.662		5207	
	7.357*	4.032	3.624	4853	5204	
4.205	6.213	2.628	3.636		6008	6011 ± 4
	6.048*	3.692	3.478	4709	6008	
	6.136	2.612	3.597		6017	
4.611	7.620	2.910	5.181		6969	6972 ± 3
	7.484	2.884	5.094		6975	

Table 10. Observed heats of dilution of aqueous erbium perchlorate solutions at 25° C

m_1	$n_2 \times 10^4$	$m_f^{1/2} \times 10^2$	-q dil.(cal)	$\overline{P}_1$	$\phi_L(m_1)$	$\overline{\phi}_L(m_1)$
0.03982	4.558	5.117	0.221		760	762 ± 17
	4.913	5.455	0.238		773	
	3.514	3.901	0.178		729	
	5.455	6.057	0.258		785	
0.1154	13.172	3.827	0.738		779	779 ± 1
	14.209	3.975	0.785		778	
0.2029	24.317	5.198	1.431		867	867
	17.622	4.427	1.094		867	
	26.036	5.382	1.512		867	
0.2307	5.795	2.541	0.413		868	873 ± 4
	5.451*	3.535	0.337	4990	872	
	5.606	2.500	0.402		870	
	5.651*	3.537	0.347	4610	870	
	20.446	4.770	1.258		876	
	22.480	5.002	1.370		880	
0.3603	35.988	6.336	2.170		926	923 ± 1
	35.939	6.332	2.153		922	
	35.922	6.323	2.152		921	
	35.872	6.319	2.152		922	
	29.807	5.757	1.855		923	
	29.768	5.754	1.845		921	

---

*Sample was diluted into the final molality of the immediately preceding sample.

Table 10. (Continued)

m_1	$n_2 \times 10^4$	$m_f^{1/2} \times 10^2$	-q dil.(cal)	$\overline{P}_1$	$\phi_L(m_1)$	$\overline{\phi}_L(m_1)$
0.5129	29.312	5.734	1.907		951	954 ± 2
	29.149	5.718	1.913		955	
	29.144	5.717	1.909		954	
	29.402	5.742	1.928		956	
0.6626	31.785	5.950	2.165		989	994 ± 2
	31.798	5.952	2.183		995	
	31.777	5.950	2.188		997	
	55.194	7.839	3.412		993	
	55.199	7.839	3.422		995	
0.8408	72.174	8.967	4.714		1063	1065 ± 1
	71.777	8.942	4.707		1065	
	53.374	7.708	3.718		1067	
	53.557	7.721	3.704		1063	
	53.466	7.714	3.720		1066	
1.055	53.019	7.682	4.322		1184	1186 ± 1
	51.130	7.544	4.194		1185	
	51.305	7.556	4.234		1190	
	51.973	7.606	4.256		1186	
	68.741	8.756	5.366		1185	
	68.889	8.765	5.386		1186	
1.227	48.139	7.347	4.684		1331	1321 ± 5
	54.400*	10.697	4.213	3030	1329	
	47.964	7.335	4.589		1315	
	55.472*	10.744	4.249	3000	1316	

Table 10. (Continued)

m_1	n_2 x 10^4	$m_f^{1/2}$ x 10^2	-q dil.(cal)	$\bar{P}_i$	$\phi_L(m_1)$	$\bar{\phi}_L(m_1)$
	47.880	7.347	4.604		1320	
	53.832*	10.682	4.149	3160	1321	
	48.035	7.311	4.613		1317	
1.498	39.663	6.664	4.932		1578	1578 ± 1
	43.349*	9.625	4.610	3250	1579	
	39.630	6.657	4.931		1578	
	42.865*	9.590	4.548	3180	1578	
1.700	29.132	5.701	4.394		1807	1808 ± 2
	31.214*	8.197	4.211	3610	1812	
	29.358	5.723	4.428		1808	
	31.064*	8.202	4.144	3300	1805	
2.033	35.765	6.319	7.000		2279	2282 ± 1
	35.072*	8.884	6.280	3310	2282	
	36.016	6.340	7.057		2282	
	34.899*	8.888	6.241	3220	2283	
2.358	32.748	6.043	8.084		2781	2781 ± 1
	28.448*	8.255	6.560	3550	2781	
	32.940	6.060	8.135		2782	
	28.209*	8.252	6.491	3420	2780	
2.676	14.870	4.067	4.630		3344	3348 ± 3
	15.175*	5.779	4.515	3870	3346	
	14.886	4.069	4.641		3348	
	15.045*	5.769	4.494	4080	3353	

Table 10. (Continued)

m_1	$n_2 \times 10^4$	$m_f^{1/2} \times 10^2$	-q dil.(cal)	$\bar{P}_i$	$\phi_L(m_1)$	$\bar{\phi}_L(m_1)$
3.086	8.377	3.051	3.320		4144	4143 ± 6
	10.045*	4.523	3.829	3620	4131	
	8.273	3.032	3.273		4136	
	9.074*	4.390	3.476	4080	4135	
	8.306	3.038	3.293		4146	
	13.035	3.807	5.122		4147	
	12.866*	5.366	4.891	4830	4152	
	12.980	3.799	5.095		4143	
	13.173*	5.392	5.020	5610	4155	
3.413	7.834	2.949	3.642		4825	4822 ± 5
	8.577*	4.267	3.874	5670	4819	
	7.800	2.942	3.628		4827	
	8.681*	4.276	3.913	5240	4815	
3.863	9.153	3.190	5.100		5760	5770 ± 6
	9.187	3.194	5.135		5777	
	8.973*	4.489	4.894	5170	5772	
4.215	14.221	3.977	9.092		6619	6627 ± 4
	14.812*	5.681	9.268	4470	6622	
	9.733	3.290	6.260		6625	
	10.899*	4.660	6.887	4350	6628	
	9.796	3.299	6.304		6629	
	10.999*	4.806	6.938	4090	6630	
	9.232	3.205	5.951		6635	

Table 10. (Continued)

m_1	$n_2 \times 10^4$	$m_f^{1/2} \times 10^2$	-q dil.(cal)	$\bar{P}_i$	$\phi_L(m_1)$	$\bar{\phi}_L(m_1)$
4.627	7.971	2.978	5.898		7577	7576 ± 4
	7.777*	4.185	5.658	3980	7573	
	7.500	2.887	5.550		7573	
	7.942*	4.142	5.800	5080	7583	

Table 11. Observed heats of dilution of aqueous lutetium perchlorate solutions at 25° C

m_1	$n_2 \times 10^4$	$m_f^{1/2} \times 10^2$	-q dil.(cal)	$\overline{P}_1$	$\phi_L(m_1)$	$\overline{\phi}_L(m_1)$
0.009869	0.8268	0.9585	0.030		426	393 ± 33
	0.7667	0.9225	0.023		360	
0.06717	5.160	2.395	0.289		704	704 ± 1
	4.472	2.228	0.255		705	
0.09880	5.193	2.402	0.313		747	750 ± 3
	5.740	2.524	0.345		752	
0.1546	8.392	3.054	0.533		812	809 ± 3
	7.946	2.970	0.503		806	
0.2496	10.511	3.418	0.689		850	854 ± 4
	12.323	3.700	0.801		857	
0.3586	23.928	5.159	1.468		882	883 ± 1
	24.995	5.271	1.525		883	
0.4944	32.418	6.007	1.974		910	911 ± 1
	33.507	6.104	2.035		911	
0.6409	46.017	7.159	2.738		937	939 ± 2
	45.501	7.115	2.725		940	
0.8068	49.117	7.397	3.166		995	996 ± 1
	48.380	7.337	3.133		996	

Table 11. (Continued)

m_1	$n_2 \times 10^4$	$m_f^{1/2} \times 10^2$	-q dil.(cal)	$\overline{P}_j$	$\phi_L(m_1)$	$\overline{\phi}_L(m_1)$
1.006	32.379	6.018	2.566		1093	1095 ± 2
	30.221*	8.354	1.898	3400	1097	
	32.383	6.016	2.566		1093	
	32.223*	8.482	2.015	3380	1097	
1.174	31.908	5.971	2.880		1202	1203 ± 2
	26.062*	8.038	1.941	3440	1205	
	28.688	5.659	2.623		1201	
1.432	24.852	5.267	2.865		1425	1425 ± 1
	24.740*	7.433	2.463	3620	1426	
	24.201	5.195	2.792		1424	
	26.437*	7.507	2.626	3630	1424	
1.676	21.130	4.854	3.025		1688	1689 ± 2
	21.491*	6.889	2.764	3600	1691	
	20.023	4.723	2.876		1687	
	21.957*	6.833	2.829	3660	1690	
1.980	15.421	4.145	2.874		2090	2091 ± 2
	16.667*	5.976	2.874	3950	2090	
	15.942	4.212	2.977		2096	
	16.095*	5.968	2.760	4370	2090	
2.232	15.226	4.116	3.405		2461	2464 ± 3
	13.344*	5.636	2.820	3780	2466	

---

*Sample was diluted into the final molality of the immediately preceding sample.

Table 11. (Continued)

m_1	$n_2 \times 10^4$	$m_f^{1/2} \times 10^2$	-q dil.(cal)	$\overline{P}_i$	$\phi_L(m_1)$	$\overline{\phi}_L(m_1)$
2.529	18.757	4.568	5.090		2958	2961 ± 2
	15.770*	6.196	4.073	3670	2962	
	16.386	4.272				
	16.077*	6.011	4.168		2964	
2.870	10.066	3.347	3.414		3583	3585 ± 2
	10.818	3.468	3.664		3583	
	11.383*	4.967	3.723	3980	3588	
3.196	11.396	3.561	4.610		4246	4238 ± 8
	10.621*	4.949	4.164	4340	4245	
	13.315	3.847	5.344		4227	
	11.411*	5.242	4.456	3590	4234	
3.567	10.850	3.475	5.240		5026	5021 ± 2
	13.107*	5.163	6.147	4530	5021	
	11.514	3.577	5.545		5017	
	10.643*	4.962	5.003	3990	5021	
4.039	12.864	3.784	7.527		6062	6049 ± 7
	13.403*	5.406	7.635	4860	6050	
	13.480	3.872	7.857		6044	
	14.150*	5.542	8.005	4170	6042	
4.634	9.975	3.331	7.215		7423	7421 ± 3
	9.695*	4.677	6.900	4250	7425	
	9.953	3.326	7.195		7419	
	10.036*	4.713	7.130	4510	7416	

Table 12. Parameters for the empirical expressions of $\bar{P}_1$ and ϕ_L below 0.007 molal for the rare earth nitrates

	A	B
$La(NO_3)_3$	6925	- 37160
$Nd(NO_3)_3$	6925	- 44290
$Gd(NO_3)_3$	6925	- 43480
$Ho(NO_3)_3$	6925	- 38630
$Er(NO_3)_3$	6925	- 39870
$Lu(NO_3)_3$	6925	- 41590

Table 13. Parameters for the empirical expressions of $\bar{P}_1$ and ϕ_L below 0.007 molal for the rare earth perchlorates

	A	B	C
$La(ClO_4)_3$	6925	- 79240	421480
$Nd(ClO_4)_3$	6925	- 82930	444610
$Gd(ClO_4)_3$	6925	- 84990	499425
$Er(ClO_4)_3$	6925	- 70670	304190
$Lu(ClO_4)_3$	6925	- 85000	524620

Table 14. Parameters for the empirical expressions of ϕ_L of rare earth nitrate solutions below 1.0 molal corresponding to Equation 7.15

	a	b	c	d	e	f
$La(NO_3)_3$	508.71	7525.9	-7118.3	-3816.5	7244.9	-3485.0
$Nd(NO_3)_3$	-1002.1	14819.0	-17550.	1241.4	10206.0	-6966.7
$Gd(NO_3)_3$	615.87	6468.1	-5957.8	-4938.4	9731.5	-5024.6
$Ho(NO_3)_3$	2509.6	-4750.3	12942.	-22838.	25827.0	-12246.
$Er(NO_3)_3$	-127.30	10822.0	-13077.	5119.1	-3235.5	1929.8
$Lu(NO_3)_3$	735.54	5464.5	-4845.0	-1689.4	1344.8	276.68

Table 15. Parameters for the empirical expressions of ϕ_L of rare earth nitrate solutions above 1.0 molal corresponding to Equations 7.17 and 7.18

	a'	b'	c'	d'	e'	f'
$La(NO_3)_3$	4686.0	7264.5	4286.0	-864.19	10.223	0.49051
$Gd(NO_3)_3$	2966.1	-2719.3	-27.876	756.80	-89.058	4.1432
$Ho(NO_3)_3$	4167.2	-4794.7	2109.6	10.203	-55.505	3.5927
$Er(NO_3)_3$	3346.1	-2559.1	-165.34	926.87	-121.38	6.3119
$Lu(NO_3)_3$	3486.0	-2807.1	-467.58	1204.6	-136.11	5.9494

	a"	b"	c"	d"	e"	f"	g"	h"
$Nd(NO_3)_3$	685.30	-440.17	1681.4	-1141.5	-2435.0	2297.7	205.24	-101.19

Table 16. Parameters for the empirical expressions of $\bar{L}_2$ of rare earth nitrate solutions below 1.0 molal corresponding to Equation 7.25

	a_1	b_1	c_1	d_1	e_1	f_1
$La(NO_3)_3$	693.00	11289.0	-11864.0	-7633.0	16905.0	-8712.5
$Nd(NO_3)_3$	-1336.1	22228.0	-29250.0	2482.8	23814.0	-17417.0
$Gd(NO_3)_3$	821.16	9702.1	-9929.7	-9876.8	22707.0	-12562.0
$Ho(NO_3)_3$	3346.2	-7125.4	21570.0	-45676.0	60263.0	-30615.0
$Er(NO_3)_3$	-169.73	16233.0	-21795.0	10238.0	-7549.5	4824.5
$Lu(NO_3)_3$	980.72	8196.7	-3075.0	-3378.8	3137.9	691.70

Table 17. Parameters for the empirical expressions of $\overline{L}_2$ of rare earth nitrate solutions above 1.0 molal corresponding to Equations 7.27 and 7.28

	a_1'	b_1'	c_1'	d_1'	e_1'	f_1'
$La(NO_3)_3$	7029.0	-14529.0	10715.0	-2592.6	40.892	2.4526
$Gd(NO_3)_3$	4449.2	-5438.6	-69.690	2270.4	-356.23	20.716
$Ho(NO_3)_3$	6250.8	-9589.4	5274.0	30.609	-222.02	17.964
$Er(NO_3)_3$	5019.2	-5118.2	-413.35	2780.6	-485.52	31.560
$Lu(NO_3)_3$	5229.0	-5614.2	-1169.0	3613.8	-544.44	29.747

	a_1''	b_1''	c_1''	d_1''	e_1''	f_1''	g_1''	h_1''
$Nd(NO_3)_3$	685.30	-586.89	2522.1	-2283.0	-5681.6	5744.2	615.72	-354.16

Table 18. Parameters for the empirical expressions of $\overline{L}_1$ for rare earth nitrate solutions below 1.0 molal corresponding to Equation 7.30

	a_2	b_2	c_2	d_2	e_2	f_2
$La(NO_3)_3$	-3.3201	-67.793	85.496	68.758	-174.03	94.179
$Nd(NO_3)_3$	6.0180	-133.49	210.79	-22.365	-245.16	188.27
$Gd(NO_3)_3$	-3.6985	-58.265	71.557	88.970	-233.77	135.79
$Ho(NO_3)_3$	-15.071	42.791	-155.44	411.45	-620.40	330.94
$Er(NO_3)_3$	0.76447	-97.485	157.06	-92.224	77.721	-52.151
$Lu(NO_3)_3$	-4.4172	-49.224	58.192	30.436	-32.304	-7.4770

Table 19. Parameters for the empirical expressions of $\bar{L}_1$ for rare earth nitrate solutions above 1.0 molal corresponding to Equations 7.32 and 7.33

	a_2'	b_2'	c_2'	d_2'	e_2'	f_2'
$La(NO_3)_3$	-42.210	130.87	-116.72	31.137	-0.55251	-0.035347
$Gd(NO_3)_3$	-26.718	48.989	0.75915	-27.268	4.8132	-0.29857
$Ho(NO_3)_3$	-37.537	86.378	-57.451	-0.36762	2.9998	-0.25890
$Er(NO_3)_3$	-30.141	46.103	4.5027	-33.396	6.5601	-0.45485
$Lu(NO_3)_3$	-31.401	50.571	12.734	-43.403	7.3562	-0.42872

	a_2''	b_2''	c_2''	d_2''	e_2''	f_2''	g_2''
$Nd(NO_3)_3$	2.6433	-15.146	20.565	58.490	-62.091	-7.3950	4.5574

Table 20. Parameters for the empirical expressions of ϕ_L for rare earth perchlorate solutions below 1.1 molal corresponding to Equation 7.16

	A	B	C	D	E	F	G
$La(ClO_4)_3$	1385.5	1982.9	000.00	-8533.8	9764.0	-3629.8	-76.093
$Nd(ClO_4)_3$	1331.5	1905.0	658.14	-10756.6	13783.8	-6164.5	0.000
$Gd(ClO_4)_3$	687.40	4790.0	-3108.0	-7578.9	11826.8	-5526.0	0.000
$Er(ClO_4)_3$	619.93	7488.0	-10923.9	7098.7	-9235.4	6107.4	0.000
$Lu(ClO_4)_3$	988.84	4413.6	-5334.6	955.41	-3186.0	3253.4	0.000

Table 21. Parameters for the empirical expressions of ϕ_L for rare earth perchlorate solutions above 1.1 molal corresponding to Equation 7.19

	A'	B'	C'	D'	E'	F'
$La(ClO_4)_3$	2108.2	-1729.1	-413.96	448.79	657.13	-176.40
$Nd(ClO_4)_3$	2275.5	-2294.3	-161.23	704.54	314.34	-85.561
$Gd(ClO_4)_3$	1725.6	-1419.6	236.48	160.72	496.69	-108.50
$Er(ClO_4)_3$	5377.1	-10874.9	8288.6	-1729.7	000.00	96.714
$Lu(ClO_4)_3$	2033.2	-1373.1	-669.55	772.18	524.09	-162.55

Table 22. Parameters for the empirical expressions of $\overline{L}_2$ for rare earth perchlorate solutions below 1.1 molal corresponding to Equation 7.26

	A_1	B_1	C_1	D_1	E_1	F_1	G_1
$La(ClO_4)_3$	1847.3	2974.4	000.0	-17067.6	22782.7	-9074.5	-228.28
$Nd(ClO_4)_3$	1775.3	2857.5	1096.9	-21513.2	32162.2	-15411.2	000.00
$Gd(ClO_4)_3$	916.53	7185.0	-5180.0	-15157.8	27595.9	-13815.0	000.00
$Er(ClO_4)_3$	826.57	11232.0	-12206.5	14197.4	-21549.3	15268.5	000.00
$Lu(ClO_4$ $_3$	1318.5	6620.4	-8891.0	1910.8	-7434.0	8133.5	000.00

Table 23. Parameters for the empirical expressions of $\overline{L}_2$ for the rare earth perchlorate solutions above 1.1 molal corresponding to Equation 7.29

	A_1'	B_1'	C_1'	D_1'	E_1'	F_1'
$La(ClO_4)_3$	2108.2	-2593.7	-827.92	1122.0	1971.4	-617.40
$Nd(ClO_4)_3$	2275.5	-3441.5	-322.46	1761.4	943.02	-299.46
$Gd(ClO_4)_3$	1725.6	-2129.4	472.96	401.80	1490.1	-379.75
$Er(ClO_4)_3$	5377.1	-16312.4	16577.2	-4324.3	000.0	338.50
$Lu(ClO_4)_3$	2033.2	-2059.7	-1339.1	1930.5	1572.3	-568.93

Table 24. Parameters for the empirical expressions of $\overline{L}_1$ for rare earth perchlorate solutions below 1.1 molal corresponding to Equation 7.31

	A_2	B_2	C_2	D_2	E_2	F_2	G_2
$La(ClO_4)_3$	-8.3204	-17.862	000.0	153.74	-234.54	98.092	2.7418
$Nd(ClO_4)_3$	-7.9959	-17.160	-7.9047	193.79	-331.14	166.59	0.0000
$Gd(ClO_4)_3$	-4.1281	-43.148	37.329	136.54	-284.10	149.33	0.0000
$Er(ClO_4)_3$	-3.7229	-67.452	131.20	-127.89	221.85	-165.05	0.0000
$Lu(ClO_4)_3$	-5.9383	-39.758	64.072	-17.213	76.531	-87.920	0.0000

Table 25. Parameters for the empirical expressions of $\bar{L}_1$ for rare earth perchlorate solutions above 1.1 molal corresponding to Equation 7.34

	A'_2	B'_2	C'_2	D'_2	E'_2
$La(ClO_4)_3$	15.575	7.4575	-12.127	-23.676	7.9446
$Nd(ClO_4)_3$	20.666	2.9046	-19.038	-11.326	3.8535
$Gd(ClO_4)_3$	12.787	-4.2602	-4.3431	-17.896	4.8866
$Er(ClO_4)_3$	97.956	-149.32	46.741	0.000	-4.3558
$Lu(ClO_4)_3$	12.368	12.062	-20.866	-18.883	7.3208

Table 26. Probable errors calculated using Equations 7.22, 7.23, and 7.24 for a number of $La(NO_3)_3$ sample solutions

m_1	$m_f^{1/2} \times 10^2$	$P^2_{\Delta H_{1-f}}$	$P^2_{\phi_L(m_f)}$	$P^2_{\phi_L(m_1)}$
0.009027	0.993	142.2	0.0001	142.2
0.01702	1.093	180.3	0.0002	180.3
0.05013	2.037	13.4	0.002	13.4
0.1599	5.137	0.64	0.08	0.72
0.2498	5.232	0.65	0.08	0.73
0.3598	5.670	0.65	0.11	0.76
0.4891	7.241	0.37	0.30	0.67
0.8101	7.758	0.27	0.39	0.66
1.000	7.200	0.32	0.29	0.61
2.092	5.415	0.63	0.09	0.72
3.606	5.042	1.46	0.07	1.53
4.608	5.523	2.55	0.10	2.65

Table 27. Probable errors calculated using Equations 7.22, 7.23, and 7.24 for a number of $La(ClO_4)_3$ sample solutions

m_1	$m_f^{1/2} \times 10^2$	$P^2_{\Delta H_{1-f}}$	$P^2_{\phi_L(m_f)}$	$P^2_{\phi_L(m_1)}$
0.03991	1.834	21.	0.006	21.
0.08912	2.827	3.2	0.067	3.3
0.1611	3.356	1.8	0.18	2.0
0.2500	4.043	1.0	0.55	1.6
0.3504	5.122	0.78	2.21	2.99
0.4939	5.426	0.53	3.11	3.64
0.6448	5.763	0.55	4.45	5.00
0.8167	5.744	0.97	4.37	5.34
1.005	6.416	0.45	8.44	8.89
2.238	4.323	3.9	0.81	4.7
3.581	5.240	18.4	2.53	20.9
4.791	2.995	54.5	0.10	54.6

Table 28. $\bar{L}_1$ values at selected concentrations for some aqueous rare earth nitrate solutions at 25° C

	$-\bar{L}_1$					
Molality	$La(NO_3)_3$	$Nd(NO_3)_3$	$Gd(NO_3)_3$	$Ho(NO_3)_3$	$Er(NO_3)_3$	$Lu(NO_3)_3$
0.10	0.278	0.167	0.238	0.414	0.390	0.377
0.20	0.240	0.079	0.230	0.702	0.691	0.611
1.00	-3.29	-0.406	-0.584	5.73	6.31	4.79
1.50	2.71	3.59	6.70	20.9	22.2	21.3
2.00	17.1	18.0	26.0	48.9	52.1	57.7
2.50	40.9	42.8	59.1	90.1	96.5	115.
3.00	73.6	78.0	105.	143.	152.	190.
3.50	115.	120.	161.	206.	216.	276.
4.00	164.	167.	224.	277.	283.	368.
4.50	221.	213.		358.	353.	458.
5.00				452.	429.	542.
5.50						619.
6.00						693.
6.50						775.
saturation	235. (4.608)	220. (4.582)	278. (4.400)	458. (5.027)	509. (5.456)	833. (6.792)

Table 29. $\bar{L}_2$ values at selected concentrations for some rare earth nitrate solutions at 25° C

	$\bar{L}_2$					
Molality	$La(NO_3)_3$	$Nd(NO_3)_3$	$Gd(NO_3)_3$	$Ho(NO_3)_3$	$Er(NO_3)_3$	$Lu(NO_3)_3$
0.10	1081	910	979	1208	1185	1137
0.20	1068	880	980	1322	1303	1231
0.50	871	765	888	1459	1443	1288
1.00	678	522	862	1763	1781	1553
1.50	817	884	1174	2371	2488	2280
2.00	1185	1336	1781	3212	3436	3436
2.50	1677	1946	2596	4181	4532	4853
3.00	2234	2644	3522	5199	5664	6374
3.50	2821	3369	4480	6216	6751	7869
4.00	3425	4062	5417	7215	7754	9241
4.50	4047	4671		8208	8675	10435
5.00				9236	9561	11434
5.50						12264
6.00						12993
6.50						13734
saturation	4184 (4.608)	4760 (4.582)	6134 (4.400)	9293 (5.027)	10415 (5.456)	14232 (6.792)

Table 30. $\bar{L}_1$ values as selected concentrations for some rare earth perchlorate solutions at 25° C

	$-\bar{L}_1$				
Molality	$La(ClO_4)_3$	$Nd(ClO_4)_3$	$Gd(ClO_4)_3$	$Er(ClO_4)_3$	$Lu(ClO_4)_3$
0.10	0.189	0.156	0.233	0.250	0.247
0.20	0.128	0.024	0.301	0.373	0.339
0.50	0.030	-0.47	0.975	1.13	0.891
1.00	6.1	3.8	8.2	11.1	10.2
1.50	35.1	30.3	38.3	45.2	41.1
2.00	94.2	84.6	93.3	105.	103.
2.50	185.	170.	178.	192.	196.
3.00	309.	289.	294.	310.	320.
3.50	462.	442.	443.	466.	472.
4.00	643.	629.	625.	667.	647.
4.50	843.	849.	837.	923.	840.
saturation	966. (4.791)	938. (4.685)	888. (4.611)	997. (4.627)	893. (4.634)

Table 31. $\bar{L}_2$ values at selected concentrations for some aqueous rare earth perchlorate solutions at 25° C

	$\bar{L}_2$				
Molality	$La(ClO_4)_3$	$Nd(ClO_4)_3$	$Gd(ClO_4)_3$	$Er(ClO_4)_3$	$Lu(ClO_4)_3$
0.10	860	818	910	915	893
0.20	841	772	938	965	931
0.50	812	679	1033	1074	1008
1.00	1234	968	1545	1769	1658
1.50	2485	2109	2871	3253	3018
2.00	4351	3824	4609	5146	4973
2.50	6593	5925	6690	7280	7264
3.00	9080	8319	9035	9662	9761
3.50	11705	10931	11579	12322	12355
4.00	14371	13699	14263	15299	14952
4.50	16990	16570	17034	18632	17465
saturation	18462 (4.791)	17649 (4.685)	17656 (4.611)	19540 (4.627)	18114 (4.634)

Table 32. Values of $T(\bar{S}_2 - \bar{S}_2^o)$ at selected concentrations for some rare earth salt solutions at 25° C

	$T(\bar{S}_2 - \bar{S}_2^o)$			
Molality	$Nd(ClO_4)_3$	$Gd(ClO_4)_3$	$Lu(ClO_4)_3$	$Er(NO_3)_3$
0.10	3278	3257	3108	3779
0.20	3385	3388	3239	4208
0.50	3022	3077	2875	4527
1.00	2038	2101	1969	4612
1.50	1339	1413	1221	4863
2.00	964	843	739	5278
2.50	845	488	439	5798
3.00	960	391	324	6327
3.50	1246	539	356	6793
4.00	1571	834	418	7161
4.50	1719	1068	279	7437
5.00				7669
saturation	2216 (4.685)	1083 (4.611)	177 (4.634)	7922 (5.456)

Table 33. Values of $T(\bar{S}_1 - \bar{S}_1^{o})$ at selected concentrations for some rare earth salt solutions at 25° C

	$- T(\bar{S}_1 - \bar{S}_1^{o})$			
Molality	$Nd(ClO_4)_3$	$Gd(ClO_4)_3$	$Lu(ClO_4)_3$	$Er(NO_3)_3$
0.10	0.825	0.914	0.928	1.25
0.20	0.948	1.18	1.19	2.32
0.50	-2.23	-1.25	-1.59	3.74
1.00	1.56	5.80	7.68	3.71
1.50	-38.0	-33.1	-33.6	7.43
2.00	-57.0	-53.4	-51.3	18.1
2.50	-70.3	-70.4	-66.2	36.2
3.00	-72.3	-79.0	-75.1	58.3
3.50	-60.3	-74.3	-77.1	81.9
4.00	-36.0	-58.2	-77.9	101.
4.50	-10.3	-45.7	-93.1	117.
5.00				132.
saturation	-3.97 (4.685)	-45.5 (4.611)	-103. (4.634)	150. (5.456)

Table 34. Observed heats of solution of rare earth nitrate hydrates in water at 25° C

	n_2 x 10^4	$m_f^{1/2}$ x 10^2	$q_{sol.}$ (cal)	$\bar{L}^{\cdot}$	Mean $\bar{L}^{\cdot}$
$La(NO_3)_3 \cdot 6H_2O$	9.843	3.307	4.601	-4465	-4462 ± 6
	13.732*	5.117	6.653	-4470	
	12.032	3.658	5.629	-4450	
	13.485*	5.327	6.550	-4463	
$Nd(NO_3)_3 \cdot 6H_2O$	10.638	3.439	4.468	-3988	-3991 ± 3
	11.630	3.594	4.901	-3994	
$Gd(NO_3)_3 \cdot 6H_2O$	15.048	4.092			-3017 ± 5
	13.774*	5.662	4.714	-3017	
	13.048	3.808	4.257	-3025	
	15.728*	5.654	5.358	-3010	
$Ho(NO_3)_3 \cdot 6H_2O$	11.614	3.592			-1026 ± 1
	13.816*	5.315	1.956	-1026	
	11.683	3.605	1.464	-1028	
	10.084*	4.920	1.411	-1025	
$Er(NO_3)_3 \cdot 6H_2O$	14.021	3.947	1.120	-557	-558 ± 3
	15.745*	5.751	1.534	-562	
	16.670	4.307	1.368	-560	
	15.029*	5.938	1.477	-553	
$Lu(NO_3)_3 \cdot 5H_2O$	10.143	3.357			2786
	13.723*	5.149	-3.315	2786	
	10.739	3.455	-2.762	2786	

*Sample was diluted into the final molality of the immediately preceding sample.

Table 35. Observed heats of solution of rare earth perchlorate hydrates in water at 25° C

	$n_2 \times 10^4$	$m_f^{1/2} \times 10^2$	$-q_{sol.}$(cal)	$\bar{L}^{\cdot}$	Mean $\bar{L}^{\cdot}$
$La(ClO_4)_3 \cdot 8H_2O$	5.125	2.386	4.769	9450	9423 ± 18
	6.089*	3.529	5.592	9432	
	5.165	2.396	4.782	9403	
	5.503*	3.444	5.041	9407	
$Nd(ClO_4)_3 \cdot 8H_2O$	5.451	2.462	5.072	9453	9430 ± 19
	8.178*	3.893	7.511	9445	
	8.062	2.992	7.449	9414	
	4.655*	3.758	4.252	9407	
$Gd(ClO_4)_3 \cdot 8H_2O$	7.599	2.905	7.651	10240	10270 ± 16
	3.161*	3.457	3.168	10283	
	5.738	2.526	5.816	10288	
	6.610*	3.705	6.615	10267	
$Er(ClO_4)_3 \cdot 8H_2O$	3.306	1.915	4.408	13453	13427 ± 26
	1.881	1.445	2.503	13401	

*Sample was diluted into the final molality of the immediately preceding sample.

Table 36. Enthalpies of solution of some rare earth nitrate and perchlorate hydrates at 25° C for the process described by Equation 7.39

Hydrate	$T\Delta S_c$ (cal/mole)	X
$La(NO_3)_3 \cdot 6H_2O$	6314	6.046
$Nd(NO_3)_3 \cdot 6H_2O$	6077	6.115
$Gd(NO_3)_3 \cdot 6H_2O$	5634	6.616
$Ho(NO_3)_3 \cdot 6H_2O$	5542	5.042
$Er(NO_3)_3 \cdot 6H_2O$	5767	4.174
$Lu(NO_3)_3 \cdot 5H_2O$	4539	3.173
$La(ClO_4)_3 \cdot 8H_2O$	-2154	3.586
$Nd(ClO_4)_3 \cdot 8H_2O$	-2883	3.848
$Gd(ClO_4)_3 \cdot 8H_2O$	-3298	4.038
$Er(ClO_4)_3 \cdot 8H_2O$	-5851	3.997

VIII. DISCUSSION AND SUMMARY

When the $\overline{P}_1$ data for aqueous solutions of $La(NO_3)_3$, $Nd(NO_3)_3$, $Gd(NO_3)_3$, $Ho(NO_3)_3$, $Er(NO_3)_3$, and $Lu(NO_3)_3$ were extrapolated to infinite dilution using a linear extrapolation function, the average of the experimentally determined limiting slopes for these salts was within 6 percent of the theoretical value. Following general practice in such cases, the data were forced to the theoretical value at infinite dilution in order to eliminate small errors in the calculated relative apparent molal heat contents due to uncertainties in the extrapolation.

A second order extrapolation function was required to represent the $\overline{P}_1$ data of the rare earth perchlorates studied in this work. The $\overline{P}_1$ data of $Gd(ClO_4)_3$, $Er(ClO_4)_3$, and $Lu(ClO_4)_3$ extrapolated to within an average of about 5 percent of the predicted value. The $\overline{P}_1$ data of $La(ClO_4)_3$ and $Nd(ClO_4)_3$ failed to approach the Debye-Hückel limiting law value of 6925. Inclusion of the distance of closest approach of the ions, a^o, taken from the conductance data of Spedding and Jaffe (70), yielded limiting slopes which did approach the theoretical limit within experimental error. The a^o parameters of the rare earth perchlorates are from 20 to 60 percent larger than those of the corresponding nitrates. The effect of this parameter should therefore be expected to be more pronounced for the perchlorates than for the nitrates. Figure 10 shows a comparison of the experimental ϕ_L curves of $La(NO_3)_3$ and $La(ClO_4)_3$ in the dilute concentration range with calculated ϕ_L curves using the Debye-Hückel theory. The dashed curves are the theoretical curves including the a^o term and are seen to approach the Debye-Hückel limiting law curve, given by the dotted line, as infinite dilution is approached. The dashed curves indicate that deviations from the Debye-Hückel limiting law expression may be expected to occur at lower concentrations as the distance of closest approach increases.

The ϕ_L values for the very dilute concentration range of the perchlorates were calculated using equations which were obtained by forcing the $\bar{P}_1$ data to the predicted value of 6925 at infinite dilution. The comparison of the ϕ_L values calculated by this method for $La(ClO_4)_3$ with those determined by Nutter (72), given in Figures 8 and 9, shows good agreement.

The ϕ_L curves for the rare earth nitrates and perchlorates studied in this work are presented in Figures 11 and 12, respectively. Interpretation of these curves is facilitated by considering three concentration regions:

(1.) $0 \leq m^{1/2} \leq 0.4$

(2.) $0.4 \leq m^{1/2} \leq 1.2$

(3.) $1.2 \leq m^{1/2}$

As previously noted the ϕ_L behavior in region (1.) is determined primarily by the influence of the a^0 parameter for both the nitrates and perchlorates.

The second region is marked by a decrease in the slope of the ϕ_L versus $m^{1/2}$ curves with a downturn occurring for the light rare earth nitrates. The extent of this effect for the nitrates can be correlated with the observed trend in the rare earth mononitrate complex stability constants across the series (75, 76). The extent of complexation increases from La to Eu and then decreases rapidly to Lu. This same trend in the degree of complexation across the series has been cited by Cullen (12) in explaining his apparent molar volume data on the rare earth nitrates.

By assuming that the heat of formation of the mononitrate complex is the same across the series it is possible to estimate the effects of the variation of the stability constants of these complexes on the measured ϕ_L values. The heat of formation of $EuNO_3^{2+}$ has been determined by Choppin and Strazik (76) to be -0.57 kcal./mole. Applying this value to $Nd(NO_3)_3$ solutions in the region of the observed downturn in ϕ_L indicates that the dissociation of the mononitrate complex upon dilution could cause the ϕ_L values to be lowered by an average of as much as 55 percent between 0.5 and 1.0 molal. The effect on ϕ_L for $Er(NO_3)_3$ solutions accompanying the dissolution of the corresponding

$ErNO_3^{2+}$ complex, assuming the same heat of formation of the mono complex, would only be about 15 percent over the same concentration range due to the lower degree of complexation exhibited by the heavier rare earth nitrates.

The equilibrium between mono- and di-nitrate complexes is shifted toward the latter as the concentration increases above 1.0 molal. Abrahamer and Marcus (77) have studied the rare earth nitrate complexes of Nd, Ho, and Er using density, molar absorptivity, and NMR measurements. They conclude from their results that the nitrates form mainly inner-sphere complexes with some outer-sphere complexation also occurring. The dissociation of inner-sphere complexes upon dilution would be expected to be exothermic and would thus tend to increase ϕ_L. This could account for at least part of the observed increase in ϕ_L above 1.0 molal. Dehydration of the ions with increasing concentration also becomes important above 1.0 molal. This would also lead to higher values of ϕ_L since energy is released when the hydration requirements of an ion are fulfilled upon dilution.

The ϕ_L curves in Figure 12 for the rare earth perchlorates also show a marked decrease in slope between 0.04 and 1.0 molal. Although the perchlorates are not considered to form complexes as in the case of the nitrates, it is not unreasonable to assume that ion pair formation may occur. Throughout this thesis the term ion pair shall refer to an outer sphere type complex with at least one water molecule separating the two ions. Evidence for the existence of $CeClO_4^{2+}$ has been reported from absorption spectra studies by Heidt and Berestecki (78) and by Sutcliffe and Weber (79). Ion pair formation between ferric ion and perchlorate ion has also been postulated by Sutton (80). Additional evidence for the existence of perchlorate complexes appears in the literature (81, 82). Dissociation of ion pairs upon dilution of a solution could account for part of the decreased slope in this region.

The increase in ϕ_L above 1.0 molal is most likely due to hydration effects. This argument is supported by the excess entropy data to be discussed later.

Values of ϕ_L at selected concentrations are plotted across the series for the perchlorates and compared with similar values for the chlorides, obtained by Pepple (10), in Figure 13. The same trend in ϕ_L is present across the series although it is less pronounced for the perchlorates. The value of ϕ_L at lower concentrations is seen to decrease from La to Nd and from approximately Tb to Lu. The ϕ_L values increase with increasing atomic number of the rare earth between Nd and Tb. This behavior has been interpreted (10) as being evidence of a change in the primary hydration coordination of the rare earth ions across the series. The rare earth ions La^{3+} to Nd^{3+} are pictured as having a hydration coordination of nine while those between Tb^{3+} and Lu^{3+} have a hydration coordination of eight. An equilibrium between both forms is said to exist between Nd^{3+} and Tb^{3+}. There is a large amount of experimental evidence supporting the hydration change described above (5,6,8,9,83,84,85,86, 87,88,89). The ϕ_L data are explained on the basis of a hydration change occurring between Nd and Tb using the following argument. The charge density of a rare earth ion increases from La to Lu. As the charge density of an ion increases the effective hydrated radius of the ion increases since more water molecules are affected by the field of the ion. Since ϕ_L is inversely proportional to the size of the ion (hydrated), one would expect ϕ_L to decrease across the series from La to Lu. The expected behavior is observed from La to Nd and from Tb to Lu, but between Nd and Tb the value of ϕ_L increases. The increase in ϕ_L over this region indicates that the hydrated ion is becoming smaller from Nd to Tb. A shift to lower hydration coordination over this region would explain this behavior.

An analogous trend in the ϕ_L data for the rare earth nitrates across the series appears to exist in dilute solutions, but the effects of complexation quickly mask any evidence for a hydration change in the data above 1.0 molal. This is shown in Figure 14. Recent partial molal volume data obtained by Cullen (12) give further support to the contention that a hydration change occurs for the rare earth nitrates and perchlorates.

The relative partial molal heat contents of the solute and solvent were calculated from empirical least squares fits of the ϕ_L data, as previously described, and are plotted in Figures 15 through 18 for the nitrates and perchlorates studied in this research.

The $\bar{L}_2$ curves closely resemble the corresponding ϕ_L curves over most of the experimental concentration range.

The $\bar{L}_1$ curves all exhibit a gradual decrease from zero concentration to 1.2 molal followed by a much faster rate of decrease above this concentration. This behavior was also found in the case of the rare earth chlorides (3, 10).

Partial molal excess entropies of the solute and solvent were calculated as described in the previous section. The curves obtained for $T(\bar{S}_2 - \bar{S}_2^o)$ and $T(\bar{S}_1 - \bar{S}_1^o)$, respectively, are shown in Figures 19 and 20 for $Nd(ClO_4)_3$, $Gd(ClO_4)_3$, and $Lu(ClO_4)_3$. These curves are quite different from those obtained for the rare earth chlorides (3, 10) and for $Er(NO_3)_3$.

Once again the curves will be discussed in terms of their behavior in three concentration regions. The first region extends from zero concentration to 0.2 molal. In this region $T(\bar{S}_1 - \bar{S}_1^o)$ decreases and $T(\bar{S}_2 - \bar{S}_2^o)$ increases with increasing concentration. This behavior is generally attributed to the polarization effect of the ions on the water molecules.

Between 0.2 molal and approximately 3 molal the entropy behavior is reversed as the excess entropy of the solvent increases and that of the solute decreases. The initial increase in the entropy of the solvent above 0.2 molal may reflect the "structure breaking" effect of the large perchlorate ions. One possible explanation for the continued increase in the entropy of the solvent, and decrease in the entropy of the solute, as the concentration increases above about 1.0 molal may be visualized by considering a competitive interaction of rare earth ion and perchlorate ion for water molecules. In dilute solution the rare earth ion would be the dominant species, binding water molecules much more effectively than the perchlorate ions. As the concentration increased, however, the perchlorate ions would tie up a larger percentage of the available water molecules since the perchlorate ion concentration increases three times as fast as the rare earth ion concentration. Due to this competition for water, an exchange rate may be set up which would have the overall effect of reducing the time average binding force on a given water molecule. This would result in an increase in the excess entropy of the solvent by restoring some degrees of freedom to the water molecules participating in this exchange process. Such a competition between a rare earth ion and a perchlorate ion for water might also lead to the formation of ion pairs which would be accompanied by a decrease in $T(\bar{S}_2 - \bar{S}_2^o)$.

At approximately 3 molal hydration effects become very important. Assuming that each perchlorate ion requires 3 or 4 water molecules to satisfy its hydration demands and that a rare earth ion needs 8 or 9 water molecules to fulfill its hydration requirements, the ions would be deficient in water of hydration at approximately 3 molal. The minima in the curves shown in Figure 19 occur at this concentration. Above 3 molal the deficiency of water would cause the ions to bind the available water molecules more firmly, thus resulting in a decrease in the excess entropy of the solvent as shown in Figure 20. As the competition for water increases some of the perchlorate and rare earth ions will be forced to share water to fulfill their hydration needs. This could result in the formation of more than one type of hydrated rare earth perchlorate species in solution. Proton relaxation data on $Gd(ClO_4)_3$ solutions (90) have led to the conclusion that both 8 and 9 are acceptable hydration coordination numbers and that both hydration forms may "contribute significantly to the solution hydrate structure". Dehydration of some of the rare earth ions to form a mixture of these two hydration forms would increase the excess entropy of the solute. The extent of this effect would be expected to vary across the series due to the increasing field intensity about the rare earth ions as one goes from Nd to Lu. This behavior is exhibited by the curves in Figures 19 and 20.

Evidence for the interaction of perchlorate ion with water appears in the literature as stated earlier. The hydrolysis of Fe^{3+} in the presence of ClO_4^- decreased with increasing perchlorate ion concentration suggesting a competition between these two ions for water (91). The spectral work of Sutton (80) has been interpreted as being evidence for the formation of an ion pair between Fe^{3+} and ClO_4^-. Supporting evidence for an interaction of ClO_4^- with H_2O has also been reported by Dryjanski and Kecki (92). These workers carried out an I.R. spectral study of HDO containing Li, Na, Mg, and Ba perchlorates at various concentrations. Their results suggested that the perchlorate ions were bound to water molecules which had their hydrogen bonds with surrounding water molecules seriously weakened or broken. The formation of contact ion pairs was also suggested as well as the existence of various hydrated forms in solution. The existence of four stable solid phases at 20° C has been shown by the solubility study of the $Ce(ClO_4)_3$-$HClO_4$-H_2O system carried out by Zinov'ev and Shchirova (62). Two of the hydrates found were

$Ce(ClO_4)_3 \cdot 9H_2O$ and $Ce(ClO_4)_3 \cdot 8H_2O$.

The downturns in the $T(\bar{S}_1 - \bar{S}_1^o)$ curves for NaOH and HCl solutions have been attributed to the interaction of the solute with the water molecules (93).

The preceding arguments are, of course, speculative, but it is clear that the perchlorate ion does interact with water to some extent. A recent paper by Bond (82) points out the fact that use of perchlorate ion as an essentially inert ion to adjust the ionic strength in studies of stability constants is not always the best choice for a given system.

The relative partial molal excess entropies of the solute and solvent in erbium nitrate solutions are shown in Figures 21 and 22, respectively. The initial rise in the $T(\bar{S}_2 - \bar{S}_2^o)$ curve in Figure 21 can be interpreted, using the Debye-Hückel theory, as due to a lessening of the polarizing effect of the ion on primary hydration sphere water caused by the influence of the oppositely charged ion cloud. The slower rate of increase following this initial rise can be explained, at least in part by the formation of outer-sphere complexes. As the concentration increases further the inner-sphere complexes become more favorable. The formation of this latter type of complex results in the freeing of bound water from the first hydration sphere of the ion into the solution. This freeing of bound water essentially "dilutes" the solute with an attendant increase in the excess entropy of the solute. This argument has been used by Walters (11) to explain the $\bar{C}p_1$ data for the rare earth nitrates.

The integral heat of solution at infinite dilution, or relative molar heat content, $\bar{L}^{\cdot}$, is plotted versus rare earth ion in Figures 23 and 24 for the rare earth nitrate and perchlorate hydrates studied in this work. The experimental values are listed in Tables 34 and 35.

The equilibrium existing between water and a hydrated crystal of a rare earth salt in a saturated solution can be described by Equations 8.1 and 8.2, where R represents the rare earth, A represents the anion,

$$RA_3 \cdot n\ H_2O_{(c)} \quad + \quad X\ H_2O_{(l)} \quad = \quad RA_3(\text{sat.}) \qquad (8.1)$$

$$\Delta H_c \quad = \quad T\Delta S_c \quad = \quad \phi_L(\text{sat.}) - \bar{L}^{\cdot} \qquad (8.2)$$

and n is the number of moles of water in one mole of the hydrated crystals. Equation 8.2 represents the entropy change associated with the addition of X moles of water to one mole of hydrated crystal to form one mole of saturated solution. This entropy change is described in terms of the relative partial molal excess entropies of the individual components by Equation 8.3.

$$T\Delta S_c = T(\bar{S}_2 - \bar{S}_2^o)_{(sat.)} + nT(\bar{S}_1 - \bar{S}_1^o)_{(sat.)}$$

$$+ XT(\bar{S}_1 - \bar{S}_1^o)_{(sat.)} - T(\bar{S}^{\cdot} - \bar{S}_2^o - n\bar{S}_1^o) \qquad (8.3)$$

Values of $T\Delta S_c$ and X are listed in Table 36. Values of $T(\bar{S}_1 - \bar{S}_1^o)_{(sat.)}$ and $T(\bar{S}_2 - \bar{S}_2^o)_{(sat.)}$ are listed in Tables 33 and 32, respectively.

In summary, the heats of dilution of aqueous $La(NO_3)_3$, $Nd(NO_3)_3$, $Gd(NO_3)_3$, $Ho(NO_3)_3$, $Er(NO_3)_3$, $Lu(NO_3)_3$, $La(ClO_4)_3$, $Nd(ClO_4)_3$, $Gd(ClO_4)_3$, $Er(ClO_4)_3$, and $Lu(ClO_4)_3$ solutions were measured over the concentration range of infinite dilution to saturation at 25° C. The integral heats of solution of $La(NO_3)_3 \cdot 6H_2O$, $Nd(NO_3)_3 \cdot 6H_2O$, $Gd(NO_3)_3 \cdot 6H_2O$, $Ho(NO_3)_3 \cdot 6H_2O$, $Er(NO_3)_3 \cdot 6H_2O$, $Lu(NO_3)_3 \cdot 5H_2O$, $La(ClO_4)_3 \cdot 8H_2O$, $Nd(ClO_4)_3 \cdot 8H_2O$, $Gd(ClO_4)_3 \cdot 8H_2O$, and $Er(ClO_4)_3 \cdot 8H_2O$ in water at 25° C. were also measured.

Empirical polynomial equations, obtained by a least squares treatment of the heat of dilution data using an IBM 360 computer, were used to express the relative apparent molal heat contents as functions of $m^{1/2}$ and $m^{1/3}$. The relative partial molal heat contents of the solute, $\bar{L}_2$, and of the solvent, $\bar{L}_1$, were calculated from the empirical equations. The relative partial molal entropies of dilution of the solute, $(\bar{S}_2 - \bar{S}_2^o)$, and of the solvent, $(\bar{S}_1 - \bar{S}_1^o)$, were determined for solutions of $Er(NO_3)_3$,

$Nd(ClO_4)_3$, $Gd(ClO_4)_3$, and $Lu(ClO_4)_3$ using the $\overline{L}_2$ and $\overline{L}_1$ values and the available activity coefficient data for these electrolytes. Values of $\overline{L}_2$, $\overline{L}_1$, $T(\overline{S}_2 - \overline{S}_2^o)$, and $T(\overline{S}_1 - \overline{S}_1^o)$ were calculated at selected concentrations.

The data indicate that these six rare earth nitrates and five rare earth perchlorates approach the Debye-Hückel limiting law in aqueous solution in the concentration range 0.001 to 0.007 molal. The ϕ_L data for the rare earth perchlorate solutions can be explained in terms of two series within the rare earths. The two series effect is attributed to a decrease in the coordination number of the rare earths occurring somewhere between Nd and Tb. The partial molal entropy data are interpreted in terms of a competitive interaction of perchlorate and rare earth ions for water. The ϕ_L data of the rare earth nitrates can be correlated with the trend in the stability constants of the rare earth mononitrate complexes.

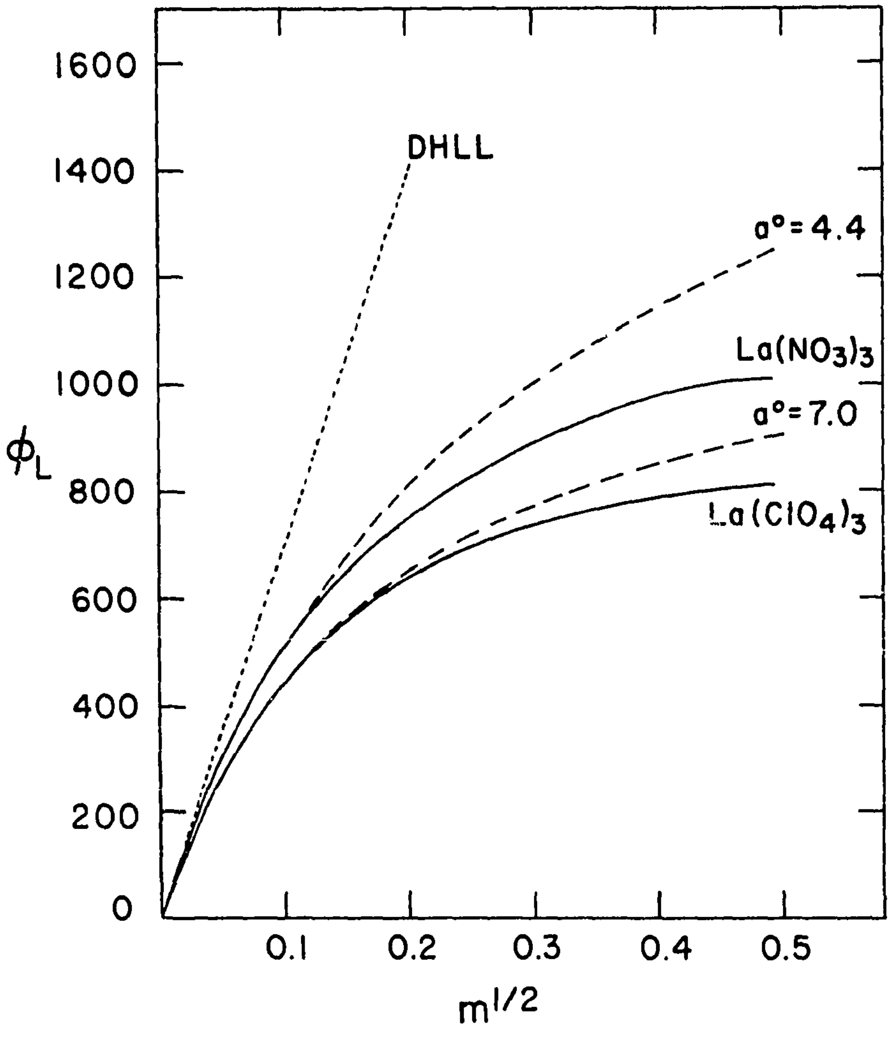

Figure 10. Comparison of the relative apparent molal heat contents of dilute aqueous solutions of $La(NO_3)_3$ and $La(ClO_4)_3$ at 25° C as determined experimentally (solid curves) and as calculated from the Debye-Hückel theory including the a^0 term (dashed curves). The dotted curve represents the Debye-Hückel limiting law slope of ϕ_L versus $m^{1/2}$

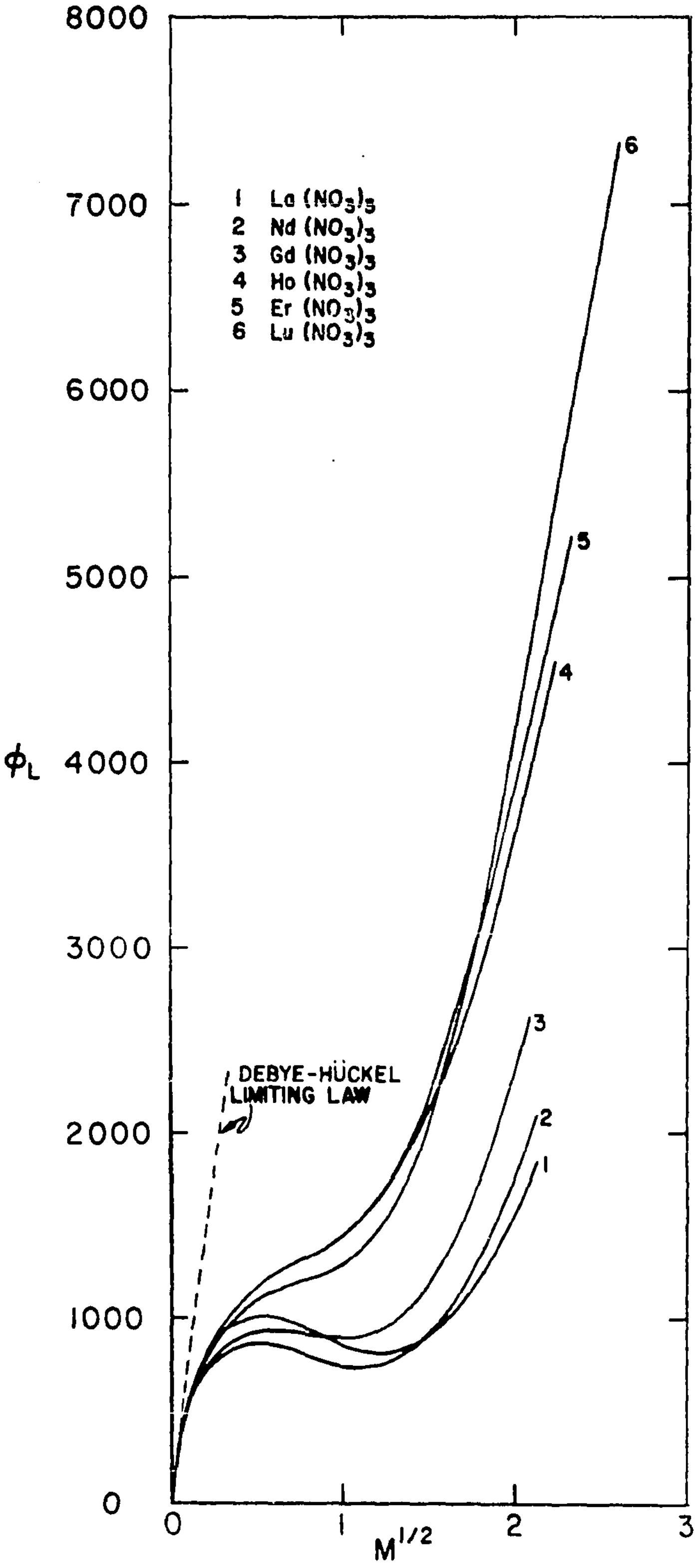

Figure 11. Relative apparent molal heat contents of six aqueous rare earth nitrate solutions versus $m^{1/2}$ at 25° C

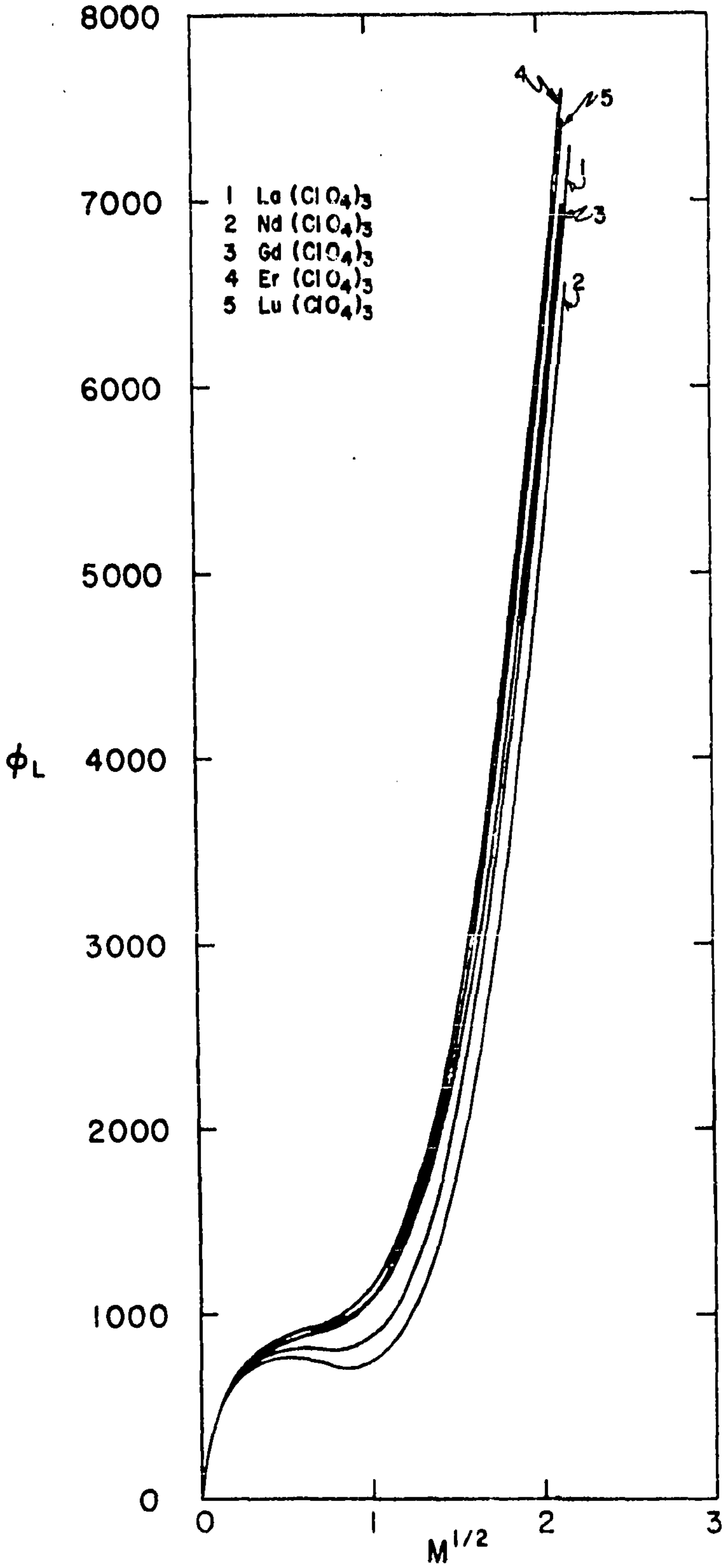

Figure 12. Relative apparent molal heat contents of five aqueous rare earth perchlorate solutions versus $m^{1/2}$ at 25° C

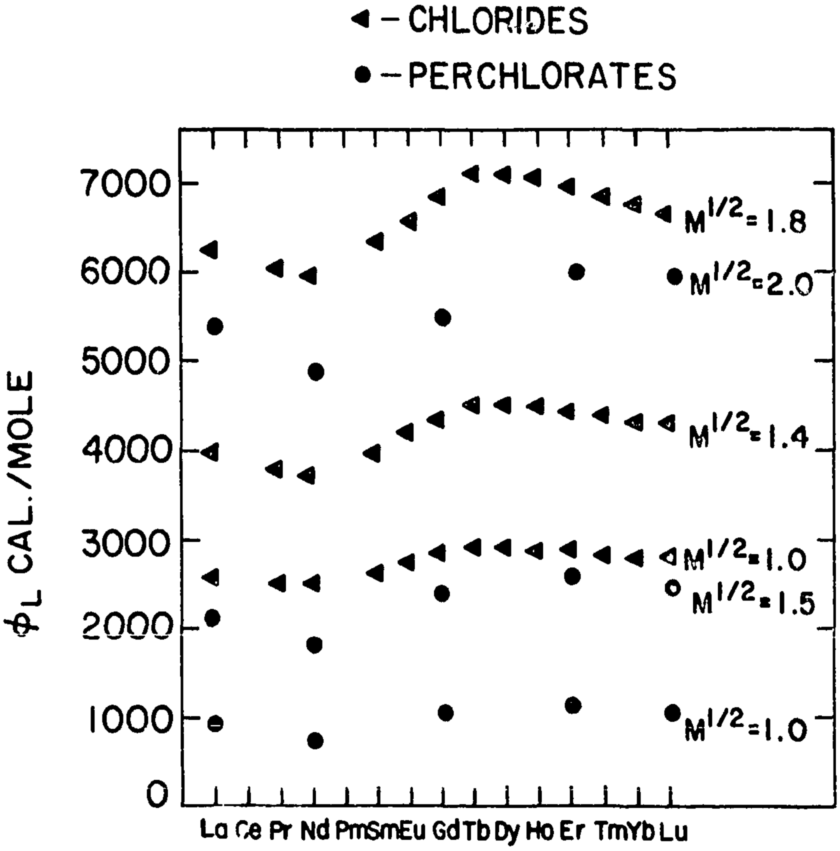

Figure 13. Comparison of the relative apparent molal heat contents of some rare earth chloride and perchlorate solutions at three similar values of $m^{1/2}$ at 25° C

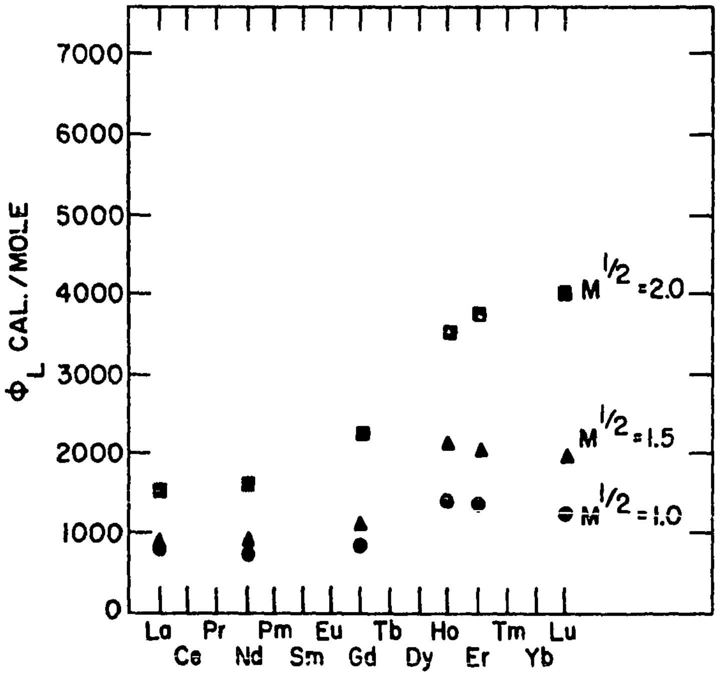

Figure 14. Relative apparent molal heat contents of six rare earth nitrate solutions at three values of $m^{1/2}$ at 25° C

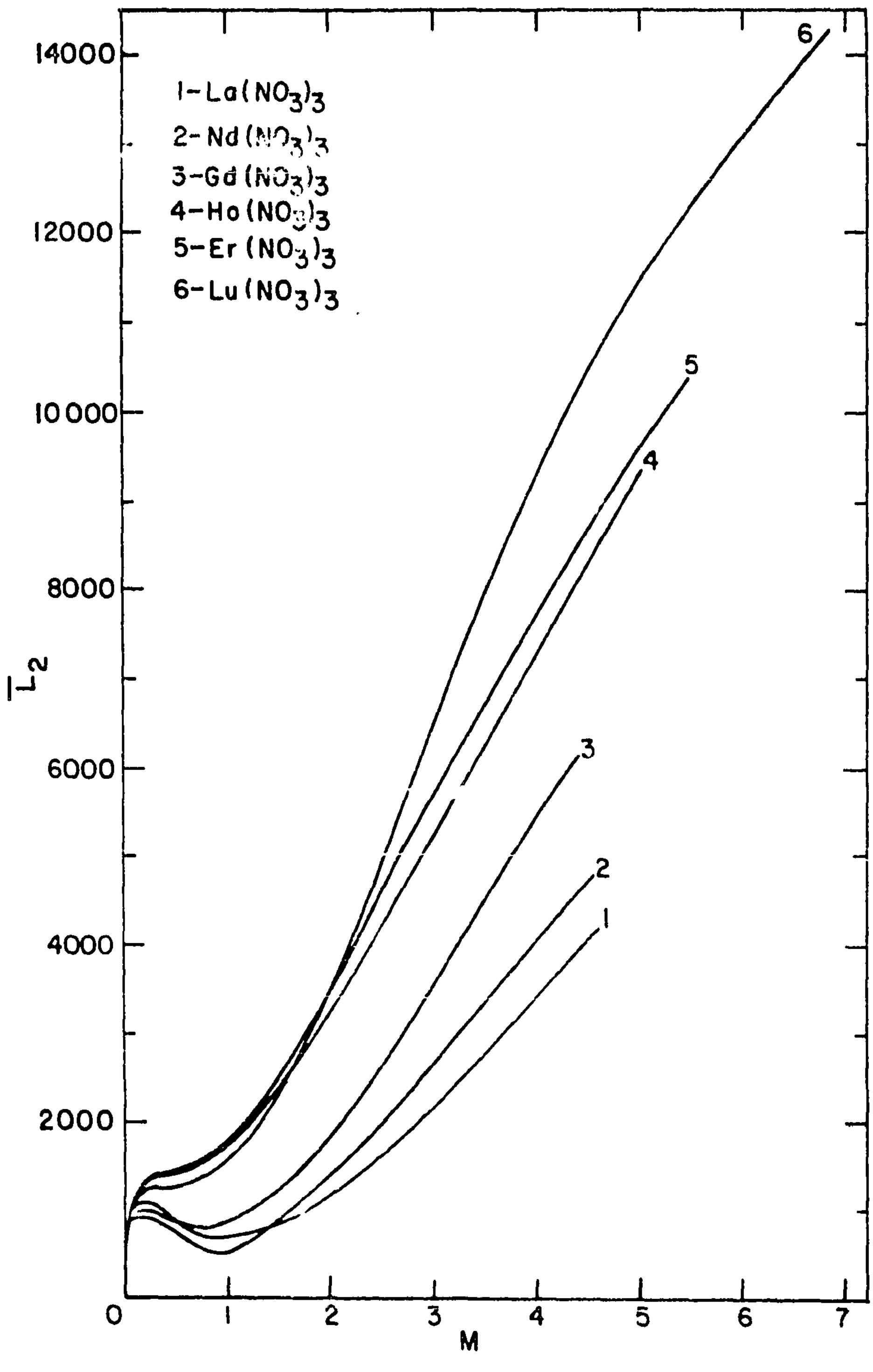

Figure 15. Relative partial molal heat contents of the solute in six aqueous rare earth nitrate solutions versus molality at 25° C

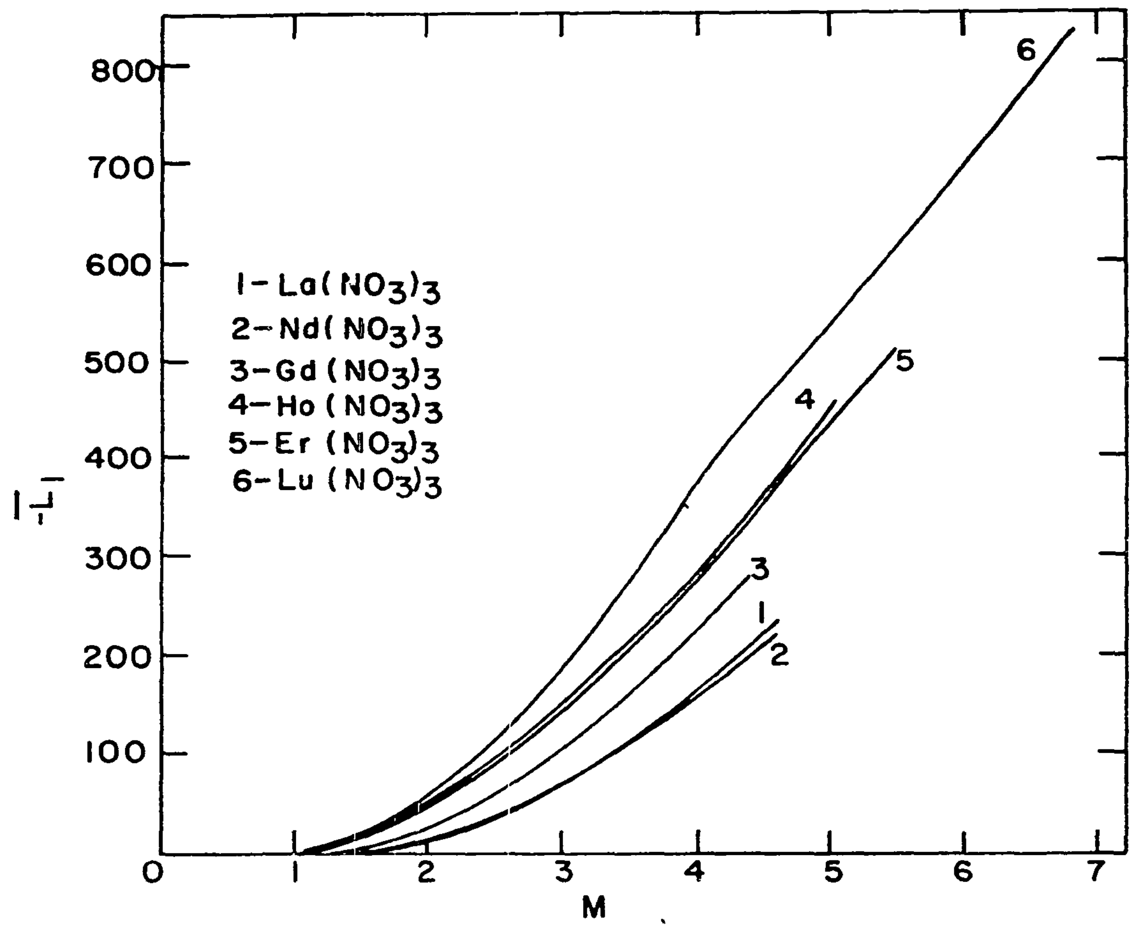

Figure 16. Relative partial molal heat contents of water in six aqueous rare earth nitrate solutions versus molality at 25° C

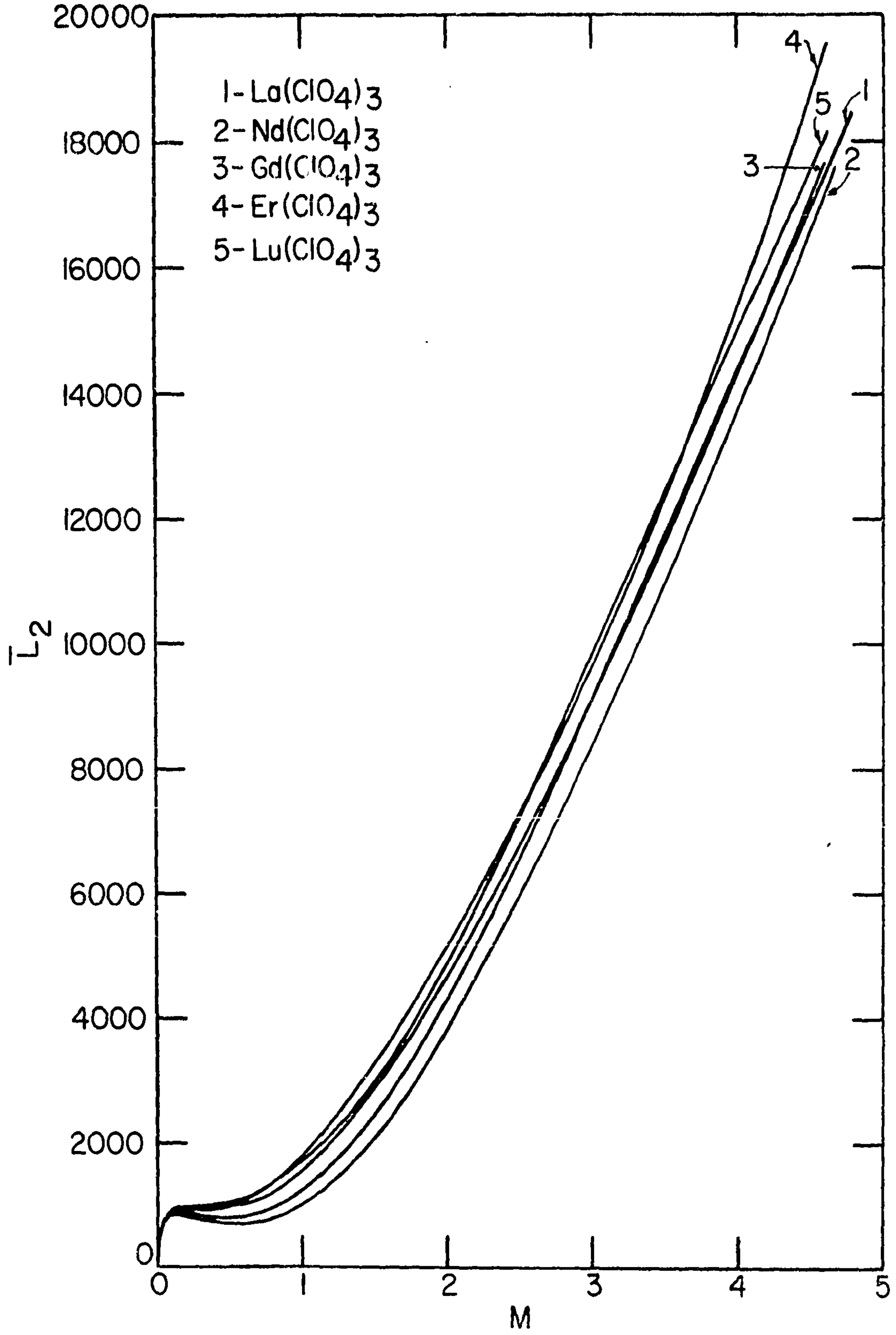

Figure 17. Relative partial molal heat contents of the solute in five aqueous rare earth perchlorate solutions versus molality at 25° C

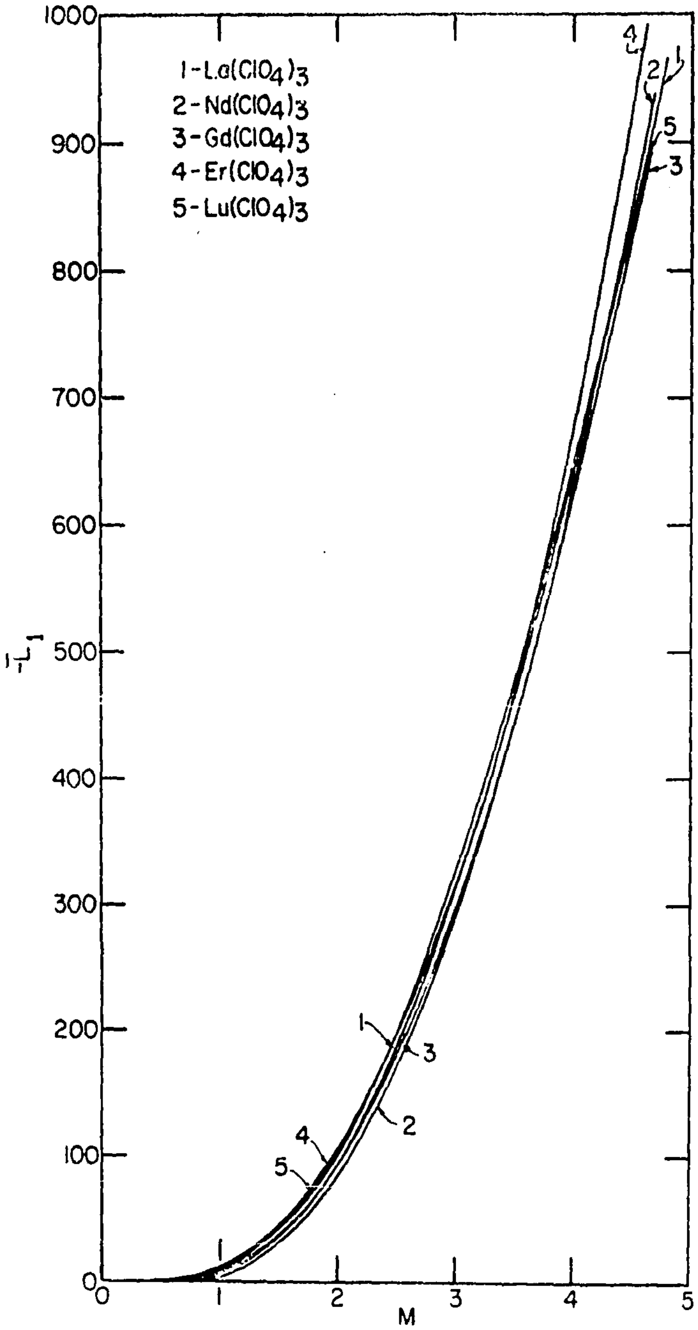

Figure 18. Relative partial molal heat contents of water in five aqueous rare earth perchlorate solutions versus molality at 25° C

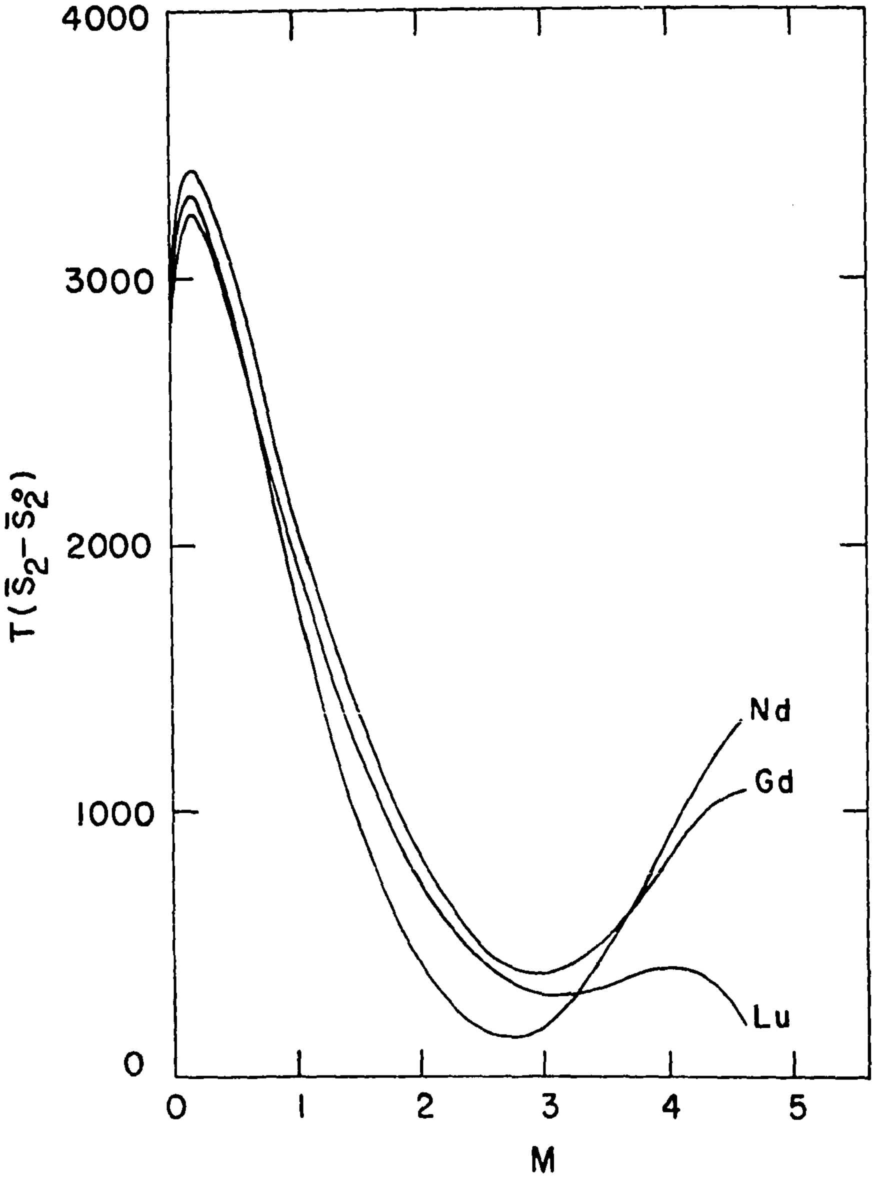

Figure 19. Partial molal excess entropies of the solute in three aqueous rare earth perchlorate solutions versus molality at 25° C

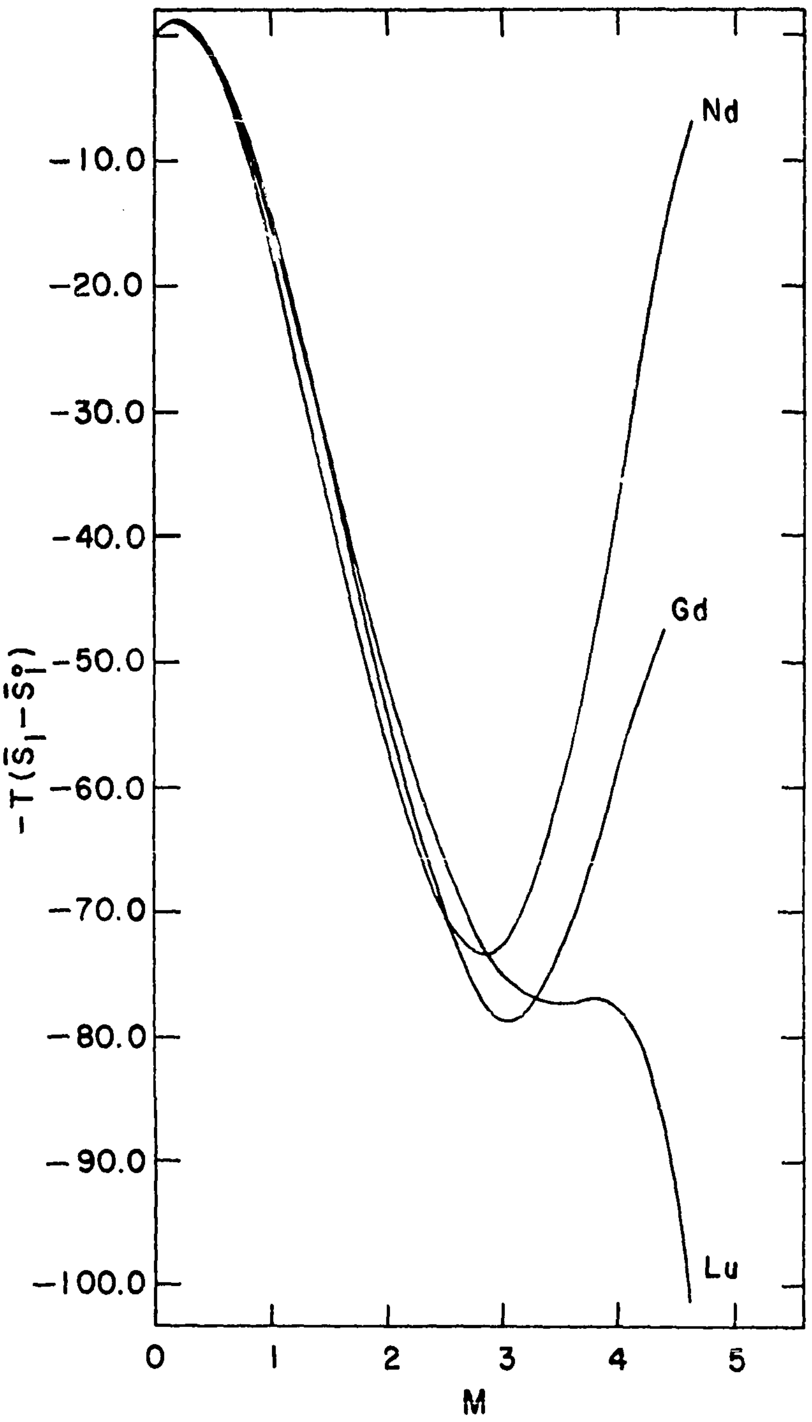

Figure 20. Partial molal excess entropies of water in three aqueous rare earth perchlorate solutions versus molality at 25° C

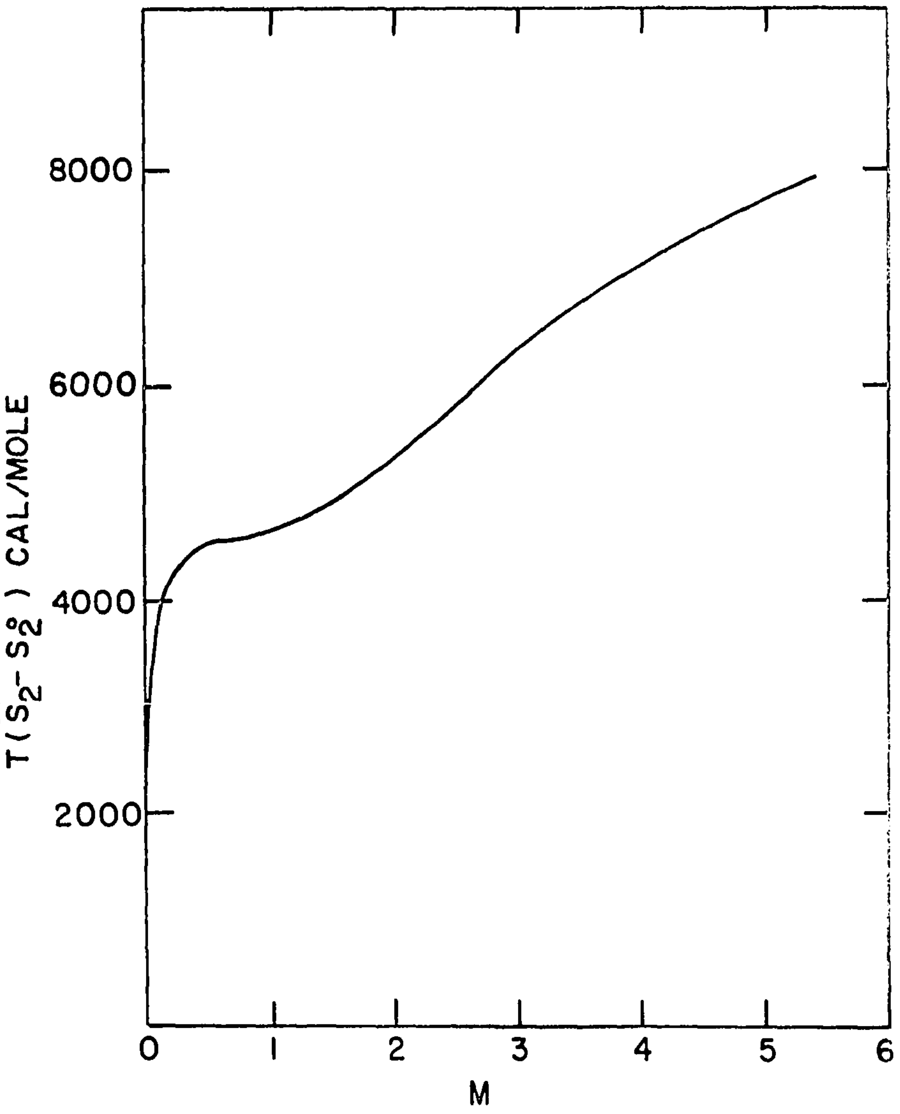

Figure 21. Partial molal excess entropy of the solute in aqueous solutions of erbium nitrate versus molality at 25° C

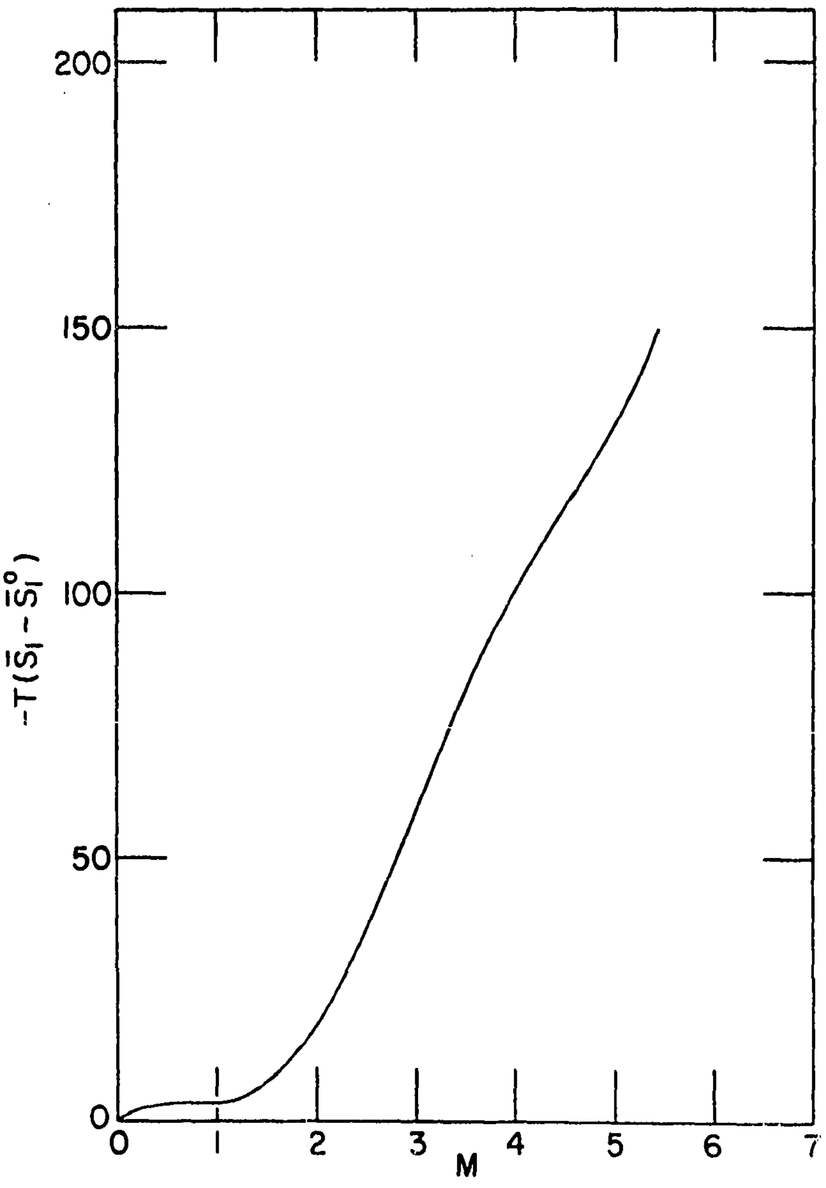

Figure 22. Partial molal excess entropy of water in aqueous solutions of erbium nitrate versus molality at 25° C

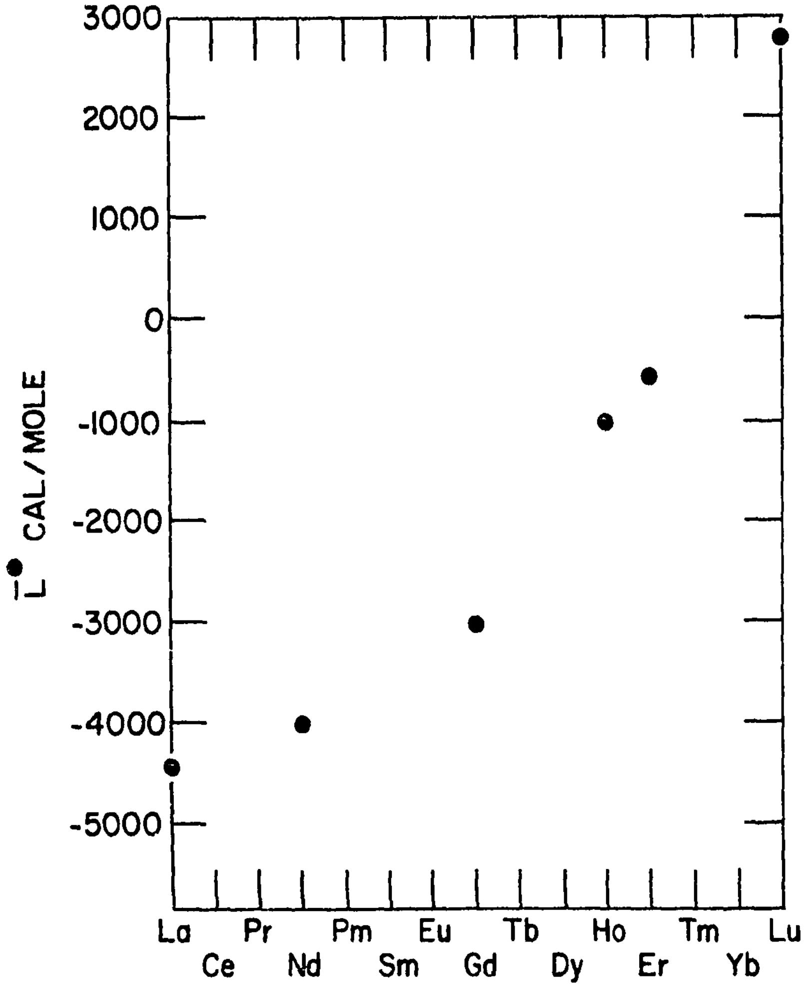

Figure 23. Relative molar heat contents of six hydrated rare earth nitrates at 25° C

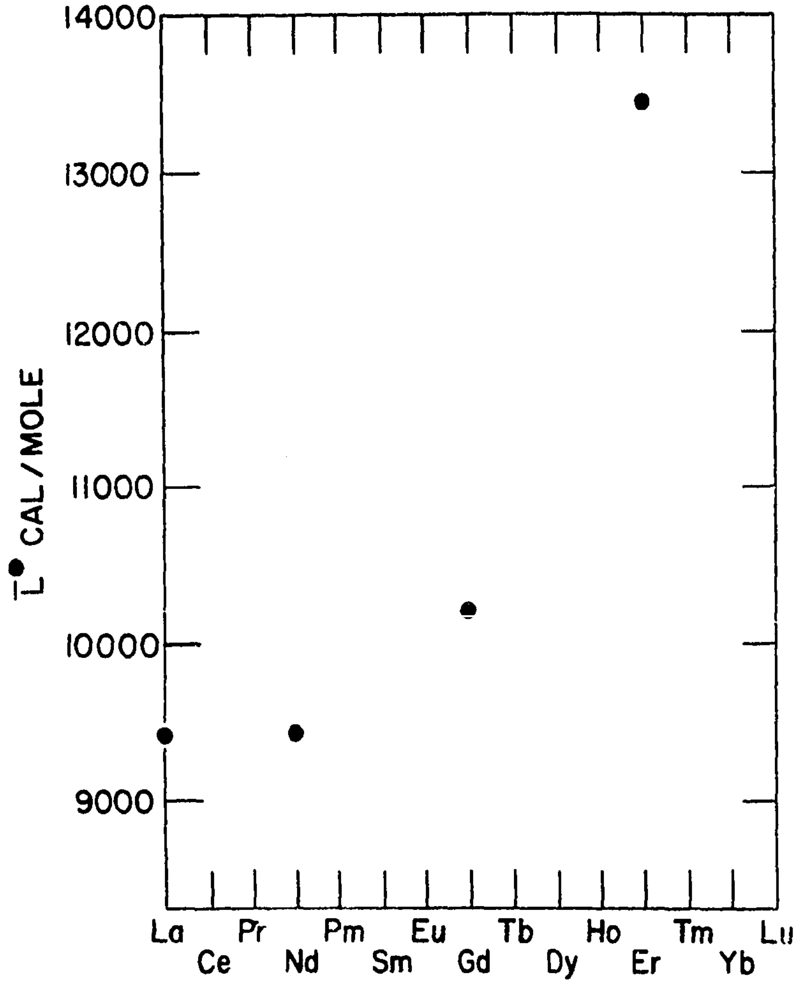

Figure 24. Relative molar heat contents of four hydrated rare earth perchlorates at 25° C

IX. BIBLIOGRAPHY

1. Debye, P. and Hückel, E., Physik. Z., 24, 185 (1923).

2. Powell, Jack E., "Separation of rare-earths by ion exchange". In Spedding, F. H. and Daane, A. H., eds. "The rare-earths", pages 55-73, John Wiley and Sons, Inc., New York, N.Y., 1961.

3. DeKock, Carroll W., "Heats of dilution of some aqueous rare-earth chloride solutions at 25° C", Unpublished Ph.D. thesis, Library, Iowa State University of Science and Technology, Ames, Iowa, 1965.

4. Spedding, F. H. and Atkinson, Gordon, "Properties of rare-earth salts in electrolytic solutions". In Hamer, Walter J., ed., "The structure of electrolytic solutions", pages 319-339, John Wiley and Sons, Inc., New York, N.Y., 1959.

5. Spedding, F. H., Csejka, D. A. and DeKock, C. W., J. Phys. Chem., 70, 2423 (1966).

6. Spedding, F. H. and Jones, K. C., J. Phys. Chem., 70, 2450 (1966).

7. Spedding, F. H., Naumann, A. W. and Eberts, R. E., J. Am. Chem. Soc., 81, 23 (1959).

8. Spedding, F. H. and Pikal, M. J., J. Phys. Chem., 70, 2430 (1966).

9. Spedding, F. H., Pikal, M. J. and Ayers, B. O., J. Phys. Chem., 70, 2440 (1966).

10. Pepple, George W., "Relative apparent molal heat contents of some aqueous rare-earth chloride solutions at 25° C", Unpublished Ph.D. thesis, Library, Iowa State University of Science and Technology, Ames, Iowa, 1967.

11. Walters, John P., "Partial molar heat capacities of some aqueous rare earth chlorides, nitrates and perchlorates from tenth molal to saturation at 25° C", Unpublished Ph.D. thesis, Library, Iowa State University of Science and Technology, Ames, Iowa, 1968.

12. Cullen, Peter F., "Apparent molal volumes of some dilute aqueous rare earth salt solutions at 25° C", Unpublished

Ph.D. thesis, Library, Iowa State University of Science and Technology, Ames, Iowa, 1969.

13. Gulbransen, E. A. and Robinson, A. L., *J. Am. Chem. Soc.*, *56*, 2637 (1934).

14. Young, T. F. and Seligmann, P., *J. Am. Chem. Soc.*, *60*, 2379 (1938).

15. Lange, E., "Heats of dilution of dilute solutions of strong and weak electrolytes". In Hamer, W. J., eds. "The structure of electrolytic solutions", pages 135-151, John Wiley and Sons, Inc., New York, N.Y., 1959.

16. Robinson, A. L. and Wallace, W. E., *J. Am. Chem. Soc.*, *63*, 1582 (1942).

17. Salman, B. C. L. and White, A. G., *J. Chem. Soc.*, (London), 3197 (1957).

18. Arrhenius, Svante, *Z. physik. Chem.*, *1*, 631 (1887).

19. van Laar, J. J., *Z. physik. Chem.*, *15*, 457 (1894).

20. Sutherland, W., *Phil. Mag.*, *3*, 167 (1902).

21. Sutherland, W., *Phil. Mag.*, *7*, 1 (1906).

22. Bjerrum, N., *Z. Electrochem.*, *24*, 321 (1918).

23. Bjerrum, N., Z. *anorg. Chem.*, *109*, 275 (1920).

24. Hertz, P., *Ann. Physik.*, *37*, 1 (1912).

25. Ghosh, I. C., *J. Chem. Soc.*, *113*, 449, 627, 707, 790 (1918).

26. Ghosh, I. C., *Trans. Faraday Soc.*, *15*, 154 (1919).

27. Ghosh, I. C., *J. Chem. Soc.*, *117*, 823, 1390 (1920).

28. Milner, R., *Phil. Mag.*, *23*, 551 (1912).

29. Milner, R., *Phil. Mag.*, *25*, 742 (1913).

30. Owen, B. B. and Brinkley, S. R., Jr., *Ann. N. Y. Acad. Sci.*, *51*, 753 (1949).

31. Swanson, James A., "Thermochemical studies; 1. Heats of dilution of perchloric acid, sodium perchlorate and barium perchlorate. 2. Heat of neutralization of perchloric acid with sodium hydroxide". Microfilm copy. Unpublished Ph.D. thesis, Library, The University of Nebraska, Lincoln, Nebraska, 1962.

32. Harned, H. S. and Owen, B. B., "The physical chemistry of electrolytic solutions", 3rd ed., Reinhold Publishing Corporation, New York, 1958.

33. Wyman, J. and Ingalls, E. N., *J. Am. Chem. Soc.*, *60*, 1182 (1938).

34. Washburn, E. W., "International critical tables of numerical data", McGraw Hill Book Co., New York, N.Y., 1930.

35. Kramers, H. A., *Proc. Acad. Sci. Amsterdam*, *30*, 145 (1927).

36. Fowler, R. H., *Trans. Faraday Soc.*, *23*, 434 (1927).

37. Onsager, L., *Chem. Rev.*, *13*, 73 (1933).

38. Kirkwood, J. G., *J. Chem. Phys.*, *2*, 767 (1934).

39. Fowler, R. and Guggenheim, E. A., "Statistical thermodynamics", Cambridge University Press, Cambridge, England, 1952.

40. Kirkwood, J. G. and Poirier, J. C., *J. Phys. Chem.*, *58*, 591 (1954).

41. Gronwall, T. H., LaMer, V. K. and Sandved, K., *Physik. Z.*, *29*, 358 (1929).

42. LaMer, V. K., Gronwall, T. H. and Greiff, L. J., *J. Phys. Chem.*, *35*, 2245 (1931).

43. Guggenheim, E. A., *Trans. Faraday Soc.*, *55*, 1714 (1959).

44. Hückel, E., *Physik. Z.*, *26*, 93 (1925).

45. Scatchard, G., *Chem. Rev.*, *19*, 309 (1936).

46. Robinson, R. A. and Stokes, R. H., *J. Am. Chem. Soc.*, *70*, 1870 (1948).

47. Wicke, E. and Eigen, M., *Z. Electrochem.*, *56*, 551 (1952).

48. Eigen, M. and Wicke, E., *J. Phys. Chem.*, *58*, 702 (1954).

49. Glueckauf, E., *Trans. Faraday Soc.*, *51*, 1235 (1955).

50. Bjerrum, N., *Kgl. Danske Videnske. Selskab.*, *7*, No. 9 (1926). Original available but not translated; cited in Harned, H. S. and Owen, B. B., "The physical chemistry of electrolytic solutions", 3rd ed., page 70, Reinhold Publishing Corporation, New York, N.Y., 1958.

51. Fuoss, R. M. and Kraus, C. A., *J. Am. Chem. Soc.*, *55*, 2387 (1933).

52. Fuoss, R. M. and Kraus, C. A., *J. Am. Chem. Soc.*, *57*, 1 (1935).

53. Mayer, J. E., *J. Chem. Phys.*, *18*, 1426 (1950).

54. Mayer, J. E. and Mayer, M. G., "Statistical mechanics", John Wiley and Sons, Inc., New York, N.Y., 1940.

55. Poirier, J. C., *J. Chem. Phys.*, *21*, 965, 972 (1953).

56. Glueckauf, E., *Proc. Roy. Soc. A.*, *310*, 449 (1969).

57. Robinson, R. A. and Stokes, R. H., "Electrolytic solutions", Butterworths Scientific Publications, London, England, 1955.

58. Naumann, Alfred W., "Heats of dilution and related thermodynamic properties of aqueous neodymium and erbium chloride solutions", Unpublished Ph.D. thesis, Library, Iowa State University of Science and Technology, Ames, Iowa, 1958.

59. Gucker, F. T., Jr., Pickard, H. B. and Planck, R. W., *J. Am. Chem. Soc.*, *61*, 459 (1939).

60. Eberts, Robert E., "Relative apparent molal heat contents of some rare-earth chlorides and nitrates in aqueous solutions", Unpublished Ph.D. thesis, Library, Iowa State University of Science and Technology, Ames, Iowa, 1957.

61. Csejka, David A., "Some thermodynamic properties of aqueous rare-earth chloride solutions", Unpublished Ph.D. thesis, Library, Iowa State University of Science and Technology, Ames, Iowa, 1961.

62. Zinov'ev, A. A. and Shchirova, N. A., *Russ. Jour. Inorg. Chem.*, *5*, 626 (1960).

63. Rossini, Frederick D., Wagman, Donald D., Evans, William H., Levine, Samuel and Jaffe, Irving, *U.S. National Bureau of Standards Circular 500* (1952).

64. Foulk, C. W. and Hollingsworth, M., *J. Am. Chem. Soc.*, *45*, 1220 (1923).

65. Vogel, Arthur II, "A text-book of quantitative inorganic analysis", 3rd ed., John Wiley and Sons, Inc., New York, N.Y., 1961.

66. Vanderzee, C. E. and Swanson, J. A., *J. Phys. Chem.*, *67*, 2608 (1963).

67. Hale, J. D., Izatt, R. M. and Christensen, J. J., *J. Phys. Chem.*, *67*, 2605 (1963).

68. Young, T. F. and Vogel, O. G., *J. Am. Chem. Soc.*, *54*, 3030 (1932).

69. Young, T. F. and Groenier, W. L., *J. Am. Chem. Soc.*, *58*, 187 (1936).

70. Spedding, F. H. and Jaffe S., *J. Am. Chem. Soc.*, *76*, 884 (1954).

71. Lange, E. and Miederer, W., *Z. Electrochem.*, *60*, 362 (1956).

72. Nutter, James D., "Heat of dilution of lanthanum perchlorate", Unpublished M.S. thesis, Library, University of Nebraska, Lincoln, Nebraska, 1961.

73. Worthing, A. G. and Geffner, J., "Treatment of experimental data", John Wiley and Sons, Inc., New York, N.Y., 1943.

74. Petheram, Harry H., "Osmotic and activity coefficients of some aqueous rare-earth chloride solutions at 25° C", Unpublished Ph.D. thesis, Library, Iowa State University of Science and Technology, Ames, Iowa, 1963.

75. Peppard, D. F., Mason, G. W. and Hucher, I., J. Inorg. Nucl. Chem., 24, 881 (1962).

76. Choppin, G. R. and Strazik, W. F., Inorg. Chem., 4, 1205 (1965).

77. Abrahamer, I. and Marcus, A., Inorg. Chem., 6, 2103 (1967).

78. Heidt, L. J. and Berestecki, J., J. Am. Chem. Soc., 77, 2049 (1955).

79. Sutcliffe, L. H. and Weber, J. R., Trans. Faraday Soc., 52, 1225 (1956).

80. Sutton, J., Nature, 169, 71 (1952).

81. Klanberg, F., Hunt, J. P. and Dodgen, H. W., Inorg. Chem., 2, 139 (1963).

82. Bond, A. M., J. Phys. Chem., 74, No. 2, 331 (1970).

83. Karraker, D. G., Inorg. Chem., 7, 473 (1968).

84. Saeger, Victor W., "Some physical properties of rare-earth chlorides in aqueous solution", Unpublished Ph.D. thesis, Library, Iowa State University of Science and Technology, Ames, Iowa, 1960.

85. Mackey, J. L., Powell, J. E. and Spedding, F. H., J. Am. Chem. Soc., 84, 2047 (1962).

86. Grenthe, I., Acta Chem. Scand., 18, 293 (1964).

87. Edelin De La Praudiere, P. L. and Stavely, L. A. K., J. Inorg. Nucl. Chem., 26, 1713 (1964).

88. Geier, G., Karlen, U. and Zeleinsky, A. V., Helv. Chim. Acta, 52, 1967 (1969).

89. Bertha, S. L. and Choppin, G. R., Inorg. Chem., 8, 613 (1969).

90. Morgan, L. O., J. Chem. Phys., 38, 2788 (1963).

91. Olsen, A. R. and Simonson, T. R., J. Chem. Phys., 17, 1322 (1949).

92. Dryjanski, Piotr and Kecki, Zkyniew, Rocz. Chem., 43, 1053 (1969).

93. Frank, H. S. and Robinson, A. L., J. Chem. Phys., 8, 933 (1940).

X. ACKNOWLEDGMENTS

The author wishes to express his appreciation to Dr. F. H. Spedding for his advice and guidance throughout the course of this research and in the preparation of this thesis. Thanks are also extended to his many associates who have contributed to this work through their cooperation, assistance and many helpful discussions. The author also extends special thanks to Mr. H. O. Weber for his efforts to provide activity data which were used in this work.